



SCUOLA
NORMALE
SUPERIORE

TESI DI PERFEZIONAMENTO

The geometry of large outerplanar and half-planar maps

CANDIDATO
Alessandra Caraceni

RELATORI

Prof. Franco Flandoli

Università di Pisa



Prof. Nicolas Curien

Université Paris Sud



Contents

Contents	1
How to read	3
I Introduction	5
1 Planar Maps and their Limits	7
1.1 About (large) planar maps	7
1.2 Scaling limits	10
1.3 Local distances and local limits	13
2 Trees	15
2.1 Rooted plane trees	15
2.2 Real trees	17
2.3 Galton–Watson trees	21
2.4 The Brownian tree	23
2.5 The critical Galton–Watson tree conditioned to survive	25
3 Quadrangulations	29
3.1 Rooted quadrangulations of the sphere	29
3.2 There and back again: some bijections for bipartite maps	31
3.3 Random quadrangulations and random labelled trees	41
3.4 The Brownian map	43
3.5 The UIPQ	48
II The scaling limit of random outerplanar maps	51
II.1 Introduction	52
II.2 Outerplanar maps and plane trees	53
II.3 Rough localisation of geodesics	56
II.4 An algorithm to compute map-distances	58
II.5 The Galton–Watson tree conditioned to survive	62
II.6 The algorithm running on the infinite bicoloured tree	65

II.7	Final proofs	70
III	The geometry of the UIHPQ	79
III.1	Introduction	80
III.2	Schaeffer-type constructions	85
III.3	The new construction	94
III.4	A study of geodesic rays in \mathcal{H}_∞	105
III.5	Scaling limits	115
III.6	The UIHPQ with a simple boundary	121
III.7	Self-avoiding walks on the UIPQ	124
	Bibliography	133

An Introduction to the Introduction: How To Read this Thesis

This thesis contains an account of results obtained by the author and others within the context of the rich probabilistic theory developed around random planar maps, a field which has been very active over the last decade (see [40, 54]).

While original results are discussed within Parts II and III, we have thought it appropriate to include a rather broad introduction to the research field, the objects it is concerned with, the issues it tries to tackle, the technical tools it typically employs and the kind of ideas it thrives on. Throughout Part I of this thesis, we shall present a variety of objects and results which we hope will provide motivation, as well as effective reference points, for the reader's adventuring in Part II and Part III.

The reader may notice a number of shaded boxes, which we refer to as "Infoboxes" throughout this work, and whose appearance is roughly as captured below; their nature is explained within Infobox 1.

About Infoboxes

1

Floating infoboxes will serve different purposes throughout this thesis: within the introduction, they will usually contain insights or examples that the author believes may help readers less familiar with the subject matter to get a clearer picture of the objects under scrutiny. Sometimes they will contain lists of extra results and references, and sometimes brief explanations of technical tools which many readers will be already familiar with, or sketches of proofs that are not considered essential to the main point of the section or chapter.

The general idea is that the content isolated within an infobox may be considered somewhat tangential to the main discussion, and should be read if and when the reader wishes; successive infoboxes within a chapter are linked to each other, providing a gallery of curiosities, lemmas, ideas and tools meant to reflect the specific interests and tastes of the author.

Within Parts II and III, fewer infoboxes are to be found: their main purpose is to give some proofs that were not included in the papers upon which such parts are based, without disrupting their original structure, so that they are easy to find for readers who follow a referral to this work in search for additional details.

Part II of this thesis presents a result by the author about the scaling limit of outer-planar maps, which is contained in a paper bearing the same title as Part II [19], having been accepted for publication by the *Annales de l'Institut Henri Poincaré*. Part III is based on joint work with Nicolas Curien, and deals with an object called the *uniform infinite quadrangulation of the half-plane*; the bulk of it follows a paper now available on the ArXiv [21], while the very last section presents results which we intend to include in a paper still in preparation [20].

Part I

Introduction

where we discuss scaling and local limits of large random planar maps, and get acquainted (or catch up) with amiable objects such as the CRT and the Brownian map.

Chapter 1

Planar Maps and their Limits

1.1 About (large) planar maps

We start by giving some very standard definitions. The reader familiar with the basic terminology of planar maps may safely skip this section.

A *multigraph* (henceforth simply a *graph*) is a pair (V, E) , where V (the *vertex set*) is any set, finite or infinite, and E (the *edge set*) is a multiset containing elements of $\{\{u, v\} \mid u, v \in V\}$. Thus a multigraph may contain multiple copies of a single edge, and edges involving a single vertex (called *loops*).

A *cellular embedding* of a graph $G = (V, E)$ on a surface S (supposed connected, compact, and without a boundary) is a representation of G as a union of simple arcs in S such that

- each vertex v in V corresponds to a point $f(v)$ in S (and $f : V \rightarrow S$ is injective);
- each edge $\{u, v\}$ corresponds to an arc between $f(u)$ and $f(v)$ in S , that is to say the image of an injective continuous map $e : [0, 1] \rightarrow S$ such that $e(0) = f(u)$ and $e(1) = f(v)$ (hence a loop when $u = v$);
- arcs may not intersect other arcs or the image of f other than in their endpoints;
- the complement of the union of all arcs representing edges is a disjoint union of connected components homeomorphic to the open disk, each of which is called a *face*.

A graph is *planar* if it admits a cellular embedding in the sphere \mathbb{S}^2 .

Definition 1.1.1. A *planar map* is a *connected, locally finite planar (multi)graph* endowed with a cellular embedding in the sphere \mathbb{S}^2 , considered up to orientation-preserving homeomorphisms of the sphere.

Notice that many of the requirements in the definition above are in fact redundant: planarity and connectedness are both consequences of the existence of a cellular embed-

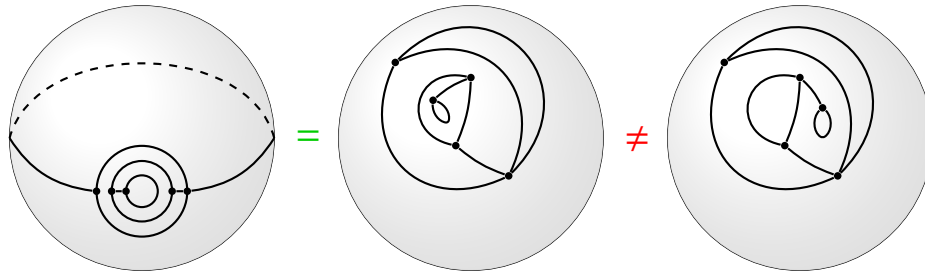


Figure I.1: The first two drawings represent the same planar map, while the third one is a *different* planar map with the same underlying graph structure.

ding in the sphere; local finiteness, on the other hand, we enforce for all infinite maps we shall be dealing with throughout this work.

Of course, a planar map will inherit all natural notions traditionally defined for graphs – it will have a vertex set and an edge set, we will say two of its vertices are *neighbours* if they are connected by an edge, and so on.

The fact that planar maps are intrinsically embedded also adds a few features and natural notions specific to them: to start with, that of *faces*. We have mentioned earlier that each connected component of the complement of the image of a cellular map is called a face; since orientation-preserving homeomorphisms of \mathbb{S}^2 “preserve” faces, their notion makes sense for planar maps; we can speak of vertices and edges as being *adjacent* to faces: each vertex can be adjacent to any number of faces (though only a finite number, thanks to the requirement of local finiteness) and each edge can be adjacent to either one or two faces.

Each edge, in fact, possesses two possible orientations; given an oriented edge, since \mathbb{S}^2 is oriented as well, we can consider the face lying to its right and that lying to its left (note that the two may coincide). We say the oriented edge is incident to the face lying to its left, and call *degree* of a face the number of oriented edges that are incident to it.

An oriented edge univocally identifies what we shall call a *corner*; informally, given an oriented edge e , we may say its corner c_e is a “very small” neighbourhood of the tail vertex e^- of e , intersected with the face f_e lying to the left of e (and, if such an intersection has more than one connected component, one needs to take the one that lies directly to

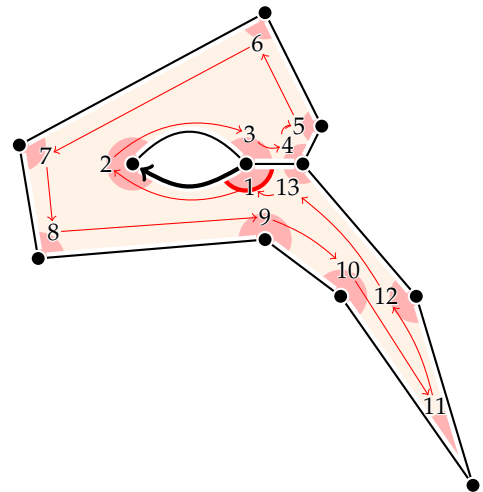


Figure I.2: A face of degree 13 and its counterclockwise contour started at the corner labelled one, which is the one associated with the thick oriented edge.

the left of e). We will say that c_e is a corner of f_e and is adjacent to the vertex e^- .

Each face has as many corners as its degree; if the face has finite degree, then its corners are naturally arranged in a cyclic order: given a corner c_1 of a face f of finite degree, we call the sequence $c_1, \dots, c_{d(f)}$ of its corners, ordered clockwise, the *clockwise contour* of f , started with c_1 ; *counterclockwise contours* can be defined analogously.

Most of the planar maps we will be dealing with throughout this work will be *rooted*, i.e. equipped with a distinguished oriented edge. Whenever they are, we shall for simplicity draw them as embedded in the plane rather than the sphere, by making the face incident to the root edge (to the left) into the unbounded face of the map in the plane. Taking rooted planar maps rather than just planar maps considerably simplifies their enumeration and treatment: rooting a map “destroys all of its symmetries”, in the sense that the only automorphism of a map that fixes the root edge and its endpoints sends all vertices and edges onto themselves.

A touch of history

1.1

The origin of the study of planar maps is often traced back to the '60's, when efforts to solve the celebrated 4-colour problem led to an increased interest in embedded planar graphs.

Tutte [63] was the first to set up a systematic enumerative theory, producing generating functions for a number of classes of planar maps. Since then, numerous links between maps and problems not strictly related to graph theory have kept the field active: from *dessins d'enfant* to knots [13] to matrix integrals [64].

Since relatively recently, one of the main sources of interest in planar maps is their relevance to theoretical physics, and in particular theories of quantum gravity [6]: being natural models for a random “discretised” surface, planar maps – and especially random planar maps – have a role to play in the context of two-dimensional field theories. The question arises of how planar maps may in fact be interpreted as approximations of a “continuous” random surface, a “Brownian” map, in the same way as random discrete walks along \mathbb{Z} can be rescaled to yield one-dimensional Brownian motion: many a work has been written by now about what is called the *scaling limit* for a number of classes of planar maps (see the next section for more details).

One of the main tools infusing life into the many combinatorial, probabilistic and physics applications is a bijective approach to maps enumeration: after the bijective descriptions in terms of permutations suggested by Cori et al. [25], the celebrated Schaeffer bijection and later versions by Bouttier, Di Francesco, Guitter [16] have provided the basis for much of the present investigation of geometric properties of large planar maps.

This is the first infobox in the chapter

Next infobox: 1.2 \leftrightarrow

1.2 Scaling limits

Given a certain class of combinatorial objects categorised according to a quantitative parameter one can think of as *size*, we wish to investigate asymptotical properties of “large” members of the family. We therefore wish to take a uniform sampling of a member of the family having size n , and to somehow compare such samplings and define a limit as $n \rightarrow \infty$.

Of course, the way to develop this idea depends on the class of objects we are considering, and on the tools at our disposal for “comparing” members of the family. Very broadly, a natural operation to perform on samplings is to normalise them in order to account for their increasing size, thus rendering them directly comparable and seeing them as increasingly detailed approximations of a “continuous” limit. The primal example of this kind of reasoning – albeit in a slightly different context – is the construction of one-dimensional Brownian motion as the scaling limit of the symmetric random walk on \mathbb{Z} .

When the combinatorial family comprises graphs or related objects, possibly with additional structure (maps, labelled maps etc.), one may exploit the natural metric structure of a graph (given by the graph distance on the set of its vertices) to compare objects as metric spaces via the Gromov–Hausdorff distance.

Given two compact metric spaces X and Y , their Gromov–Hausdorff distance $d_{\text{GH}}(X, Y)$ aims to measure how “similar” they are by trying to superimpose one on the other, embedding the two isometrically into a suitable common “ambient” metric space. More formally, we have

Definition 1.2.1. Given two compact (nonempty) metric spaces X, Y , their Gromov–Hausdorff distance $d_{\text{GH}}(X, Y)$ is

$$\inf_{Z, \varphi_X: X \rightarrow Z, \varphi_Y: Y \rightarrow Z} d_{\text{Haus}}(\varphi_X(X), \varphi_Y(Y)),$$

where the infimum is taken over all compact metric spaces Z and isometries $\varphi_X : X \rightarrow Z$, $\varphi_Y : Y \rightarrow Z$, and d_{Haus} is the Hausdorff distance, that is

$$d_{\text{Haus}}(\varphi_X(X), \varphi_Y(Y)) = \max \left\{ \max_{x \in \varphi_X(X)} d_Z(x, \varphi_Y(Y)), \max_{y \in \varphi_Y(Y)} d_Z(y, \varphi_X(X)) \right\}.$$

The Gromov–Hausdorff distance (see Infobox 1.2 for more details) provides us with a way to gauge “nearness” of graphs as metric spaces and discuss convergence of random samplings with increasing size. Of course, in order to obtain an “interesting” limit, some kind of rescaling is necessary: since the graphs being sampled get bigger and bigger, each sampling is far from the next in terms of Gromov–Hausdorff distance. The rescaling will be done by a function of the size n , which is not necessarily equal to n itself: our preferred notion of size for the combinatorial objects – usually the number of edges – may not coincide with the one “perceived” by the Gromov–Hausdorff distance, which in the case of graphs is going to be related to the diameter: see Infobox 1.3.

More on the Gromov–Hausdorff distance

1.2

The following alternative definition of the Gromov–Hausdorff distance will be useful in Section II.7 of Part II, and is often handy for estimating the Gromov–Hausdorff distance of two compact metric spaces.

Definition 1.2.2. Given two metric spaces (A, d_A) and (B, d_B) , a *correspondence* between the two is a set $\mathcal{R} \subseteq A \times B$ such that its projection on A is A and its projection on B is B .

The *distortion* of a correspondence \mathcal{R} is

$$\text{dis}(\mathcal{R}) = \sup_{(a,b),(a',b') \in \mathcal{R}} |d_A(a, a') - d_B(b, b')|.$$

Proposition 1.2.1. Given two (nonempty) compact metric spaces X, Y , we have

$$d_{\text{GH}}(X, Y) = \frac{1}{2} \inf_{\mathcal{R} \subseteq X \times Y} \text{dis}(\mathcal{R}),$$

where the infimum is taken over all correspondences $\mathcal{R} \subseteq X \times Y$.

This alternative definition will be mostly used in the form of its obvious corollary

Corollary 1.2.2. Given a bijection ψ between two compact metric spaces (X, d_X) and (Y, d_Y) , we have

$$d_{\text{GH}}((X, d_X), (Y, d_Y)) \leq \frac{1}{2} \max_{x, x' \in X} |d_X(x, x') - d_Y(\psi(x), \psi(x'))|.$$

↔ **Previous infobox:** 1.1

Next infobox: 1.3 ↔

One can define a space \mathbb{K} of equivalence classes of (nonempty) compact metric spaces, on which d_{GH} is indeed a distance – the resulting metric space $(\mathbb{K}, d_{\text{GH}})$ is *complete* and *separable*. One needs to put a little care in a formal definition of \mathbb{K} , but informally we can just think of \mathbb{K} as the set of compact metric spaces, considered up to isometries. Given a sequence of compact metric spaces that is Cauchy for d_{GH} , we can consider its Gromov–Hausdorff limit in \mathbb{K} ; similarly, given a sequence of *random* elements of \mathbb{K} , we look for a limit in distribution for the distance d_{GH} .

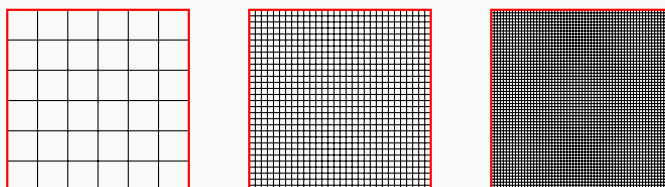
All definitions given above (including those from Infobox 1.2) can be adapted to deal with *pointed* compact metric spaces, which is what we will mostly need. The Gromov–Hausdorff distance between two such spaces will be computed by only considering isometries that match the distinguished points in the two spaces, giving them the same image (in Proposition 1.2.1, we only consider correspondences containing the pair (ρ_1, ρ_2) of the distinguished points in the two spaces). Again, one may take limits in the complete separable metric space $(\mathbb{K}^\bullet, d_{\text{GH}})$ of (isometry classes of) pointed compact metric spaces, endowed with the “pointed” Gromov–Hausdorff distance.

*Scaling limits**1.3*

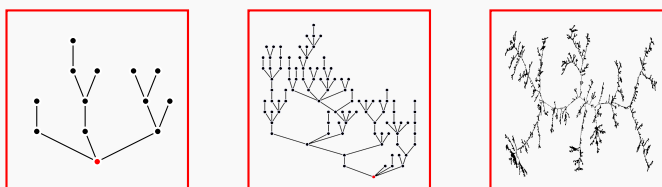
Here are some examples that might help give an idea of what taking scaling limits entails:

- As an extremely simple example of a scaling limit in a deterministic context, take the $n \times n$ grid graph C_n ; we may see its vertex set as a metric space $(V(C_n), d_{\text{gr}})$. Then the sequence of metric spaces $(V(C_n), \frac{1}{n} \cdot d_{\text{gr}})_{n>0}$ converges to the euclidean square $[0, 1]^2$ for the Gromov–Hausdorff distance.

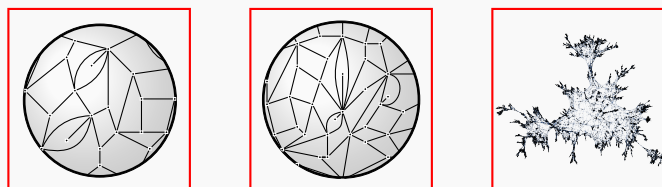
To see this, it is enough to embed each metric space $(V(C_n), \frac{1}{n} \cdot d_{\text{gr}})$ into $[0, 1]^2$ as the set $\{\frac{i}{n} | 1 \leq i \leq n\}^2$. Since the maximum distance of a point in $[0, 1]^2$ to the image of $V(C_n)$ is less than $\frac{2}{n}$, we have $d_{\text{GH}}((V(C_n), \frac{1}{n} d_{\text{gr}}), [0, 1]^2) \leq \frac{2}{n}$.



- We will see in Section 2.4 how for a *uniform random plane tree* θ_n of size n , the random metric spaces $(V(\theta_n), \frac{1}{\sqrt{n}} d_{\text{gr}})$, pointed in the roots of the random trees, converge to a random compact pointed metric space called the *continuum random tree* as $n \rightarrow \infty$.



- If Q_n is a (uniform) random rooted quadrangulation, the sequence $(V(Q_n), \frac{1}{n^{1/4}} d_{\text{gr}})$ converges to an object called *the Brownian map* (see Section 3.4).



↔ Previous infobox: 1.2

Next infobox: 1.4 ↔

1.3 Local distances and local limits

In roughly the same spirit as before – that of investigating the structure of the “large” elements in a combinatorial family – one could take a completely different approach than that of scaling limits; namely, suppose we are dealing with variants of pointed graphs (plane trees, rooted maps etc.), and that we take an interest in what a typical large graph in the family looks like *locally around its distinguished vertex* (or edge).

To this end, we need a way to compare the relevant objects only in terms of certain “centred” neighbourhoods; increasing both the size of the objects and the size of the neighbourhoods, one would wish to build a limit that encodes information about the typical asymptotical behaviour of centred neighbourhoods in large members of the family.

The appropriate tool for comparing two objects in this context is a so-called *local distance*, whose definition will depend on the chosen class of objects; let us suppose – as will always be the case for us – we are dealing with pointed planar maps (that is to say, planar maps with one distinguished vertex: notice that rooted maps, for example, can be seen as being pointed in the tail of their root edge). Given a planar map m pointed in a vertex δ and a natural number r , we write $[m]_r$ for the *ball of radius r around the vertex δ* , that is the map obtained by erasing all vertices u of m such that $d_{\text{gr}}(u, \delta) > r$ and edges involving such vertices, pointed in δ .

Given two planar maps m and m' , each pointed (in vertices $\delta_m, \delta_{m'}$ respectively), we set

$$d_{\text{loc}}(m, m') = \left(1 + \sup \left\{n \in \mathbb{N} \mid [m]_n = [m']_n\right\}\right)^{-1} :$$

in other words, two maps are “near” for the local distance d_{loc} if they coincide up to a great distance from the respective distinguished vertices.

A local distance can be defined on most all of the sets of pointed spaces we might want to work with: all that gets updated is the notion of a “ball” of radius r around the distinguished point and that of “equality” (being equality of maps, labelled maps, graphs etc. according to the situation).

Given a sequence of *random* pointed maps $(M_n)_{n \in \mathbb{N}}$ one may take, if it exists, its limit in distribution for the local distance d_{loc} ; such a limit M_∞ may be characterised as being a planar map such that the law of the random variable $[M_\infty]_r$, for each non-negative integer r , is itself the limit of the laws of the balls $[M_n]_r$, as n is sent to infinity. In other words, if one sits in the distinguished vertex of the limit map M_∞ and “looks around” within a finite range r , the random landscape is essentially the one they would come to expect after looking out from the distinguished vertex of M_n for an increasingly large n . By extension, we call M_∞ the local limit of the sequence $(M_n)_{n \in \mathbb{N}}$.

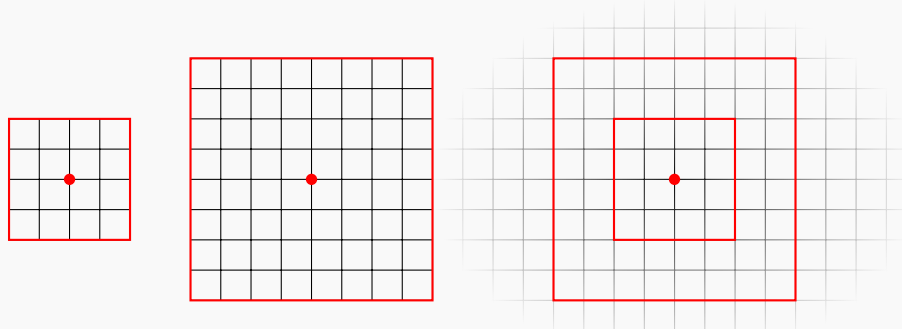
Usually we take n to be a measure of *size*: the local limit of a sequence of (random) pointed maps $(M_n)_{n \in \mathbb{N}}$ such that M_n has n edges (or vertices, or faces...), if such a limit exists, is always an infinite map: the following infobox gives a few relevant easy observations and examples, as well as references to the part of this thesis where we shall discuss local limits further.

Local limits

1.4

We give some very simple examples with which to test one's intuitive understanding of local limits.

- In order for a sequence of (deterministic) finite pointed maps to converge it is necessary (though of course not sufficient) for the degree of the distinguished vertex to be eventually constant: the distance between two maps whose distinguished vertex has different degree is always equal to 1.
- Consider the planar map given by a $2n + 1 \times 2n + 1$ grid, pointed at the vertex $(n + 1, n + 1)$; the local limit of the sequence of such maps, when n is sent to infinity, is clearly the map given by \mathbb{Z}^2 (embedded as a grid), pointed in one of its vertices, since the balls of radius r in \mathbb{Z}^2 are the same as those in all large enough finite grids.



- Consider now this very simple sequence of random pointed maps: P_n is a path of length n , pointed in a vertex chosen uniformly at random among the $n + 1$ vertices of the path. The local limit P_∞ of the sequence is almost surely “constant”, and may be built as a doubly infinite path, its vertices indexed by \mathbb{Z} , pointed in vertex 0. Indeed, the probability that $[P_n]_r$ is the same as $[P_\infty]_r$, which is a path of length $2r$, pointed in its “central” vertex, is (as long as $n > 2r$) the probability that the distinguished point in the random pointed map P_n is at distance at least r from either end of the path, that is to say $(n + 1 - 2r)/(n + 1)$, which tends to 1 when n is sent to infinity.
- We shall later examine the local limit of the sequence of uniform random plane trees, that is the *geometric Galton–Watson tree conditioned to survive* (Section 2.5) and the local limit of uniform quadrangulations, called the *uniform infinite quadrangulation of the plane* (Section 3.5), as well as the local limit of uniform quadrangulations with a boundary.

↩ Previous infobox: 1.3

This is the last infobox in the chapter

Chapter 2

Trees

2.1 Rooted plane trees

Definition 2.1.1. A *rooted plane tree* (from now on referred to as simply a *tree* or a *plane tree*) is a rooted planar map with a single face. The *size* of a plane tree τ , denoted $|\tau|$, is the number of its edges. The tail of the root edge of τ is named the *root vertex* of τ .

Notice that the above definition agrees with the traditional ‘graph-theoretic’ one, in the sense that a plane tree, when seen as a graph, is indeed connected and devoid of any cycles. Also notice that, according to our definition of a “planar map” (see Definition 1.1.1), we can have both finite and infinite plane trees, where infinite trees are required to be locally finite; we shall call T_n the set of all plane trees of size n .

The information that the embedding and distinguished oriented edge (or, equivalently, distinguished corner – see Figure I.1) add to the abstract graph amounts to a genealogical structure induced on vertices, where each generation is naturally ordered. In fact, given a plane tree τ , one can build a partition $(A_i)_{i \in \mathbb{N}}$ of its vertices according to their graph distance from the root vertex ρ of τ (so that $A_0 = \{\rho\}$, A_1 is the set of neigh-

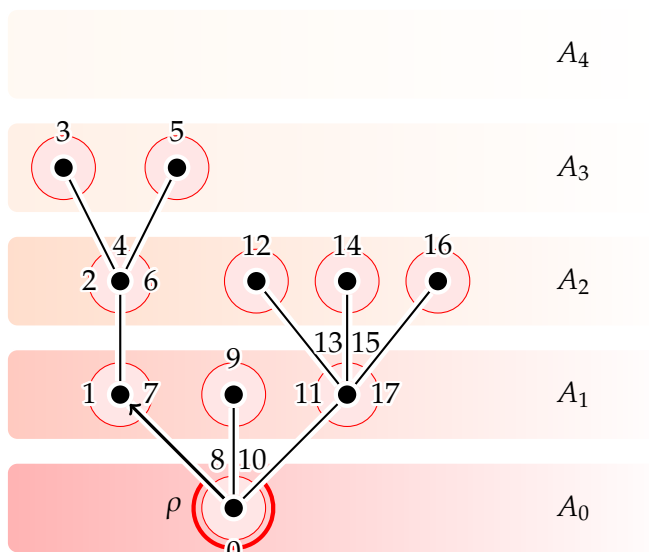


Figure I.1: A **plane tree** of size 9 and height 3, whose 18 corners are labelled according to their order in the (counterclockwise) contour of its face; the tree is rooted in the marked oriented edge, or equivalently has the corner labelled 0 as a distinguished corner.

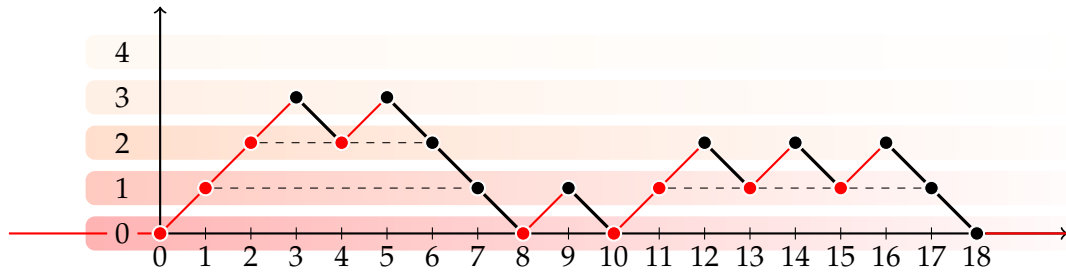
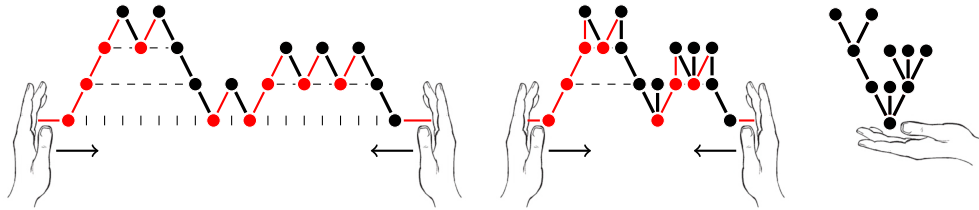


Figure I.2: Here is the (extended) contour function for the tree from Figure I.1; the dashed lines represent the equivalence classes of corners adjacent to a single vertex; notice that we can interpret ‘down-steps’ of the contour function as edges of the tree joining equivalence classes of corners.



bours of ρ , and in general A_{i+1} is the set of neighbours of vertices in A_i that do not belong to A_{i-1}). For a vertex u of τ we say it has height i , and write $|u| = i$, if it belongs to A_i . Notice that there is a natural map $p : A_{i+1} \rightarrow A_i$ sending each vertex u in A_{i+1} to its unique neighbour in A_i , named the *parent* of u . Furthermore, we call vertices in the set $p^{-1}(u)$ *children* of u , and write $k(u)$ for the number of children that u possesses (thanks to the requirement of local finiteness, $k(u)$ is always finite even for infinite trees); vertices with no children are called *leaves*.

From here onwards, we shall suppose our plane trees are *finite*, so that we can take the contour of their unique face; infinite plane trees will have a role to play in later sections (see Section 2.5), but shall not be mentioned again until then. Notice that the counterclockwise contour of the single face of a plane tree τ , started at the distinguished corner (from now on dubbed *the contour of τ* for simplicity), induces an order on corners and a partial order on vertices of τ : we say that a vertex u lies *strictly to the left* of a vertex v if the latest occurrence of a corner adjacent to u in the contour happens before the earliest occurrence of a corner adjacent to v ; if the reverse holds, we say that u lies *strictly to the right* of v . In both cases, vertices u and v are said to be *unrelated*: neither is an ancestor of the other (i.e. neither can be obtained from the other by iterating the parent function). The abstract graph structure, the root vertex and the left-to-right order on pairs of unrelated vertices are enough to determine τ as a plane tree.

A simple way to encode a tree using its contour is the so-called *contour function*. Given a plane tree τ , consider the function $C_\tau : \{0, 1, \dots, 2|\tau|\} \rightarrow \mathbb{N}$ that maps i to the height of the vertex adjacent to the i -th corner in the contour of τ (where the distinguished corner corresponds to $C_\tau(0)$, hence also to $C_\tau(2|\tau|)$: since τ has $|\tau|$ edges, and each edge

– depending on its orientation – can represent 2 distinct corners, τ has exactly $2|\tau|$ corners); naturally, since the distinguished corner is adjacent to the root vertex, we have $C_\tau(0) = C_\tau(2|\tau|) = 0$. Also $|C_\tau(i) - C_\tau(i-1)| = 1$ for all $i = 1, \dots, 2|\tau|$. In other words, C_τ is a so-called *Dyck path* of length $2|\tau|$: a sequence of $2|\tau| + 1$ non-negative integers, starting and ending with 0, and proceeding by steps of ± 1 .

It is not hard to recover τ from C_τ : corners of τ correspond to integers between 1 and $2|\tau|$, in the order induced by the contour (where $2|\tau|$ corresponds to the distinguished corner of τ). Two corners i and j (where we suppose $i < j$) are adjacent to the same vertex if $C_\tau(i) = C_\tau(j)$ and $C_\tau(k) \geq C_\tau(i)$ for all k between i and j . Via C_τ , it is thus very natural to see vertices of τ as equivalence classes of corners; genealogical relationships are easily recovered in this framework: for any pair of vertices u, v , we have $v = p(u)$ in τ if $i \in u$, $i+1 \in v$ and $C_\tau(i) - C_\tau(i+1) = 1$ for some corner i . The partial order on vertices is induced by C_τ exactly as described before: we have $u < v$ (u lies to the left of v) if $i < j$ for all corners $i \in u$ and $j \in v$.

Notice that there is a convenient way to write the equivalence relation grouping together corners adjacent to the same vertex; the condition described above is equivalent to

$$i \sim j \quad \text{if} \quad C_\tau(i) + C_\tau(j) - 2 \min_{i \wedge j \leq k \leq i \vee j} C_\tau(k) = 0, \quad (\text{I.1})$$

which is an expression we shall find useful later.

One may in fact go a step further and show (see Figure I.2) that the correspondence between each tree τ and its contour function C_τ is a bijection between the set \mathbb{T}_n of all plane trees of size n and the set of all Dyck paths of length $2n$. In particular, this is one of many elementary ways to obtain the following classical enumerative result:

Enumeration result I.1. *There are exactly $\text{Cat}(n) = \frac{1}{n+1} \binom{2n}{n}$ plane trees of size n (i.e. with exactly n edges).*

2.2 Real trees

Take now a finite plane tree τ with its contour function $C_\tau : \{0, \dots, 2|\tau|\} \rightarrow \mathbb{N}$. Note that we may extend the map C_τ so that it becomes a function sending real numbers to real numbers, by defining $C_\tau(t)$ to be 0 whenever $t \notin (0, 2|\tau|)$, and making C_τ linear on intervals of the type $[i, i+1]$, for $i \in \mathbb{Z}$. The result is the continuous function depicted in Figure I.2.

We may also extend the equivalence relation (I.1) to all of \mathbb{R} by simply prescribing that, for each pair $s, t \in \mathbb{R}$,

$$s \sim t \quad \text{if} \quad d_{C_\tau}(s, t) := C_\tau(t) + C_\tau(s) - 2 \min_{s \wedge t \leq x \leq s \vee t} C_\tau(x) = 0. \quad (\text{I.2})$$

It is not hard to see that the map $d_{C_\tau} : \mathbb{R}^2 \rightarrow \mathbb{R}$, as we have just defined it, is a pseudodistance on \mathbb{R} (all that is needed to show this is some casework for the relative position of points in the triple for which one wishes to check the triangle inequality). Hence we can consider the metric space obtained by taking the quotient of (\mathbb{R}, d_{C_τ}) by

*Notation on real trees***2.1**

Informally, a real tree could be seen as a disjoint union of line segments, some of whose endpoints are pairwise identified, all in such a way that no loops get created. What the two parts of the definition make sure of is that there is a unique geodesic path between any two points, which is also the only available (simple) path up to reparameterisation. Notice that both parts of the definition are important to identify a class of objects that will look like trees: the second part excludes the presence of cycles while the first one enforces path-connectedness.

Many essential elements and features of plane trees can be redefined for real trees: given a (rooted) real tree (\mathcal{T}, d) the *degree* of a point x is the number of connected components of $\mathcal{T} \setminus \{x\}$; we call x a *branching point* if $\mathcal{T} \setminus \{x\}$ has at least 3 connected components, and we say x is a *leaf* if $\mathcal{T} \setminus \{x\}$ is connected. Naturally, a point x in a real tree does not necessarily have finite degree (no more local finiteness!).

We can also recognise, in some sense at least, a genealogical structure: given two points $x, y \in \mathcal{T}$, consider the two sets $\varphi_{\rho,x}([0, |x|])$ and $\varphi_{\rho,y}([0, |y|])$, ρ being the root of (\mathcal{T}, d) and $|\cdot|$ representing, by analogy with plane trees, the distance $d(\rho, \cdot)$ (also called *height*); then there is a unique $z \in \mathcal{T}$ such that the intersection of the two sets is of the form $\varphi_{\rho,z}([0, |z|])$. We call z the *least common ancestor* of x and y . If $z = x$, then x is an *ancestor* of y .

Notice, however, that the “union of segments” imagery can only bring us so far: while perfectly adequate for the most “tame” examples, such as our $(\mathcal{T}_{C_\tau}, d_{C_\tau})$, the next box will show some of the complexity of real trees which sets them apart from plane trees. While the notion of “ancestors” can be mutated from plane trees, one cannot define anything like a parent function, not even on the set of branching points.

This is the first infobox in the chapter

Next infobox: 2.2 \leftrightarrow

the equivalence relation \sim , which we shall call $(\mathcal{T}_{C_\tau}, d_{C_\tau})$. This is a compact metric space which *could* be embedded in the plane (so that its own metric agrees with the induced intrinsic metric) in order to obtain the plane tree τ ; it is, however, missing information that is crucial to fully recover τ as a plane tree: while it’s mostly possible to tell whether a point in \mathcal{T}_{C_τ} represents a vertex of τ by the number of connected components of its complement (already vertices with just one child may represent a problem), and two vertices are neighbours if there’s a path in $(\mathcal{T}_{C_\tau}, d_{C_\tau})$ joining the two and not containing any other vertex, the left-to-right order on vertices is completely lost in passing to the quotient.

It does seem that the space $(\mathcal{T}_{C_\tau}, d_{C_\tau})$ should have the right to be called a tree; it falls, in fact, under the denomination of a *real tree*, according to the following definition:

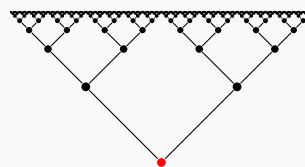
Definition 2.2.1. A (compact) *real tree* is a compact metric space (\mathcal{T}, d) such that for each pair of points $a, b \in \mathcal{T}$

Some facts about real trees

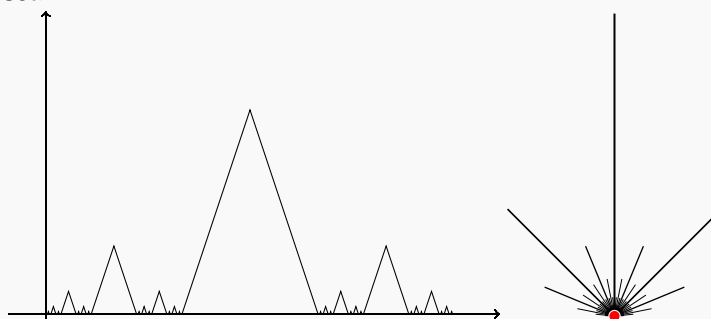
2.2

Here are some facts about real trees that may help get a better intuition of what a *general* specimen looks like.

- **The set of leaves in a real tree may be uncountable.** As an example, take a compact realisation of the infinite complete binary tree: build a metric space (\mathcal{T}, d) as the completion of the union of an increasing sequence of metric spaces (\mathcal{T}_n, d_n) , for $n \geq 0$, where $\mathcal{T}_0 = \{\rho\}$ and $(\mathcal{T}_{i+1}, d_{i+1})$ is built by attaching two branches of length 2^{-i-1} to each leaf of (\mathcal{T}_i, d_i) . The leaves of (\mathcal{T}, d) can be bijectively sent to the set of all infinite sequences of 0's and 1's, which in turn can be taken to represent real numbers between 0 and 1. Notice that the representation is not unique (the natural projection of (\mathcal{T}, d) onto the embedded tree in the picture is not injective!).



- **A vertex in a real tree may have infinite degree (but its complement has at most countably many connected components).** Given a point v of height h in real tree (\mathcal{T}_g, d_g) , consider the set $g^{-1}(h) \subset [0, 1]$, which contains the preimage of v ; $g^{-1}(h)$ may be uncountable, but it is closed by continuity of g , hence its complement is a countable union of (disjoint) intervals, and the set of such intervals can be sent surjectively to the set of connected components of $\mathcal{T}_g \setminus \{v\}$, which is thus finite or countable. For an example where $g^{-1}(0)$ is indeed uncountable, take $g(t)$, for $t \in [0, 1]$, to be the distance of t from the Cantor set.



- **The set of branching points in a real tree is countable.** This is not hard to show if one knows Proposition 2.2.1: take a real tree (\mathcal{T}_g, d_g) coded by a function $g \in C([0, 1], \mathbb{R}_{\geq 0})$ and let $I \subset [0, 1]$ be the set of all strict local minima of g . The set of branching points of (\mathcal{T}_g, d_g) is contained within the projection of I , and the set of possible values for their height is contained within $g(I)$. Since $g(I)$ is countable, if the set of branching points were uncountable, then there would be $h \in g(I)$ such that the set of branching points of height h in the tree is uncountable; this would imply that there is an uncountable set $I_h \subseteq g^{-1}(h) \cap I$ such that for any $a < b \in I_h$ there is $x \in (a, b)$ such that $g(x) < h$ (or a and b would be identified in the quotient). But I_h , being uncountable, must have an accumulation point which is itself an element of I_h , say a ; given any sequence $(b_n)_{n \geq 0}$ converging to a (suppose $b_n > a$) there is a sequence $(x_n)_{n \geq 0}$ such that $x_n \in (a, b_n)$ (hence $x_n \rightarrow a$) and $g(x_n) < h$. But this is a contradiction, because a cannot then be a local minimum.

- there is a unique isometry $\varphi_{a,b} : [0, d(a, b)] \rightarrow \mathcal{T}$ such that $\varphi_{a,b}(0) = a$ and $\varphi_{a,b}(d(a, b)) = b$;
- given any continuous injective map $f : [0, 1] \rightarrow \mathcal{T}$ such that $f(0) = a$ and $f(1) = b$, its image $f([0, 1])$ is exactly the image $\varphi_{a,b}([0, d(a, b)])$ of $\varphi_{a,b}$.

Though compactness is not essential, we shall only deal with compact real trees, so we follow Le Gall and Miermont [47] in including a requirement of compactness directly in the definition of a real tree; see Infobox 2.1 for more information and an attempt at some intuitive insight into the above definition. Notice that, in spite of this requirement, real trees may still be very complex objects: see Infobox 2.2 for a few facts about (locally) compact real trees.

The space $(\mathcal{T}_{C_\tau}, d_{C_\tau})$ is – indeed – a real tree, and the construction performed with the function C_τ can be generalised to one that yields a real tree from any continuous function $g : [0, 1] \rightarrow \mathbb{R}_{\geq 0}$ such that $g(0) = g(1) = 0$ (from now on we work with functions defined on the unit interval for convenience: notice that we would have obtained the same metric space $(\mathcal{T}_{C_\tau}, d_{C_\tau})$ if we had taken the quotient of $[0, 1]$, endowed with the pseudometric induced by $C_\tau(2|\tau|\cdot) : [0, 1] \rightarrow \mathbb{R}$, by the appropriate equivalence relation). One can say even more: real trees are *exactly* the metric spaces obtained by the process of ‘folding’ such continuous functions (see Figure I.3), as clarified by the following proposition:

Proposition 2.2.1 (Le Gall). *The set of compact real trees is exactly the set of metric spaces (\mathcal{T}_g, d_g) , where $g : [0, 1] \rightarrow \mathbb{R}_{\geq 0}$ is any continuous function such that $g(0) = g(1) = 0$ and (\mathcal{T}_g, d_g) is obtained by taking the quotient of $[0, 1]$ by the relation $s \sim t \Leftrightarrow d_g(s, t) = 0$, where*

$$d_g(s, t) = g(s) + g(t) - 2 \min_{s \wedge t \leq x \leq s \vee t} g(x),$$

and we also write d_g for the quotient metric obtained from the pseudodistance defined above.

In other words, (compact) real trees can be coded by real continuous functions on the unit interval.

Real trees are extremely well-suited to help formalising Gromov–Hausdorff convergence of plane trees as metric spaces. On the one hand, it’s quite clear that for a finite plane tree τ , the Gromov–Hausdorff distance between the metric space (τ, d_{gr}) and the real tree $(\mathcal{T}_{C_\tau}, d_{C_\tau})$ is easy to control (simply embedding one into the other in the natural way shows it is at most the “length of an edge”, that is to say 1). On the other hand, convergence of continuous functions for the uniform norm on $C([0, 1], \mathbb{R})$ implies convergence of the corresponding real trees, as expressed by the the following lemma:

Lemma 2.2.2. *Let f, g be two continuous functions from $[0, 1]$ to $\mathbb{R}_{\geq 0}$ such that $f(0) = g(0) = f(1) = g(1) = 0$; we have*

$$d_{\text{GH}}((\mathcal{T}_f, d_f), (\mathcal{T}_g, d_g)) \leq \sup_{t \in [0, 1]} |f(t) - g(t)|.$$

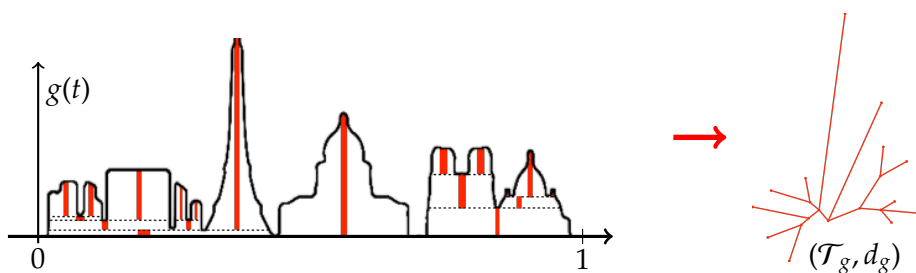


Figure I.3: The real tree (\mathcal{T}_g, d_g) coded by a continuous function $g : [0, 1] \rightarrow \mathbb{R}_{\geq 0}$.

We will thus be able to glean convergence results for sequences of random plane trees from the convergence (in law) of certain random real functions – in other words, convergence of stochastic processes – for which all the tools of stochastic analysis are at our disposal.

2.3 Galton–Watson trees

Now that most of the deterministic notation regarding trees is dealt with, the time has come to start introducing randomness to our setting.

Namely, *how should one define a random tree?* How do we apply the concepts from Chapter 1 to random trees – can we take scaling and local limits of random trees? What kind of objects do we obtain?

A reasonable starting point for an effort to tackle such questions is to simply take a *uniform* plane tree of size n (i.e. with n edges), which we shall call θ_n , and compute the scaling and/or local limit, as defined in Sections 1.2 and 1.3, of the sequence $(\theta_n)_{n \geq 0}$. Notice, however, that a uniform random plane tree is not the only reasonable model for a plane tree of size n : one might want to consider models with restrictions on the degree of vertices (binary trees, for example), or abstract trees that have not been embedded in the plane and are considered distinct only up to graph isomorphisms, or various classes of labelled trees (such as Cayley trees).

We shall soon come back to the idea of uniform plane trees, but we shall first introduce a more general notion of a random plane tree, which was known and employed since the 19th century: Galton–Watson trees were first introduced in order to investigate the probability of extinction for the names of noble families; though the model proves way too simplistic to give any reliable insight into onomastics, it has since found a plethora of applications in pure and applied mathematics, as well as physics and biology.

Let μ be a probability measure on \mathbb{N} such that $\mu(0) > 0$ and that

$$\sum_{n>0} n\mu(n) \leq 1; \tag{I.3}$$

consider the measure \mathbb{GW}_μ on the set \mathbb{T} of all plane trees defined so that, if τ is finite,

$$\mathbb{GW}_\mu(\{\tau\}) = \prod_{u \in \tau} \mu(k(u))$$

and $\mathbb{GW}_\mu(\{\tau\}) = 0$ if τ is infinite. One can show that \mathbb{GW}_μ is a probability measure on \mathbb{T} (concentrated on the set of finite plane trees). We call a random variable θ taking values in \mathbb{T} and having law \mathbb{GW}_μ a Galton–Watson tree with offspring distribution μ .

Galton–Watson trees and uniform random trees 2.3

Here are some examples of offspring distributions μ such that conditioned versions of the Galton–Watson law \mathbb{GW}_μ are uniform on “interesting” classes of trees.

- If we set $\mu(0) = \mu(2) = \frac{1}{2}$, the probability measure $\mathbb{GW}_\mu(\cdot \mid |\cdot| = n)$ is uniform, for each $n \in \mathbb{N}$, on the set of *binary plane trees* of size n .
- More generally, setting $\mu(d) = \frac{1}{d}$ and $\mu(0) = \frac{d-1}{d}$ yields a measure $\mathbb{GW}_\mu(\cdot \mid |\cdot| = n)$ which is uniform on the set of all d -ary trees of size n , for each $n \in \mathbb{N}$.
- Consider the set \mathbb{C}_n of all Cayley trees of size n , that is the set of all ‘graph-theoretic’ trees (V, E) on the vertex set $V = \{1, \dots, n+1\}$ (notice they must *not* be taken up to graph isomorphisms, and instead the “labels” of the vertices matter: the trees $\mathbf{1-2-3}$ and $\mathbf{1-3-2}$ are distinct). Now take μ to be the Poisson law of parameter 1, and consider a random element of \mathbb{T}_n distributed according to $\mathbb{GW}_\mu(\cdot \mid |\cdot| = n)$; then taking its graph structure (forgetting the root and embedding) and selecting an assignment of the “names” $1, \dots, n+1$ to its vertices uniformly at random yields a uniformly random element of \mathbb{C}_n .
- As remarked upon outside this infobox, taking $\mu(i) = 2^{-i-1}$ for $i \in \mathbb{N}$ yields a law \mathbb{GW}_μ which gives the same weight to elements in \mathbb{T}_n .

↔ Previous infobox: 2.2

Next infobox: 2.4 ↔

Different offspring distributions give rise to different models for random trees, and one may take an interest in both critical (i.e. such that equality holds in (I.3)) and subcritical ones. Throughout this thesis, however, we shall generally deal with *critical geometric Galton–Watson trees*, that is to say Galton–Watson trees whose offspring distribution is specifically the geometric law ν (defined so that $\nu(n) = 2^{-n-1}$), which is clearly critical.

Geometric Galton–Watson trees lead us back to uniform plane trees: since $\mathbb{GW}_\nu(\{\tau\}) = 2^{-\sum_{u \in \tau} (k(u)+1)} = 2^{-2|\tau|-1}$ (notice this follows from an immediate double counting of the number of corners of τ), a geometric Galton–Watson tree θ conditioned on having size $|\theta| = n$ is actually distributed as θ_n , that is to say uniformly over all plane trees with exactly n edges.

Furthermore, the contour function $(C_\theta(i))_{0 \leq i \leq 2|\theta|}$ of a critical geometric Galton–Watson tree θ is nothing but an excursion of the simple symmetric random walk on \mathbb{Z} . By this we mean that the law of $(C_\theta(i))_{0 \leq i \leq 2|\theta|}$ is that of $(S(i))_{0 \leq i \leq l}$, where $(S(i))_{i \geq 0}$ is a random sequence of integers such that $S(0) = 0$ and the differences $S(i+1) - S(i)$ are distributed as independent Bernoulli random variables of parameter $1/2$, while $l = \inf\{i | S(i) = -1\} - 1$. Showing this fact is straightforward if one uses the fact that the correspondence $\tau \leftrightarrow C_\tau$ is a bijection between the set \mathbb{T}_n and the set of all Dyck paths of length $2n$ (see Section 2.1). For any fixed Dyck path C_τ of length $2|\tau|$ (representing a certain plane tree τ), the probability that $S(i) = C_\tau(i)$ for $i = 1, \dots, 2|\tau|$ and that $S(2|\tau| + 1) = -1$ is exactly $2^{-2|\tau|-1}$, which is also the probability that $\theta = \tau$, hence that $C_\theta = C_\tau$.

We refer to Infobox 2.3 for other examples of Galton–Watson trees and their conditioned versions.

2.4 The Brownian tree

The Brownian tree, or CRT (for *continuum random tree*), was introduced by Aldous in [3]; it is a random real tree – or rather a random variable taking values in the set \mathbb{K} (or \mathbb{K}^\bullet , if we see it as a rooted real tree) as defined in Section 1.2 – that arises as the scaling limit of uniform plane trees, seen as metric spaces in $(\mathbb{K}^\bullet, d_{\text{GH}})$ themselves (or, indeed, as the scaling limit of various different classes of random trees and random maps).

The CRT will play a major role in Part II of this work, which will be entirely devoted to showing that a certain class of planar maps (*outerplanar* maps) admits the CRT as a scaling limit. Although no real knowledge of the object itself is necessary to follow the proof, which essentially consists in showing that outerplanar maps admit *the same* scaling limit as uniform random plane trees, up to an explicitly determined (constant) scaling factor, we shall devote this section to a brief overview of basic results about the CRT. We will not, however, go into very much detail; many surveys and lecture notes devoted to this and broader topics already exist: we refer the reader to [42] for proofs of Theorem 2.4.1 and Corollary 2.4.2, as well as various generalisations.

It should already be quite clear from Sections 1.2, 2.2 and 2.3 how one might go about building a scaling limit for uniform random plane trees: we can switch from a uniform plane tree θ_n having size n to its (random) contour function C_{θ_n} , which is a uniform random Dyck path of length $2n$, and consider the limit in distribution of the extended version of C_{θ_n} , rescaled by an appropriate factor (which turns out to be \sqrt{n} , as per Infobox 1.1). If we were to find a limit for the sequence of contour functions (as random variables taking values in $(C([0, 1], \mathbb{R}), \|\cdot\|_\infty)$), we would then be able to use it as in Section 2.2 to build a random real tree, which would automatically be the scaling limit of uniform random plane trees by the argument sketched at the end of Section 2.2 (see Lemma 2.2.2 and the paragraph above).

The question therefore becomes essentially that of determining the limit of an excursion of the simple symmetric random walk, conditioned on having length $2n$, if one rescales time by n , space by \sqrt{n} , and sends n to infinity. A description of such a limit

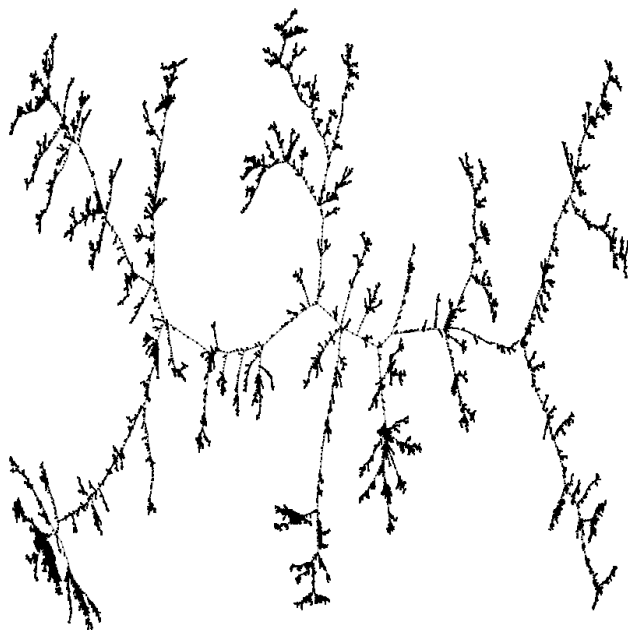


Figure I.4: Aldous' Brownian CRT.

requires some notation and a little background in stochastic analysis. Intuitively, since the scaling is exactly the one giving rise to Brownian motion from the simple symmetric random walk, one would expect to obtain an excursion of one-dimensional Brownian motion, conditioned on having length 1.

For anyone familiar with the definition of the Itô measure \mathbf{n} and its conditioned version, we set \mathbf{e}_t to be a normalised excursion of Brownian motion (hence a random continuous function from $[0, 1]$ to the non-negative real numbers, distributed according to the measure $\mathbf{n}_{(1)}$). Formal definitions of \mathbf{n} and the conditioned version $\mathbf{n}_{(1)}$ can be found in any number of places: see [57, Chapter VI] and [42]. We give a brief description of the normalised Brownian excursion in Infobox 2.4.

This being said, here is the result of convergence of contour functions to the normalised Brownian excursion, stated in a little more generality than we need for dealing with uniform plane trees (i.e. for general critical Galton–Watson trees rather than only geometric ones):

Theorem 2.4.1 (Aldous). *Let θ be a μ -Galton–Watson tree, where μ is a critical probability measure of finite variance σ^2 and let θ_n be the random plane tree θ , conditioned on having size n ; let C_{θ_n} be the (extended) contour function of θ_n (hence a random variable taking values in the*

The normalised Brownian excursion

2.4

Given one-dimensional Brownian motion $(\beta_t)_{t \geq 0}$, an *excursion* is a maximal open interval that β_t spends away from 0.

One quick way to introduce the *normalised Brownian excursion* $(\mathbf{e}_t)_{t \in [0,1]}$ is to consider the first excursion of β_t having length at least 1. Such an excursion does almost surely occur and is well-defined; suppose it is (a, b) , where a and b are random non-negative real numbers, and $\beta_a = \beta_b = 0$, while $|\beta_t| > 0$ for $t \in (a, b)$. We may define the normalised Brownian excursion as the process

$$\mathbf{e}_t = \frac{1}{\sqrt{b-a}} |\beta_{a+t(b-a)}|,$$

considered for $t \in [0, 1]$.

↔ **Previous infobox:** 2.3

Next infobox: 2.5 ↔

space $C^0(\mathbb{R}, \mathbb{R})$ of real continuous functions on \mathbb{R}). Then we have the convergence

$$\frac{\sigma}{2\sqrt{n}} C_{\theta_n}(2nt)|_{t \in [0,1]} \rightarrow \mathbf{e}_t,$$

in distribution, for the uniform norm on $C([0, 1], \mathbb{R})$.

From this, convergence of real trees follows:

Corollary 2.4.2. Consider a μ -Galton–Watson tree θ , where μ is critical of finite variance σ^2 , and take its conditioned version θ_n having size n . The random pointed compact metric space $(V(\theta_n), \frac{\sigma}{2\sqrt{n}} d_{gr})$ (with the root of θ_n being the distinguished vertex) seen as a random element of $(\mathbb{K}^\bullet, d_{GH})$, converges in distribution as $n \rightarrow \infty$ to the random rooted real tree (\mathcal{T}_e, d_e) (again, seen as a random variable taking values in $(\mathbb{K}^b_{ullet}, d_{GH})$, with the distinguished point in \mathcal{T}_e being the image of 0 via the natural projection from $[0, 1]$).

For a general idea of what the Brownian CRT looks like, see Figure I.4; the metric of this embedded realisation of the CRT is *not* entirely correct (concessions have been made by the visualisation algorithm in order to obtain an embedded version that is easier on the eye), but the object does give a strong impression of self-similarity, and many of its properties are indeed well depicted by the picture. We have compiled a small list of known properties of the CRT, which can be found within Infobox 2.5.

2.5 The critical Galton–Watson tree conditioned to survive

We now discuss a different kind of limit for uniformly random plane trees – their so-called *local limit*.

*Some properties of the CRT**2.5*

Here are some known facts about the CRT:

- the CRT has Hausdorff dimension 2 (almost surely);
- the CRT has a property of *universality* akin to that of Brownian motion: many classes of uniform random trees have been shown to converge to the CRT, including Cayley trees, unordered binary trees [50], unordered unrooted binary trees [60] and others; some classes of maps have also been shown to converge towards the CRT, for example random dissections [27], random outerplanar maps (Part II of this thesis) and variants thereof [56, 61].
- the CRT is almost surely a binary tree in the sense that all its branching points have degree 3;
- furthermore, the CRT has (almost surely) a unique topology; this can be seen as a consequence of the so-called “stick-breaking construction” of the CRT, see [3].

↔ **Previous infobox:** 2.4

This is the last infobox in the chapter

The general notion of local limit for a sequence of planar maps has been introduced in Section 1.3; in the case of plane trees, notation can be adapted a little to take into account the specific notions from Section 2.1. Given a plane tree τ (this time, suppose it can be finite or infinite) and a non-negative integer n , the ball $[\tau]_n$ around its root is obtained by erasing all generations A_i , with $i \geq n + 1$, and contains all vertices of the original tree τ having height at most n , each with the same parent as in τ , and the same left-to-right order with respect to unrelated vertices.

Given a *critical* offspring distribution μ , consider a Galton–Watson tree θ distributed according to GW_μ ; one can show that there is a probability measure $\widehat{\text{GW}}_\mu$ on the set of infinite plane trees such that, if T_∞ is a random infinite plane tree distributed according to $\widehat{\text{GW}}_\mu$, one has

$$[\theta \mid |\theta| = n]_m \xrightarrow{n \rightarrow \infty} [T_\infty]_m$$

in law, for all $m \geq 0$.

The random infinite tree T_∞ is called the *critical Galton–Watson tree conditioned to survive* with offspring distribution μ , sometimes referred to as Kesten’s tree due to its description in [34], and can in fact be generalised to the case of subcritical probability measures; see Abraham and Delmas [2] for a very complete account of local limits for Galton–Watson trees.

One can give a very explicit description of T_∞ (essentially as a multi-type Galton–Watson tree, a concept which we will introduce in Section 3.3); T_∞ may be generated as

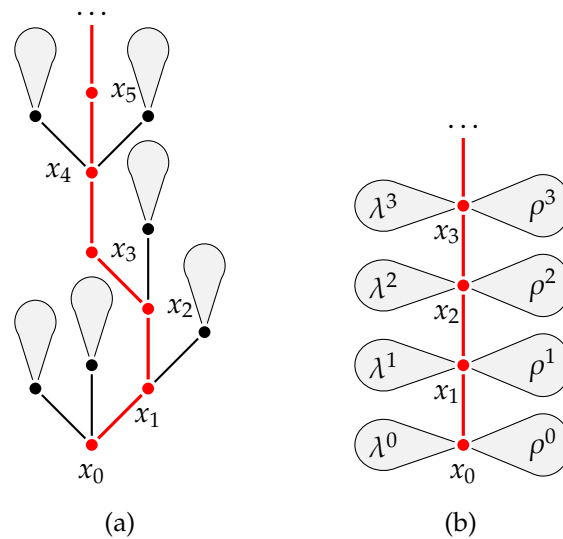


Figure I.5: The *geometric* critical Galton–Watson tree conditioned to survive, seen either as an enlarged spine to which Galton–Watson trees are attached (their roots being identified with each leaf) or a spine having geometric Galton–Watson trees on its left and right.

follows:

- start with the root, call it x_0 ;
- let x_0 have k children with probability $k\mu(k)$; notice that the latter is indeed a probability distribution by criticality of μ , and that (almost surely) the root will have at least one child;
- choose one of the children uniformly at random, and call it x_1 ;
- repeat the process above with x_1 : let the number of its children be independent from that of its siblings, and again distributed according to $k\mu(k)$; choose one at random and call it x_2 ;
- repeat the process indefinitely until you have a (random) infinite tree, which we will call the *enlarged spine* of T_∞ , made up of an infinite branch $S = \{x_0, x_1, \dots\}$, called the *spine*, and some vertices directly attached to elements of the spine;
- finally, for each vertex v in the enlarged spine which is not on the spine itself, determine its descendants by attaching a μ -Galton Watson tree to v by the root (so that v has offspring distribution μ , and so do its children); choose such a tree T^v independently from T^w for $v \neq w$.

The case we are most interested in is that of μ being the geometric distribution, because – the conditioned tree θ_n being a uniform plane tree of size n in that case – the

critical *geometric* Galton–Watson tree conditioned to survive is the local limit of uniform random plane trees.

In this specific case, as we shall see again in Section II.5, T_∞ admits an alternative description, and exhibits some especially nice properties.

Let R_i be the number of children of x_i that lie to the right of x_{i+1} ; clearly, for distinct i and j , R_i and R_j are independent. Computing the law of R_i is immediate and yields

$$\widehat{\text{GW}}(R_i = k) = 1 - \sum_{j=0}^{k-1} \mu(j).$$

It can now be observed that in the case where μ is the geometric offspring distribution ($\mu(k) = 2^{-k-1}$) we witness peculiar behaviour, since

$$\widehat{\text{GW}}(R_i = k) = 1 - \sum_{j=0}^{k-1} \mu(j) = 1 - \sum_{j=0}^{k-1} 2^{-j-1} = 2^{-k-1} = \mu(k).$$

Therefore the local limit T_∞ of uniform random plane trees can also be described as an infinite spine x_0, x_1, \dots , to which independent (finite) random plane trees (in particular, geometric Galton Watson trees) are attached, to the left and to the right, at each level (see Figure I.5). We shall use this description in Section II.5 to prove a lemma that will be useful throughout Part II of this thesis.

Chapter 3

Quadrangulations

3.1 Rooted quadrangulations of the sphere

Definition 3.1.1. A *quadrangulation* is a planar map all of whose faces have degree 4.

Notice that, thanks to Definition 1.1.1, we see a quadrangulation as automatically planar and locally finite; we call \mathcal{Q} the set of all *rooted* quadrangulations and \mathcal{Q}_n the set of all rooted quadrangulation of *area* n , where by area we mean the number of faces. Notice that the number of edges and vertices can both be recovered in terms of the area: since each face has exactly 4 oriented edges, and each edge has 2 possible orientations, Euler's formula for a quadrangulation q reads as

$$\#V(q) - \#E(q) + \text{Area}(q) = \#V(q) - \text{Area}(q) = 2,$$

hence:

$$\text{Area}(q) = n \quad \Rightarrow \quad \#E(q) = 2n; \quad \#V(q) = n + 2.$$

Quadrangulations occupy a privileged position as an emblematic class of planar maps for a number of reasons, one of which is the fact that there is a bijection between the set \mathcal{Q}_n of all rooted quadrangulation having area n and the set of all planar maps with n edges, hence the problem of enumerating general planar maps can be reduced to that of enumerating quadrangulations. This "trivial" bijection is due to Tutte [63] (see Figure I.1): it suffices to draw a vertex within each face of a general planar map, draw edges joining each "new" vertex to the corners of the face it occupies and erase all original edges to obtain a quadrangulation, which can be rooted in the edge newly drawn to join a "face-vertex" to the corner identified by the original root of the map, oriented away from the latter.

The inverse of such a correspondence is also easily described: given a rooted quadrangulation, considering the parity of the distance of vertices from the tail of the root edge is enough to determine whether or not they were part of the original planar map: draw an edge within each face, joining the two corners in the face that are adjacent to vertices having even distance from the root vertex (since a quadrangulation is *bipartite*, there are exactly two), and erase all vertices having odd distance from the root vertex

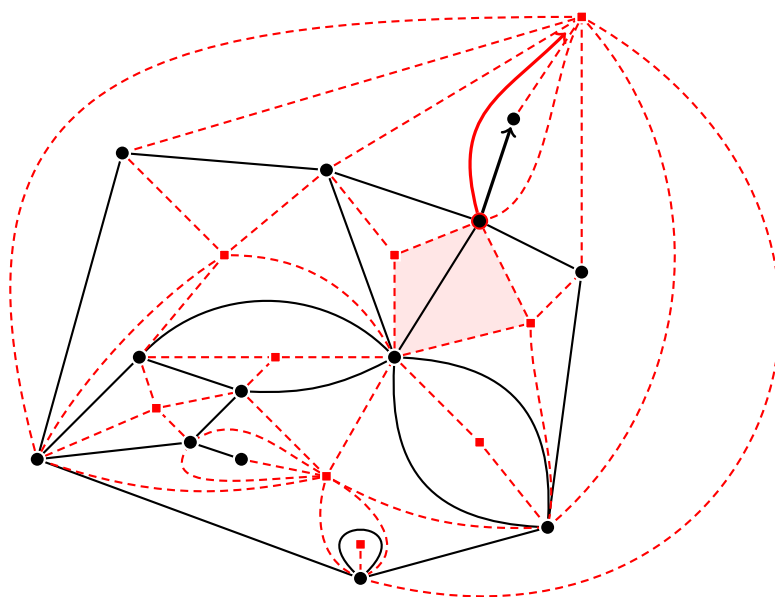


Figure I.1: Given a rooted planar map (black vertices and edges in the picture), the corresponding quadrangulation (red and black vertices, red dashed edges) has one face for each edge of the original map (look for example to the shaded red face, which encloses the single black edge joining its two black vertices). The map is recovered from the quadrangulation by drawing the edge in each face, which joins the two corners adjacent to black vertices.

(together with all original edges); the map thus obtained is then rooted in the edge drawn within the face adjacent to (the right of) the root edge of the quadrangulation, oriented away from the root vertex.

We mention this “trivial” bijection not because it will be used as a tool in further sections, but because it already contains some of the usual ingredients of more elaborate bijections that will be employed throughout this thesis. Namely, the construction of a new map from a quadrangulation can take advantage of the fact that a quadrangulation is automatically *bipartite* (its vertices can be partitioned into two sets so that two vertices cannot be neighbours if they fall into the same set; equivalently, the graph distance to the root vertex of two neighbours cannot be the same), as is the case with all planar maps all of whose faces have even degree.

We shall see in Section 3.2 how a construction not entirely dissimilar to that of the “trivial bijection” establishes precious links between quadrangulations – or, indeed, general bipartite planar maps – and decorated plane trees or forests of plane trees.

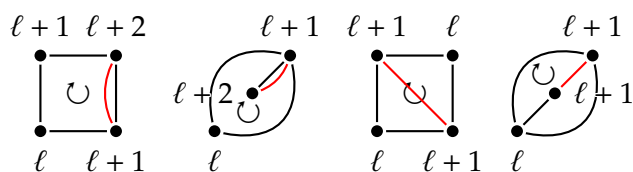


Figure I.2: The four (more like two!) types of faces one can encounter in a quadrangulation, their two down-step corners joined by a red edge; the first and second examples, and the third and fourth, have exactly the same sequence of corner labels, but all four drawings have been included to completely clarify what happens in case of a double edge.

3.2 There and back again: some bijections for bipartite maps

Part III of this thesis will rely on variants of a bijection by Bouttier, Di Francesco and Guitter [16] which generalises Schaeffer’s bijection between (rooted) planar maps and a specific class of labelled plane trees to the set of all *bipartite* planar maps. Though material about such bijections already exists, we set this section aside for an organic presentation of the different variants of such correspondences, in the hope that their juxtaposition may help the reader understand how they relate to one another. We shall not delve into the details of proofs – for which we refer the reader to the original papers [25, 58, 16, 17] in which the bijections in question were presented – but we will try nonetheless to give an idea of how and why the constructions do work as claimed.

3.2.1 The “positive” Schaeffer bijection

Definition 3.2.1. A *labelled tree* is a pair (τ, l) , where τ is a plane tree and l is an integer-valued labelling on the set of its vertices, such that, if u and v are neighbours in τ , then $|l(u) - l(v)| \leq 1$ (in other words, children of a vertex labelled n are labelled either $n + 1, n - 1$ or n themselves). A labelled tree is *positive* if its labelling l only takes strictly positive values.

Throughout this work we shall call LT the set of *finite* labelled trees and LT_k – for $k \in \mathbb{Z}$ – the set of labelled trees in LT whose root is labelled k . Similarly, we call LT^+ the subset of LT containing all (finite) *positive* labelled trees, and we define LT_k^+ , for $k > 0$, as the set of all finite positive labelled trees whose root is labelled k .

We shall soon see how the set LT has some nice properties (the set of labelled trees of size n in LT_k is very easy to enumerate!); though the class of *positive* labelled trees is a little less straightforward to deal with, we start by discussing Schaeffer’s original construction, which builds a positive labelled tree out of a rooted quadrangulation. Namely, we have the following:

Theorem 3.2.1 (Schaeffer⁺). *There is a bijection between the set \mathcal{Q}_n of all (rooted) quadrangulations having area n and the set $\{\tau \in \text{LT}_1^+ \mid |\tau| = n\}$.*

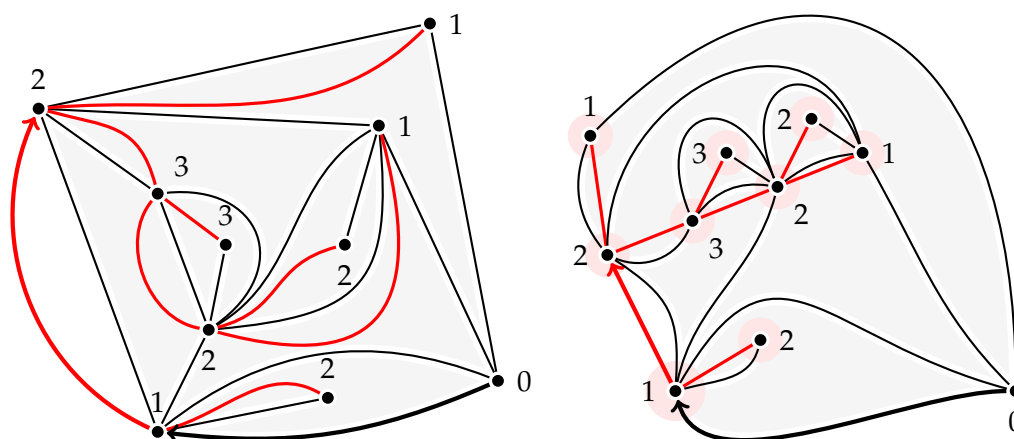
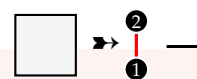


Figure I.3: The positive Schaeffer construction.

Given a quadrangulation $q \in \mathcal{Q}_n$, perform the following construction:

Quadrangulation to positive labelled tree: $q \rightarrow (\tau, l)$



- label all vertices in q with their graph distance to the root vertex; for each face of q , read the labels of the vertices adjacent to its four corners cyclically according to a *clockwise* contour. Given two successive corners c_i and c_{i+1} in a clockwise contour of a face f , we say c_i is a down-step corner of f if the label of c_{i+1} is strictly smaller than that of c_i (notice that, since the map is bipartite, the label of c_{i+1} is either one more or one less than that of c_i , hence each face has exactly 2 down-step corners);
- draw a new edge within each face of q , joining its two down-step corners (see Figure I.2);
- consider the corner corresponding to the root edge of q , which belongs to the face f lying *left* of the root edge itself (which is the unbounded face in Figure I.3), and is labelled 0; the next corner counterclockwise within f – call it c – is adjacent to the arrow of the root edge of q : it must be labelled 1 and be a down-step corner in f ; select as new root the edge joining c to the other down-step corner of f , oriented away from c ;
- erase all original edges and the original root vertex of the map (from which we have issued no new edge, since its label is strictly minimal, so none of the corners adjacent to it can be a down-step).

The rooted map (a priori *union* of maps, since connectedness is not clear) thus

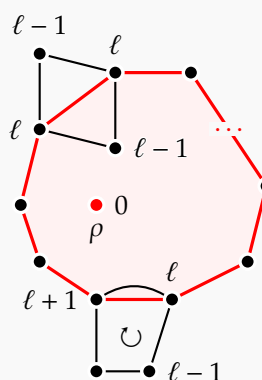
obtained is a plane tree: it has n edges, where n is the area of q , since a new edge is drawn for each face of q , and $n + 1$ vertices (q had $n + 2$ vertices, and the root vertex of q is the only one to be erased); it is enough to show that the graph is acyclic (see Infobox 3.1 for a sketched proof) to obtain that the result of the construction is indeed a plane tree.

Moreover, the root of the tree is labelled 1 by construction, and any two neighbouring vertices are down-steps of the same face, hence their labels differ by 0, 1, or -1 (see Figure I.2) as per our definition of a labelled plane tree.

It's a tree!

3.1

Consider the map obtained *before* rerooting and erasing all original edges of the quadrangulation q : for convenience we will call its edges “black” and “red”, according to whether they are original edges of q or newly drawn ones. Providing we have not crossed any black edges when drawing the red ones, which is clearly doable (see Figure I.2) this is a (rooted) planar map which we call m , whose vertices are labelled and whose edges are of two types (“black” and “red”); we wish to show that the *graph* of red edges is acyclic. Indeed, suppose it has a cycle: taking the complement of its embedded image yields two distinct connected components of the sphere (or the plane, if that is where the embedding takes place; regardless, we call the two parts the “inside” and “outside” of the cycle). Suppose the root vertex ρ of q (labelled 0) is within the *inside* of the red cycle and let ℓ be the minimum label appearing on vertices of the cycle; notice that any path of q joining ρ to a vertex outside the cycle must pass through a vertex of the cycle, which implies that all vertices outside are at distance at least ℓ from the root vertex. This, however, is a contradiction: if all vertices of the cycle are labelled ℓ (or indeed if there are two consecutive vertices labelled ℓ , see the figure above) then there is a vertex labelled $\ell - 1$ outside the cycle; if this is not the case, then reading labels *clockwise* around the cycle yields an ℓ followed by an $\ell + 1$, which again implies the existence of a label $\ell - 1$ outside the cycle (see also Figure I.2).



This is the first infobox in the chapter

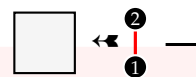
Next infobox: 3.2 \leftrightarrow

The inverse construction – starting with a labelled tree (τ, l) in LT_1^+ such that $|\tau| = n$ to obtain a rooted quadrangulation – is fairly simple and generalises readily to the more general constructions we shall later describe. The proof that the two constructions are each other’s inverses involves a fair amount of work, for which this is not the most suitable of places – the interested reader may refer to [58] (or [16]) directly for full proofs. A less meticulous reader should find Figure I.3 convincing enough: compare the quadrangulation-to-tree construction and the tree-to-quadrangulation construction;

it is not hard to see that the two quadrangulations are indeed the same.

Here is the way to re-obtain a quadrangulation from a tree $(\tau, l) \in \text{LT}_1^+$:

Positive labelled tree to quadrangulation: $(\tau, l) \rightarrow q$



- ◀ consider the counterclockwise contour $(c_i)_{i=0}^{2n-1}$ of the face of τ , started at the distinguished corner, to be read cyclically (so that, for $k \in \mathbb{Z}$, we have $c_k = c_{k \pmod{2n}}$);
- ◀ for each corner c_i labelled at least 2, set $k = \min \{j > 0 \mid l(c_{i+j}) = l(c_i) - 1\}$; join c_i to c_{i+k} , usually called the *successor* of c_i , with an edge (so that edges being drawn do not cross: see Figure I.3);
- ◀ draw a new vertex δ in the unbounded face and join each corner labelled 1 to it with a new edge;
- ◀ root the map thus obtained in the edge joining the root of τ to δ , oriented away from δ (again, so as not to cross any previously drawn edges);
- ◀ erase all edges of τ and forget all labels.

Remark 3.2.1. Notice that the construction described above does something more than pairing a quadrangulation with a labelled tree and vice-versa; there is a natural identification between the set $V(q) \setminus \{\rho\}$, where ρ is the root vertex of the quadrangulation $q \in \mathbf{Q}_n$, and the vertices in the corresponding labelled tree (τ, l) . We will make this identification implicitly in all that follows; furthermore, for each $u \in V(\tau)$ we have by construction $d_{\text{gr}}(u, \rho) = l(u)$, where by d_{gr} we mean the graph distance in the quadrangulation q .

3.2.2 The “unconstrained” Schaeffer bijection

The main advantage of the previously described bijection is that a fair amount of interesting geometrical information about a rooted quadrangulation is very easily accessible from its corresponding labelled tree; since labels originally represented distances from the root vertex, they bear very strong geometrical significance.

A bijection with a set of “unconstrained” labelled trees of fixed size and fixed root label, however, would certainly have advantages as well. We have defined a labelled tree as a pair (τ, l) , where l is a labelling of vertices, but we can equivalently see (τ, l) as a triple (τ, k, s) , where k is an integer and s is a labelling of τ 's edges, taking values in $\{0, 1, -1\}$: we just define k to be $l(\rho)$, where ρ is the root of τ , and set $s(\{u, p(u)\}) = l(u) - l(p(u))$ ($\{u, p(u)\}$ being the edge that joins a vertex u to its parent $p(u)$).

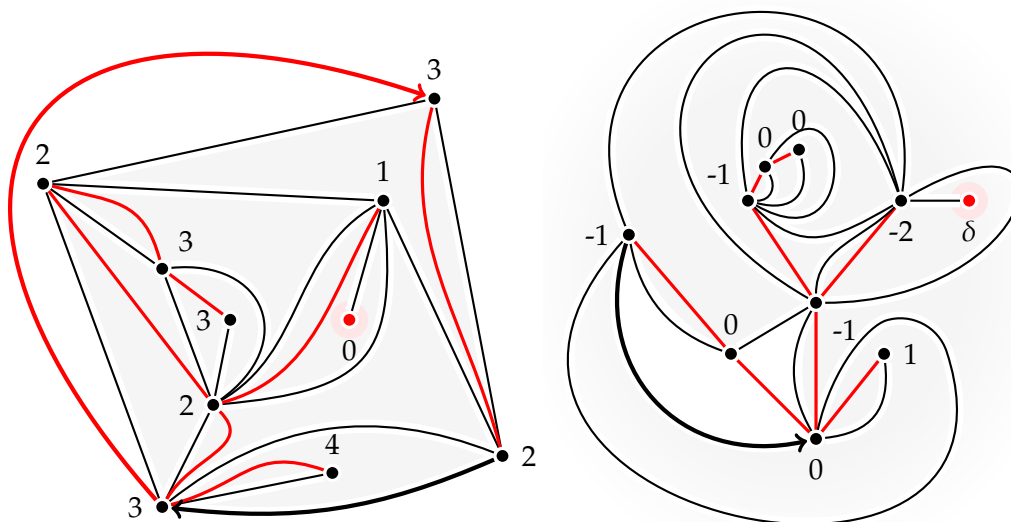


Figure I.4: The unconstrained Schaeffer bijection. The two quadrangulations are the same, although the unbounded face in the embedding on the left corresponds to the white inner face on the right.

This alternative definition of labelled trees via edge labellings makes them easy to enumerate: choosing a labelled tree of size n and root label k amounts to choosing a plane tree of size n and selecting an element of $\{0, 1, -1\}$ for each of its edges, so that

Enumeration result I.2. *The number of labelled trees in LT_k having size n is*

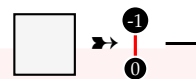
$$3^n \#T_n = 3^n \text{Cat}(n).$$

This being said, the relevance of the following result should be clear:

Theorem 3.2.2 (Schaeffer $^\pm$). *There is a bijection between the set \mathbf{Q}_n^\bullet of all pointed (rooted) quadrangulations having area n – that is $\mathbf{Q}_n^\bullet = \{(q, v) \mid q \in \mathbf{Q}_n, v \in V(q)\}$ – and the set*

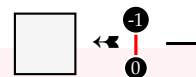
$$\{((\tau, l), \varepsilon) \mid (\tau, l) \in \text{LT}_0, |\tau| = n, \varepsilon = \pm 1\}.$$

The construction is not at all dissimilar to the “positive” one; given a quadrangulation $q \in \mathbf{Q}_n$, pointed in a vertex δ , perform the following steps:

Quadrangulation to labelled tree: $(q, \delta) \rightarrow ((\tau, l), \varepsilon)$


- label all vertices in q with their graph distance to the distinguished vertex δ ;
- draw a new edge within each face of q , joining its two down-step corners (as defined in Section 3.2.1);
- consider the root edge (e_-, e_+) of q , and let f_l and f_r be the faces lying *left* and *right* of (e_-, e_+) respectively (of course, the two may coincide); if $l(e_-) < l(e_+)$, set $\varepsilon = 1$ and choose as new root the edge being drawn between a corner adjacent to e_+ and the other down-step corner of f_l , oriented away from e_+ ; if $l(e_-) > l(e_+)$, set $\varepsilon = -1$ and root in the edge drawn between a corner of e_- and a down-step corner of f_r ;
- subtract $d_{\text{gr}}(e_-, \delta)$ (if $\varepsilon = -1$) or $d_{\text{gr}}(e_+, \delta)$ (if $\varepsilon = 1$) to all labels (where d_{gr} is intended as the graph distance in q); this way the label of the new root is 0;
- erase all original edges and the distinguished vertex δ .

It should not be hard to tell that restricting the above construction to quadrangulations pointed in the root vertex yields the construction from Section 3.2.1 (with ε always being set to 1). The converse construction is equally similar to the one we already described, with a little adjustment in order to root the quadrangulation correctly.

Labelled tree to quadrangulation: $((\tau, l), \varepsilon) \rightarrow (q, \delta)$


- ⚡ consider the counterclockwise (cyclic) contour $(c_i)_{i=0}^{2n-1}$ of the face of τ , started at the distinguished corner, and let ℓ be the minimal label appearing on vertices of τ ;
- ⚡ for each corner c_i labelled at least $\ell+1$, set $k = \min \{j > 0 \mid l(c_{i+j}) = l(c_i) - 1\}$; join c_i to c_{i+k} with an edge (so that edges being drawn do not cross, see Figure I.4);
- ⚡ draw a new vertex δ in the within the unbounded face of the tree and join each corner labelled ℓ to δ with a new edge (again, so as not to cross any previously drawn edges);
- ⚡ root the map thus obtained in the newly drawn edge issued from the distinguished corner of τ , oriented away from the root of τ if $\varepsilon = -1$, towards it if

$\varepsilon = 1$; make δ the distinguished vertex;
 ← erase all edges of τ and forget all labels.

Remark 3.2.2. The identification of $V(q) \setminus \{\delta\}$ with the set $V(\tau)$ (the pair (τ, l) being the labelled tree which corresponds to the pointed quadrangulation (q, δ)) is of course still possible; this time, we have $l(u) = d_{\text{gr}}(u, \delta) - d_{\text{gr}}(\rho, \delta)$ for every $u \in V(\tau)$, where d_{gr} is the graph distance in q and ρ is the root vertex of q .

3.2.3 A general bijection for bipartite maps

The more general bijection we now describe is due to Bouttier, Di Francesco and Guittier [16], and provides the basis for our discussion of the UIHPQ in Part III of this thesis.

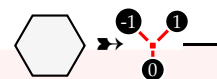
Definition 3.2.2. A *mobile* (τ, l) is given by a plane tree τ whose vertices are of two types – *labelled* and *unlabelled* – and an integer-valued labelling l on the labelled vertices of τ , such that the following hold:

- (i) if two vertices of τ are neighbours, then one is labelled, the other unlabelled;
- (ii) the root of the plane tree (also considered to be the root of the mobile) is labelled 0;
- (iii) if you pick an unlabelled vertex and read the sequence of labels of its neighbours cyclically proceeding around it clockwise, each successive label is at least the previous one minus 1 (that is, labels read around an unlabelled vertex clockwise may increase by any amount at each step, but not decrease by more than 1).

We call *size* of a mobile the number of unlabelled vertices it possesses.

Theorem 3.2.3 (BDFG). There is a bijection between the set BM_n^\bullet of all pointed (rooted) bipartite maps having area n and the set of pairs $((\tau, l), \varepsilon)$, where $\varepsilon = \pm 1$ and (τ, l) is a mobile of size n .

Map to Mobile



- ➔ label all vertices of m with their graph distance from the distinguished vertex δ ;
- ➔ draw an unlabelled vertex within each face of m ;

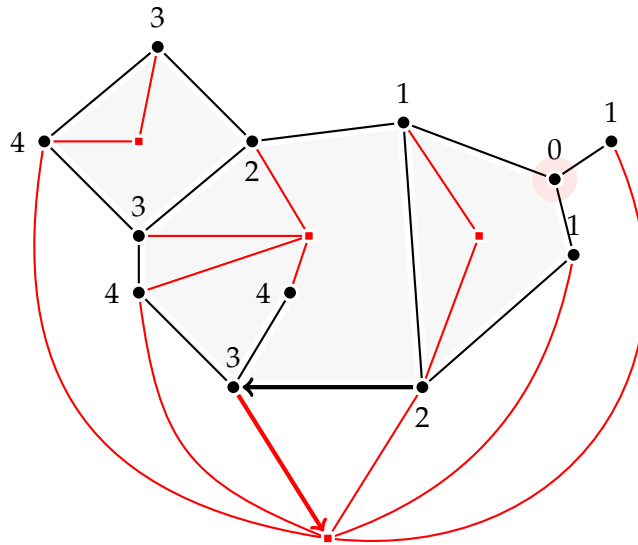


Figure I.5: Construction of a mobile of size 4 (red edges, black and red vertices) from a pointed rooted bipartite map (black vertices, black edges) with 4 faces.

- ➔ for each face f of m , join each down-step corner to the unlabelled vertex drawn within;

At this point, we have the full graph structure of a mobile of size n , which is given by the “new” edges: by construction, two labelled or two unlabelled vertices cannot be joined by a new edge; the number of unlabelled vertices is n , and each has degree $d(f)/2$, where $d(f)$ is the degree of its corresponding face in m ; furthermore, each vertex of m except for δ is incident to a new edge and therefore included in the mobile, because it must have a neighbour that is nearer to δ (possibly δ itself), hence be adjacent to a corner that is a down-step in some face. Summing up, the graph obtained by erasing δ and all original edges has n unlabelled vertices, $\#V(m) - 1$ labelled vertices, and $\#E(m)$ edges; by Euler’s formula, this amounts to saying that the number of vertices is one more than the number of edges, and an argument perfectly analogous to the one from Infobox 3.1 shows that the graph is acyclic, hence a tree.

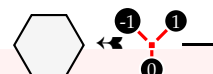
The next steps of the construction fix ε and the root corner of the mobile.

- Consider the root edge e of m , disregarding for the time being its orientation; its two endpoints e_1 and e_2 have labels that differ by ± 1 , say ℓ and $\ell + 1$ respectively. Consider the face f incident (to the left) to the root edge of m , re-oriented from e_2 to e_1 ; then (see Figure I.5) an edge will be drawn by the construction between the leftmost corner adjacent to e_2 in f and the unlabelled vertex within f . Root the mobile in (the corner corresponding to) this new edge oriented towards the unlabelled vertex. If e was oriented from e_2 to e_1 we set $\varepsilon = 1$, otherwise we set $\varepsilon = -1$.
- Finally, erase all original edges of m together with δ , and subtract to all labels the label of the new root of the mobile, so that its label becomes 0.

It is quite clear that the final object is indeed a mobile: the fact that the graph structure is that of a tree and that condition (i) from Definition 3.2.2 holds has already been established; the final shift of all labels yields (ii), and (iii) is none other than the condition one obtains from the fact that we have joined down-step of faces to the corresponding unlabelled vertices (see Figure I.5).

Reconstructing the map from the mobile is done essentially in the same way as in the Schaeffer bijection; the construction is simple enough, although work is needed to show that it is indeed the inverse of the one we have just described. The reader interested in the proof may refer to [16]; Figures I.5 and I.6 show the construction of a mobile from a pointed bipartite map and the recovery of the same map from the mobile, which happens in a way entirely analogous to Section 3.2.2:

Mobile to Map



- ← draw an extra vertex δ in the single face of the mobile;
- ← consider a (cyclic) counterclockwise contour of the face of the mobile; for each labelled corner, set its *successor* to be the next corner in the contour to bear a (strictly) smaller label; if a corner bears the minimal label in the mobile, set the corner around δ to be its successor;
- ← join each labelled corner to its successor (so that edges being drawn do not cross);
- ← erase all edges of the mobile, forget labels;

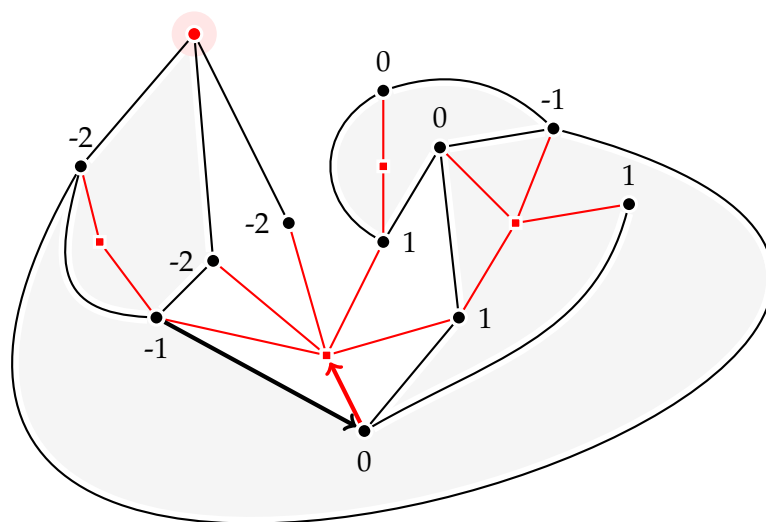


Figure I.6: The construction of an “unconstrained” mobile from a bipartite, rooted, pointed map.

- ◀ root the map obtained in the edge that has been drawn to join the corner corresponding to the root edge of the mobile to its successor, oriented from smaller to larger label if $\varepsilon = 1$, from larger to smaller otherwise;
- ◀ make δ the distinguished vertex of the map.

It is not hard to see that the bijection of Section 3.2.2 is but a special case of this construction: if all faces have degree 4, then one obtains a mobile whose unlabelled vertices all have degree 2; simply erasing all unlabelled vertices and joining the two labelled neighbours of each (or joining the down-step corners directly instead of going through an unlabelled vertex added within the face) yields the labelled tree from the Schaeffer construction.

While this bijection morally corresponds to the “unconstrained” Schaeffer bijection, one may also consider a “positive” version, which is obtained by simply restricting the construction above to rooted bipartite maps that are pointed in their own root vertex – that is to say, rooted bipartite maps tout court. In particular,

Theorem 3.2.4 (BDFG⁺). *There is a bijection between the set \mathbf{BM}_n of all rooted bipartite maps having area n and the set of mobiles of size n whose labels are all non-negative.*

This is a direct corollary of Theorem 3.2.3: if one takes a map in \mathbf{BM}_n^\bullet such that its distinguished vertex is the same as its root vertex, the construction will yield a mobile by subtracting one to all labels, which start out non-negative: the only label to become negative is that of the distinguished vertex, which has no down-step corners adjacent to it, hence is erased; for this very reason, the construction always sets $\varepsilon = 1$.

Conversely, the image of the pair $((\tau, l), 1)$, where (τ, l) is a mobile whose labels are all non-negative, will be pointed in an added vertex δ , which is also the successor of the distinguished corner of (τ, l) (which bears a minimal label, i.e. 0); since $\varepsilon = 1$, the map being reconstructed will be rooted in the new edge joining the distinguished corner of (τ, l) to δ , oriented towards the former. The vertex δ is therefore both the distinguished vertex and the root vertex of the resulting map.

The distinct advantage of the “positive” version of the bijection is the fact that labels in the mobile represent distances to the root vertex (diminished by exactly 1) in the corresponding bipartite planar map.

3.3 Random quadrangulations and random labelled trees

What the preceding section shows is that the task of enumerating – hence uniformly sampling – (rooted and/or pointed) quadrangulations of fixed size is amenable to that of generating uniform elements of certain classes of labelled trees.

Section 3.2.2 in particular is of great use in enumerating the set \mathbf{Q}_n : as we have seen at the very beginning of this chapter, quadrangulations with n faces have $n + 2$ vertices, so that there is an $(n + 2)$ -to-1 mapping from the set \mathbf{Q}_n^\bullet to the set \mathbf{Q}_n ; thanks to Theorem 3.2.2 and Enumeration Result I.2, we thus have

Enumeration result I.3. $\#\mathbf{Q}_n = \frac{2}{n+2}3^n \text{Cat}(n)$.

This, in turn, is also the cardinality of the set of all positive labelled trees of size n with root label 1 (by Theorem 3.2.1).

In order to replicate scaling and local limit results for quadrangulations, one needs to understand random generation of labelled trees a little better. We have seen in Section 2.3 that a critical geometric Galton–Watson tree conditioned on having size n is a uniform random tree in \mathbf{T}_n – i.e. that the measure GW_μ on \mathbf{T} such that $\text{GW}_\mu\{\tau\} = 2^{-2|\tau|-1}$ for each finite tree $\tau \in \mathbf{T}$ is a probability measure and gives equal weight to members of \mathbf{T}_n .

The same measure GW_μ can also be obtained by considering the generating function $\sum_{n \geq 0} \#\mathbf{T}_n x^n = \sum_{n \geq 0} \text{Cat}(n)x^n$ and determining its radius of convergence, which is $1/4$; since $\sum_{n \geq 0} \text{Cat}(n)4^{-n} = 2$, assigning measure 4^{-n} to all members of \mathbf{T}_n gives finite measure (equal to 2) to the set of all finite plane trees, and rescaling the measure by 2 yields a probability measure on such a set, which is none other than GW_μ .

This method can be used in many circumstances to yield a probability measure on a set of combinatorial objects that will automatically give equal weight to members of the set having “size” n (for some notion of size). It can be used, for example, for *positive* labelled trees bearing root label k : thanks to natural equations involving the generating functions $R_i(x) = \sum_{n \geq 0} \#\text{LT}_i^{+,n} x^n$ (see Infobox 3.2) such generating functions can be explicitly determined; their radius of convergence is always $1/12$, and one finds that $R_i(1/12) = \frac{2i(i+3)}{(i+1)(i+2)}$ (a quantity that we shall henceforth call w_i). As before, for each $i \geq 1$ we can consider the measure ρ_i^+ on the set LT_i^+ such that $\rho_i^+(\{\tau\}) = 12^{-|\tau|}/w_i$; it is

automatically a probability measure and gives equal weight to members of LT_i^+ having the same size.

Thanks to the (positive) Schaeffer bijection between \mathbf{Q}_n and LT_1^+ , the measure ρ_1^+ can be interpreted as a measure on the set of all finite rooted quadrangulations, which gives the same weight to quadrangulations with the same area; we call such a measure the *free Boltzmann measure on quadrangulations*. More details will be given in Section III.2.1.2, since the explicit form of $R_1(x)$ will be needed to some extent in Part III of this thesis, as well as a variant of R_1 built with cardinalities of certain sets of quadrangulations *with a boundary*.

For now, let us remark upon the fact that random trees distributed according to ρ_i^+ can be interpreted – at least in a certain sense – as Galton–Watson trees.

We have noted before that a uniform element of LT_0^n is actually a uniform tree from \mathbf{T}_n , endowed with a random labelling of its edges taking values in the set $\{-1, 0, 1\}$. We may therefore slightly alter the law GW_μ of a critical geometric Galton–Watson tree in order to obtain a measure ρ_0 which gives equal weight to trees of size n in LT_0 : in fact, we may simply take $\rho_0(\{\tau\}) = \text{GW}_\mu(\{\tau\})3^{-|\tau|} = 12^{-|\tau|}/2$. Notice that there is an obvious bijection between LT_0 and LT_i that preserves size (given by adding i to all labels), so that the same definition yields a measure on LT_i with the same property of being uniform on sets of trees of the same size. A random labelled tree distributed according to ρ_0 can be generated by selecting the number of descendants of each vertex independently according to the geometric law, and then selecting the label of a child of a vertex u uniformly at random in the set $\{u - 1, u, u + 1\}$.

The labelling of a tree distributed according to ρ_i^+ has a stronger dependence on the shape of the tree, in the sense that the label of a vertex influences the number of its children (in general a vertex with a small label will tend to have fewer descendants than a vertex with a larger label). Given a vertex u bearing a certain label ℓ in a random labelled tree θ^+ distributed according to ρ_i^+ , the cardinality and labels of u 's offspring only depend on ℓ ; in fact, θ^+ can be obtained by recursively generating the offspring of its vertices: given a vertex u labelled ℓ , add its children one by one, from left to right, by repeatedly selecting one of the following outcomes, until the last one is selected:

- with probability $w_{\ell-1}/12$, add a child labelled $\ell - 1$;
- with probability $w_{\ell+1}/12$, add a child labelled $\ell + 1$;
- with probability $w_\ell/12$, add a child labelled ℓ ;
- with probability $1/w_\ell$, declare the offspring of u complete.

This makes θ^+ a direct analogous of a geometric Galton–Watson tree: we do not only have independence of cardinality and labels of the offspring of unrelated vertices (given the label of the parents), but independence of the label and the number of right siblings of a vertex from the number of its left siblings and their labels. This is the kind of property that allows for the specific presentation of the Galton–Watson tree conditioned to survive from Section 2.5, and that will be very useful in dealing with local limits of positive labelled trees (hence quadrangulations) and related objects.

Generating functions for positive labelled trees **3.2**

Given a tree τ in LT_k^+ having size $n > 0$, let ρ be its root and u be its leftmost child; τ can be decomposed into two trees whose sizes sum to $n-1$: the tree τ^u of descendants of u , rooted in u , whose root is labelled $k, k+1$ or $k-1$, and the tree of descendants of ρ that lie (strictly) to the right of u , rooted in ρ itself. This decomposition yields

$$\#\text{LT}_k^{+,n} = \sum_{i=0}^{n-1} \text{LT}_k^{+,n-i-1} (\text{LT}_k^{+,i} + \text{LT}_{k-1}^{+,i} + \text{LT}_{k+1}^{+,i})$$

which translates to the relation

$$R_k = 1 + xR_k(R_{k-1} + R_k + R_{k+1})$$

between the generating functions $R_k(x)$, $R_{k-1}(x)$ and $R_{k+1}(x)$ (for $k \geq 1$), where $R_0 = 0$ by definition, and R_1 can be computed thanks to Theorems I.3 and I.4:

$$R_1(x) = \sum_{n \geq 0} \frac{2}{(n+2)(n+1)} 3^n \binom{2n}{n} x^n = \frac{18x - 1 + (1 - 12x)^{3/2}}{54x^2}.$$

Solutions for the above equations are first found in [15] (and also provided in [23] with a different proof).

↔ **Previous infobox:** 3.1

Next infobox: 3.3 ↔

3.4 The Brownian map

Let \mathcal{Q}_n be a uniform random rooted quadrangulation in \mathcal{Q}_n , and consider the problem of weak convergence of the sequence of random metric spaces $(V(\mathcal{Q}_n), d_{\text{gr}})_{n \geq 1}$, viewed as random variables taking values in the space $(\mathbb{K}, d_{\text{GH}})$ introduced in Section 1.2.

By Theorem 3.2.2, \mathcal{Q}_n is distributed as $\Phi(\theta_n, l)$, where θ_n is a uniform random plane tree of size n , and $l : V(\theta_n) \rightarrow \mathbb{Z}$ is a random integer-valued labelling of $V(\theta_n)$ (obtained by assigning label 0 to the root of θ_n and choosing $l(u) - l(p(u))$, for each $u \in V(\theta_n)$, uniformly at random in $\{0, 1, -1\}$); Φ is the “unconstrained” Schaeffer bijection – which yields a pointed rooted quadrangulation – in conjunction with the forgetful map that ignores the distinguished vertex.

One can code the pair (θ_n, l) by a pair (C, V) of random continuous functions on \mathbb{R} ; to begin with, consider the set $\{0, \dots, 2n-1\}$ as the set of corners of θ_n , ordered according to the counterclockwise contour started at the distinguished corner of θ_n , and set $V(i)$, for $i \in \{0, \dots, 2n-1\}$, to be the label of the vertex adjacent to corner i in the labelled tree (θ_n, l) . As was done with the contour function, extend V to the reals by making it linear on intervals $[i, i+1]$, with $i \in \mathbb{Z}$, and constantly null outside of the

interval $[0, 2n)$. The function V will be occasionally called the *label contour function* of (θ_n, l) , and the pair (C_{θ_n}, V) – where C_{θ_n} is the extended contour function of θ_n – fully encodes a uniform random labelled tree of size n with root label 0 (hence a uniform random quadrangulation of area n). The first step in an attempt to investigate scaling limits for the random maps \mathcal{Q}_n is to establish the joint convergence of the pair (C_{θ_n}, V) , once the two functions are appropriately rescaled in space and time. A result of this kind has been established by Chassaing and Schaeffer in [24]; in order to describe the limiting objects, one needs to introduce a process called *the Brownian snake*, which plays an important role whenever one takes scaling limits of labelled trees, and has been extensively studied (see [41]); we give an informal description of the process in Infobox 2.3. A convergence result for the pair (C_{θ_n}, V) (given in a form that is slightly different from the original result, which involved the label contour process of positive trees rather than “unconstrained” ones) is the following:

Theorem 3.4.1. *Given the functions C_{θ_n} and V as described above (i.e. the contour function and the label contour function of a uniform random labelled tree of size n with null root label), the following convergence holds in distribution, on the space $C([0, 1], \mathbb{R})^2$ endowed with the uniform norm:*

$$\left(\frac{1}{\sqrt{2n}} C_{\theta_n}(2nt), \left(\frac{9}{8n} \right)^{\frac{1}{4}} V(2nt) \right) \rightarrow (\mathbf{e}_t, Z_t),$$

where \mathbf{e}_t is a normalised Brownian excursion (see Infobox 2.4) and Z_t is the head of a Brownian snake driven by \mathbf{e}_t .

Though Theorem 3.4.1 is not enough to determine Gromov–Hausdorff convergence of the sequence of random metric spaces $(V(\mathcal{Q}_n), d_{\text{gr}})_{n \geq 1}$, it is a step in the right direction, and enables Le Gall and others to compute scaling limits for various functionals on uniform random quadrangulations (e.g. radius and profile of distances from the root for different models of random quadrangulation and random planar maps [24, 51, 49]).

Existence of the Gromov–Hausdorff limit was shown after many of its fundamental properties were already established: a compactness argument showed that limits did exist up to the extraction of a subsequence, and many properties (such as having Hausdorff dimension equal to 4 [43]) were shown for all possible subsequential limits, uniqueness being for a time conjectural.

One would expect, however, the limit to be essentially unique and expressible as a function of the CRT endowed with the labelling process Z_t , somehow arising as a “continuous version” of the Schaeffer bijection on finite labelled trees. It turns out that this is indeed the case.

Given a finite labelled tree (τ, l) , consider its label contour function $V : \{0, \dots, 2|\tau|\} \rightarrow \mathbb{Z}$ (where we interpret the set $\{0, \dots, 2|\tau| - 1\}$ as the set of corners of τ); what the Schaeffer bijection does is join corner i to corner j , where $i < j$, if one of the following holds:

- $V(j) = V(i) - 1$ and $V(t) \geq V(i)$ for $i \leq t < j$ (that is, corner j is the successor of corner i); or

*The Brownian Snake***3.3**

Consider the space \mathcal{W} of all continuous paths $w : [0, \zeta_{(w)}] \rightarrow \mathbb{R}$, where $\zeta_{(w)}$ is a non-negative real number called the *lifetime* of w , and we write \hat{w} for the endpoint of w , that is $w(\zeta_{(w)})$. For each $x \in \mathbb{R}$, we can see one-dimensional Brownian motion issued from x and stopped at a (possibly random) time T as a random variable taking values in \mathcal{W} . Equip \mathcal{W} with the following metric:

$$d(w, w') = |\zeta_{(w)} - \zeta_{(w')}| + \sup_{t \geq 0} |w(\min\{t, \zeta_{(w)}\}) - w'(\min\{t, \zeta_{(w')}\})|.$$

We can build the Brownian snake as a continuous process taking values in \mathcal{W} : given a lifetime process ζ_s , consider a process W_s such that

- for every $s \geq 0$, W_s is a random element of \mathcal{W} with lifetime ζ_s ; conditionally on ζ_s , W_s is distributed as a Brownian motion started at 0 and stopped at time ζ_s ;
- take $s < s'$, and set $m(s, s') = \inf_{s \leq r \leq s'} \zeta_r$; then $W_{s'}(t) = W_s(t)$ for all $0 \leq t \leq m(s, s')$, while conditionally on $W_s(m(s, s'))$ the path $W_{s'}(m(s, s') + t) : [0, \zeta_{s'} - m(s, s')] \rightarrow \mathbb{R}$ is independent of W_s and distributed as a Brownian motion started at $W_s(m(s, s'))$ and stopped at time $\zeta_{s'} - m(s, s')$.

The process W_s is called a Brownian snake with lifetime process ζ_s , or *driven* by the process ζ_s . In this section, ζ_s is a normalised Brownian excursion, but it could be a different process (as we shall see in Section III.5.1).

Intuitively, W_s can be built by progressively erasing the path from the endpoint backwards when the lifetime process ζ_s decreases, and adding an infinitesimal length of one-dimensional Brownian motion, independent of what came before, at the very tip of the path, whenever ζ_s increases.

When W_t is driven by a normalised Brownian excursion \mathbf{e}_t , it is quite natural to see the process $Z_t = \widehat{W}_t$ (which is no longer path-valued, but only records the trajectory of the endpoint of the random path W_t) as a form of one-dimensional Brownian motion indexed by the CRT $T_{\mathbf{e}}$. It is in fact clear that, if two points $s, t \in [0, 1]$ are identified in the CRT (i.e. if $s \leq t$ and $\mathbf{e}_s + \mathbf{e}_t - 2 \inf_{r \in [s, t]} \mathbf{e}_r = 0$), then $\widehat{W}_s = \widehat{W}_t$ almost surely: the condition leading to the identification of the two point of the CRT can be read as the fact that $m(s, t) = \mathbf{e}_s = \mathbf{e}_t$, so that the entire paths W_s and W_t must coincide up to $m(s, t)$, i.e. up to their endpoint. If one bears in mind the “acyclic union of intervals” imagery from Infobox 2.1, the intuitive picture of the Brownian snake driven by the contour process of a real tree is a set of short tracts of linear Brownian motion, arranged in a tree-like structure.

↔ **Previous infobox:** 3.2

Next infobox: 3.4 ↔

- $V(i) = V(j) - 1$ and $V(t) \geq V(j)$ for $t \geq j$ and for $t < i$ (corner i is the successor of corner j).

If, whenever $a \geq c$, we take $a < b < c$ to mean “ $b > a$ or $b < c$ ”, the above condition can be rewritten as

$$V(i) + V(j) - 2 \max \left(\min_{i \leq t < j} V(t), \min_{j \leq t < i} V(t) \right) = -1.$$

It should therefore not be surprising that the first step in an attempt to reconstruct the Schaeffer bijection on the CRT is to define a function $D^\circ : [0, 1]^2 \rightarrow \mathbb{R}$ as

$$D^\circ(s, t) = Z_s + Z_t - 2 \max \left(\inf_{s \leq u \leq t} Z_u, \inf_{t \leq u \leq s} Z_u \right);$$

one expects to then identify points of the CRT having pre-images in $[0, 1]$ for which D° is null (since Z_t is no longer discrete but continuous, and heuristically the condition of having bounded difference in the discrete setting will turn into a condition of full equality in the continuous case).

The function D° is a pseudodistance on $[0, 1]$ (which represents the set of “corners” of the CRT in some sense); one could define a version of D° directly on T_e^2 as

$$D^\circ(a, b) = \inf \left\{ D^\circ(s, t) \mid p(s) = a, p(t) = b \right\}$$

where p is the usual projection sending $[0, 1]$ to the CRT (see Section 2.4). It is not surprising, however, that D° is *not* a pseudo-distance on T_e (in fact, notice that D° does not come from a distance at the discrete level, as \mathbf{e}_t did in Section 2.4). We expect D° to still somehow encode quadrangulation distances on the CRT, but only in a very local sense; this justifies the idea of considering $D^* : T_e^2 \rightarrow \mathbb{R}_{\geq 0}$, defined as

$$D^*(a, b) = \inf \left\{ \sum_{i=1}^{k-1} D^\circ(a_i, a_{i+1}) \mid k \geq 2, a = a_1, a_2, \dots, a_k = b \right\},$$

which does in fact turn out to be a pseudo-distance on T_e . Taking the quotient of T_e by the equivalence relation $D^* = 0$ and endowing it with the quotient metric yields a random (pointed) metric space (M, D^*) which is usually called *the Brownian map*.

Theorem 3.4.2 (Miermont; Le Gall). *Given a uniform random rooted quadrangulation \mathcal{Q}_n with n faces, we have*

$$\left(V(\mathcal{Q}_n), \left(\frac{9}{8n} \right)^{\frac{1}{4}} d_{\text{gr}} \right) \longrightarrow (M, D^*)$$

in distribution, where (M, D^) is the Brownian map (and all random variables take values in the space $(\mathbb{K}^\bullet, d_{\text{GH}})$).*

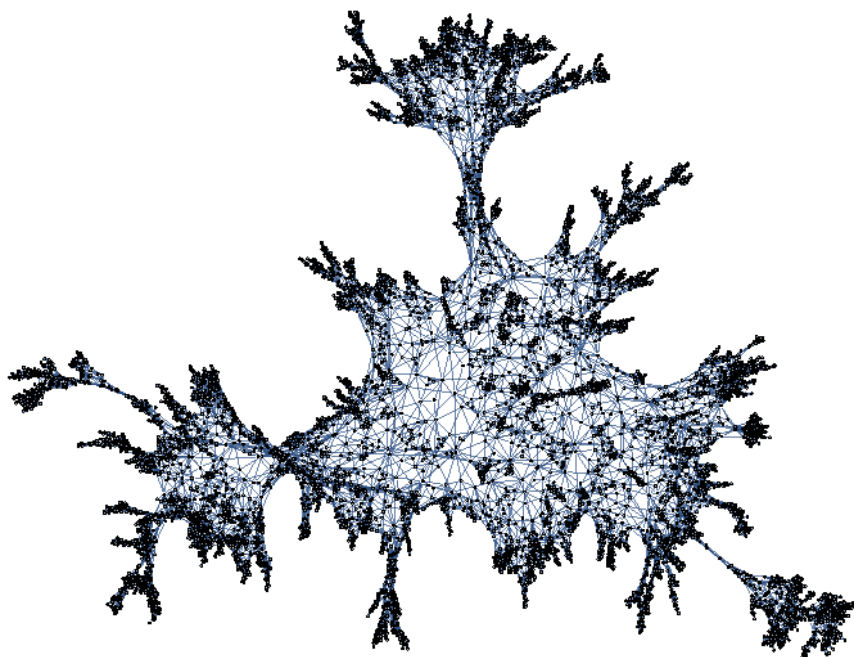


Figure I.7: The Brownian Map, or rather a very large uniform random triangulation (image credit to Nicolas Curien).

Some facts about the Brownian map

3.4

- Many classes of random maps have been shown to converge to (a scalar multiple of) the Brownian map in the scaling limit; these include uniform random quadrangulations with n faces [44, 55], uniform random p -angulations (for $p = 3$ or p even) with n faces [44], uniform random bipartite planar maps with n edges [1], uniform planar maps with n edges [12];
- the Brownian map has the topology of the sphere \mathbb{S}^2 [48];
- the Brownian map has Hausdorff dimension 4 [43].

↔ **Previous infobox:** 3.3

This is the last infobox in the chapter

3.5 The UIPQ

A study of the local limit for the sequence $(\mathcal{Q}_n)_{n \geq 1}$ of uniform random rooted quadrangulations of area n was initiated by Krikun [36] as well as Chassaing and Durhuus [23], following works of Angel and Schramm [9] on the local limit of uniform triangulations.

The weak limit of the sequence $(\mathcal{Q}_n)_{n \geq 1}$, seen as random variables taking values in the set of all planar maps equipped with the local distance (see Section 1.3) is a random infinite quadrangulation called the UIPQ (for *uniform infinite quadrangulation of the plane*).

One way to describe such an object is via the unconstrained Schaeffer bijection (as done by Curien, Ménard and Miermont in [30]); the bijection from Theorem 3.2.2 can be extended to a continuous map $\Phi : \text{LT}_0 \rightarrow \mathcal{Q}$, where LT_0 is the set of all labelled trees, finite or infinite, having a single spine, and \mathcal{Q} is the set of all (locally finite) rooted quadrangulations (in fact, Φ is obtained by extending the Schaeffer bijection – and the forgetting of the distinguished vertex – in the natural way, see Figure I.8).

We have already encountered the local limit of uniform random plane trees, which is the *geometric Galton–Watson tree conditioned to survive* (see Section 2.5); it should be quite intuitive that the local limit of uniform random *labelled* plane trees (with unconstrained labels and root label 0, labels being included in the definition of the local distance as mentioned in Section 1.3) is the same object, endowed with a random labelling l which can be generated by choosing $l(u) - l(p(u))$ uniformly at random in $\{0, 1, -1\}$. Continuity results for Φ imply that the UIPQ, which we shall denote \mathcal{Q}_∞ , can be obtained from such a random infinite labelled tree by applying Φ .

Alternatively, the UIPQ can also be constructed via the *positive* Schaeffer bijection (see Section 3.2.1), as the image of a random labelled tree with an infinite spine that Chassaing and Durhuus describe in [23], where they compute explicit transition probabilities of labels along the spine, and give laws of the left and right finite trees attached to it in terms of the laws ρ_i^+ that we introduced in Section 3.3. The fact that such a “positive” construction does yield the local limit of uniform random rooted quadrangulations has been shown by Ménard in [53].

Both the “unconstrained” and the “positive” approach result in precious insights into the geometry of \mathcal{Q}_∞ . While the former is very well suited for a study of infinite geodesics in the UIPQ (see [30], where Curien, Ménard and Miermont show that there is an essentially unique infinite geodesic – or rather a single “geodesic pencil” – hence in a certain sense a single point at infinity), the latter can be used to investigate geometric properties that depend specifically on distances from the root vertex of the UIPQ (e.g. asymptotics for the volume of balls centred in the root vertex, see what Le Gall and Curien do in [29]).

Le Gall and Curien’s work leads to the computation of the scaling limit for the profile of distances of the UIPQ, and to the introduction of a “continuous” random metric space called the *Brownian plane*, to which we will propose an analogue in Section III.5.3.

In fact, the entirety of Part III of this thesis, based on joint work with Nicolas Curien, employs methods similar to the ones described above to investigate the geometry of the local limit of *uniform quadrangulations with a boundary* (when both the area and

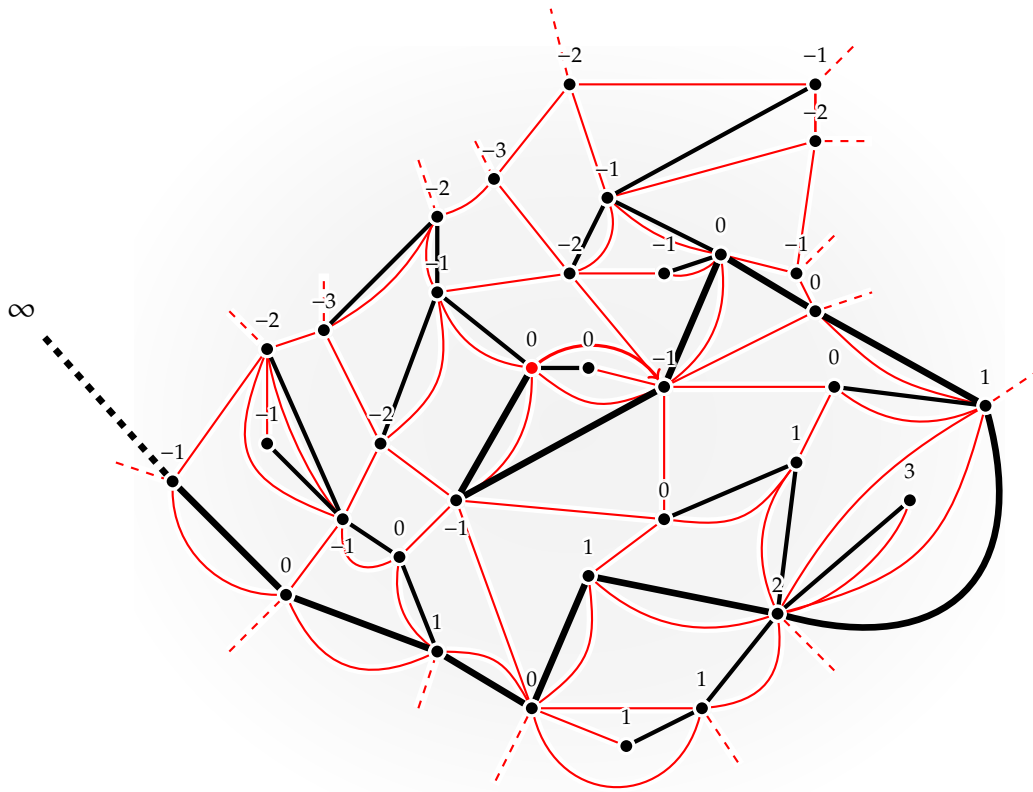


Figure I.8: The UIPQ, represented as the image of the geometrical Galton–Watson tree conditioned to survive, with unconstrained labels; the thicker black path represents the spine of the tree, along which the \liminf of labels can be shown to be $-\infty$ almost surely. Though the face of the tree is of infinite degree, its corners can still be ordered “counterclockwise” with respect to infinity (though their sequence is indexed by \mathbb{Z} rather than being a finite set); each corner has a successor defined exactly as in Section 3.2 (because it is always eventually followed by a corner with strictly smaller label according to the counterclockwise order). Joining corners to successors (red edges) and erasing tree (black) edges yields the UIPQ.

perimeter are sent to infinity). We shall see that many results obtained for the UIPQ can be essentially replicated for such a limit, called the UIHPQ (or *uniform infinite quadrangulation of the half-plane*). In Section III.6 and III.7, we begin to study how the UIPQ and UIHPQ relate to one another, and whether one can be obtained from the other by certain surgical operations.

Part II

The scaling limit of random outerplanar maps

where we show that random uniform outerplanar maps with n vertices suitably rescaled by a factor $1/\sqrt{n}$ converge in the Gromov–Hausdorff sense to $7\sqrt{2}/9$ times Aldous’ Brownian tree. The content of this part is mostly mutated from the author’s paper [19].

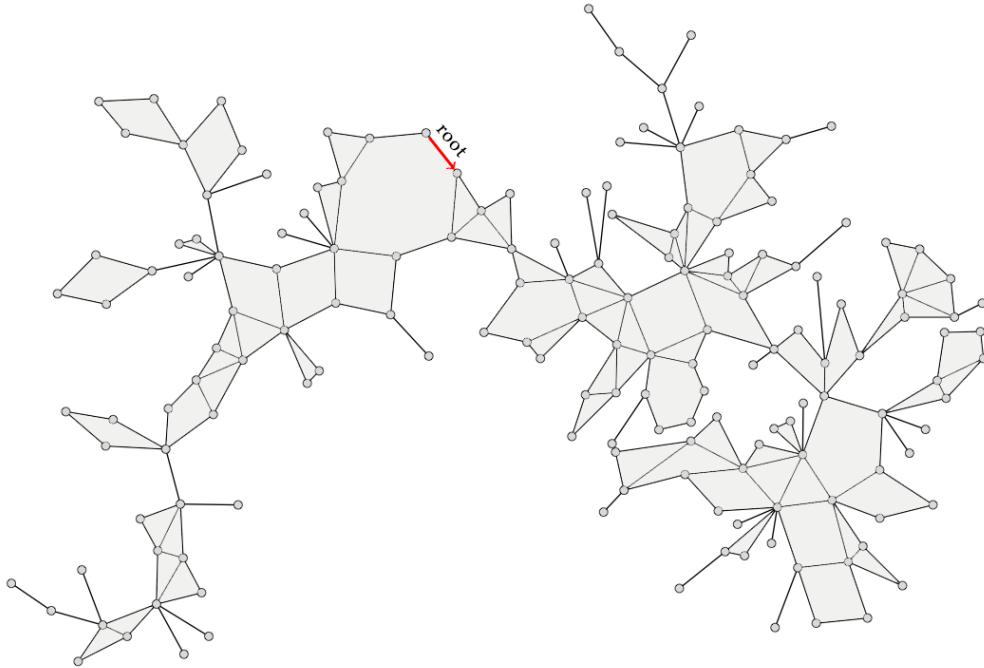


Figure II.1: A rooted, simple outerplanar map.

II.1 Introduction

A significant portion of Part I of this thesis provided an introduction to the study of scaling limits for large random combinatorial objects, a field which has been very active since the early 90's; in particular, we have discussed in Section 2.4 one of its most emblematic results, that is the construction of the continuum random tree (CRT) by Aldous [3, 4, 5] as the scaling limit of various classes of oriented trees. On the other hand, we have also described in Section 3.4 the more recent breakthrough achieved by Le Gall and Miermont [44, 55], who showed that several classes of random planar maps admit the so-called Brownian map as scaling limit.

It has meanwhile been observed that – for some particular regimes – random planar maps with a unique macroscopic large face have a tree-like structure and admit the CRT (rather than the Brownian map) as scaling limit; see [11, 17, 33, 56]. The present part of this thesis shall provide a confirmation of this phenomenon, as already mentioned in Infobox 2.5, for the case of a class of planar maps named *outerplanar maps*.

We say a planar map is *outerplanar* if all of its vertices are adjacent to the same face, which is dubbed the *outerface* and usually drawn as the infinite face in a planar embedding. Outerplanar maps constitute a class of well-studied combinatorial structures; in particular, they have a simple characterisation in terms of minors (a graph is outerplanar if and only if it does not contain $K_{2,3}$ nor K_4 as a minor [22]). See [62] for more

characterisations of outerplanar graphs. In this work we shall restrict ourselves to *simple* outerplanar maps, with no loops or multiple edges. All of the maps considered here are *rooted*, that is endowed with a distinguished oriented edge such that the outerface is lying on its left. The tail of the root edge will be called the *root vertex*. More generally, we will make use of standard notation for planar maps and plane trees as introduced in Chapters 1 and 2 of this thesis.

Our main result is the following:

Theorem II.1.1. *Let \mathbf{M}_n be a random uniform rooted simple outerplanar map with n vertices, and denote by d_{gr} the graph distance on the set of its vertices $V(\mathbf{M}_n)$. We have the following convergence in distribution for the Gromov–Hausdorff topology:*

$$\left(V(\mathbf{M}_n), \frac{d_{\text{gr}}}{\sqrt{n}} \right) \xrightarrow[n \rightarrow \infty]{(d)} \left(\mathcal{T}_{\mathbf{e}}, \frac{7\sqrt{2}}{9} d_{\mathbf{e}} \right),$$

where $(\mathcal{T}_{\mathbf{e}}, d_{\mathbf{e}})$ is the Brownian CRT of Aldous. We adopt here the normalisation of Le Gall [42] by considering $\mathcal{T}_{\mathbf{e}}$ as constructed from a normalised Brownian excursion (see Section 2.4).

The first ingredient in our proof is a way to relate outerplanar maps to plane trees; this will be done using the bijection of Bonichon, Gavaille and Hanusse [14] between the set of (simple and rooted) outerplanar maps with n vertices and a special class of bicoloured plane trees with n vertices which is described in Section II.2. The plan of the proof then partially follows that of [27], in which Curien, Haas and Kortchemski prove the convergence of random dissections to a scalar multiple of the CRT. More specifically, we will show that the distances on an outerplanar map are roughly proportional to the distances on the associated tree. To this end, we describe throughout Section II.4 an algorithm that, given a bicoloured tree and a vertex v , yields the length of a geodesic path from v to the root vertex in the associated outerplanar map. When applied to the model of a bicoloured Galton–Watson tree conditioned to survive (presented in Sections 2.5 and II.5) this algorithm yields a Markov chain whose mean increment (under the stationary distribution) gives the asymptotic proportionality constant between the metric on a large outerplanar map and that of its associated tree. The distances between arbitrary pairs of points are finally controlled by a large deviations estimate, see Sections II.6 and II.7.

II.2 Outerplanar maps and plane trees

As mentioned earlier, the first ingredient needed for our discussion is a bijection found in [14], which enables the coding of outerplanar maps as bicoloured trees of a certain class. More specifically,

Definition II.2.1. We say that a rooted plane tree τ is *bicoloured* if each of its vertices is coloured either black or white; we shall say that τ is *well bicoloured* if it is bicoloured and all of the vertices in its rightmost branch are coloured white (see Figure II.2a). We shall

henceforth simply write *well bicoloured tree* when referring to a well bicoloured rooted plane tree.

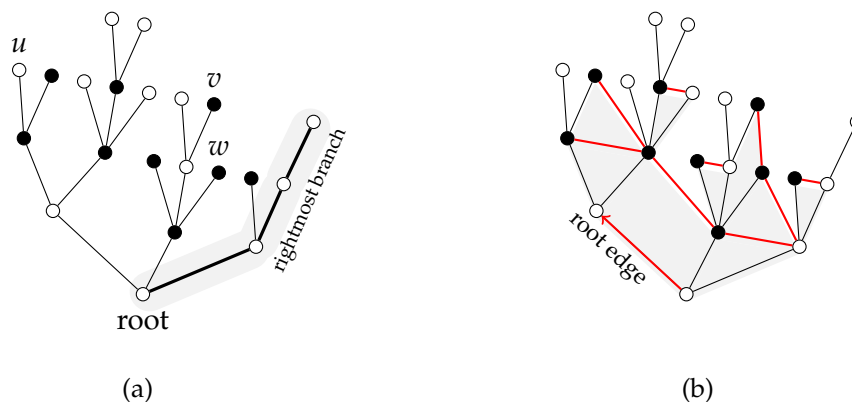


Figure II.2: Figure (a) shows a well bicoloured tree. Vertices u and v are *unrelated*. Vertex w is the *target* of v . Figure (b) represents its image via the map Ψ .

Some working knowledge of the explicit bijection is needed in the sections that follow, and thus part of the construction is included for future reference. For the reader who wishes to better understand both directions of the bijection, a more complete account is given within Infobox II.1. We adopt notation consistent with that of [14], as already introduced in Section 2.1: given two distinct vertices in a plane tree, we call them *unrelated* if neither is an ancestor of the other.

Let now τ be a well bicoloured tree. For each black vertex v of τ define the *target* of v to be its next unrelated vertex in the contour of τ (defined – see Section 2.2 – as the counterclockwise contour of the face of τ , started at the corner corresponding to the root edge). Define $\Psi(\tau)$ as the rooted map obtained by joining each black vertex of τ to its target (via an edge that leaves the rightmost corner of the black vertex and enters the target from the leftmost corner available); note that the map is rooted in the same oriented edge as the tree; finally, forget the colouring of τ (see Figure II.2b for an example).

Notice that the order in which the additional edges are drawn is not relevant, and that the root edge will have the unbounded face on its left side. The map $\Psi(\tau)$ is easily seen to be outerplanar. Moreover, the inverse of Ψ can be constructed explicitly (see Infobox II.1). All that we will need, however, is the following:

Theorem II.2.1 (Bonichon, Gavoille, Hanusse [14]). *The map Ψ is a bijection between well bicoloured trees with n vertices and simple rooted outerplanar maps with n vertices.*

Such a bijection, together with the fact that the scaling limit for uniform random plane trees is the CRT, constitutes the basis for our future discussion; notice that, however, it is not at all clear how the colouring affects the metric in the switch from tree to map: distances between corresponding vertices are, in general, smaller when computed on the map (if two vertices are adjacent in the tree then they are in the corresponding

map, but not vice-versa). This means we cannot easily employ the result for plane trees to make deductions on outerplanar maps. Most of the following sections will develop ways to control the outerplanar map metric via easily readable information about its corresponding tree.

More about the BGT bijection

ii.1

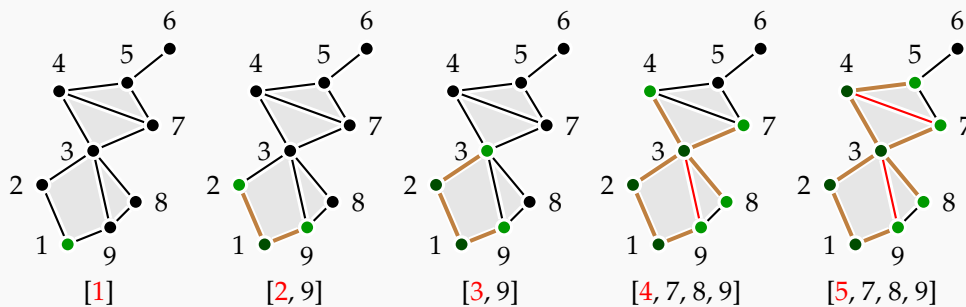
For the interested reader, here is a description of the inverse of the mapping Ψ from Theorem II.2.1. Given a rooted outerplanar map m with n vertices, the well bicoloured tree τ such that $\Psi(\tau) = m$ can be constructed as a spanning tree for m (i.e. a plane tree obtained from m by erasing certain edges, but keeping all of m 's vertices intact).

The spanning tree can be built recursively by marking certain edges as to keep and erasing others. In order to better explain the algorithm, we use a last-in-first-out stack which will contain vertices of m , called the *bud* stack; elements are added to the stack one by one, and "popping" an element from the stack removes the element which was most recently added. Initially, the stack contains the root vertex e^- , where (e^-, e^+) is the root edge of m ; the algorithm terminates when the stack is empty.

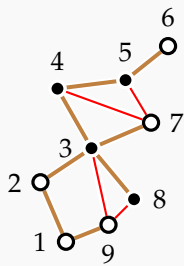
At each run of the main loop, one vertex is popped from the *bud* stack and some vertices are (possibly) added; the algorithm decides on a *parent* for such vertices, thus marking the edges that join them to their parent as "to keep". We can therefore assume that each vertex being popped from the stack has a parent, except for e^- . Also, it will be clear from the description of the algorithm that vertices enter the stack only once.

main loop

Pop the first vertex from the *bud* stack; call it v . Consider the set $C(v)$ containing all neighbours of v that are not at present within the *bud* stack, and have never yet been in it. We may order $C(v)$ as $c_1, \dots, c_{n(v)}$, by taking its elements *counterclockwise* around v in such a way that the edge $\{v, p(v)\}$ is between edges $\{v, c_1\}$ and $\{v, c_{n(v)}\}$, or (in the case of v being the root vertex e^-) in such a way that $c_{n(v)} = e^+$. We add $c_1, \dots, c_{n(v)}$ to the *bud* stack in *this order* (so that $c_{n(v)}$ will be the next vertex to be popped), and set $p(c_i) = v$ for $i = 1, \dots, n(v)$ (edges $\{c_i, v\}$ will thus belong to the spanning tree).



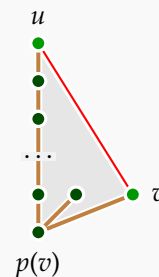
Notice that every vertex of m will go through the *bud* stack, since the set of vertices that do go through the stack is closed under the operation of taking neighbours, and m is connected. Also, edges marked as “to keep” form a connected graph after each iteration of the main loop, and are always one less than the number of vertices having been in the stack; the final graph is therefore connected, has n vertices (as many as $V(m)$) and $n - 1$ edges. Hence the map τ obtained by erasing all edges that never get marked as “to keep” by the algorithm (notice that (e^-, e^+) does belong to τ , and we consider it to be its root edge) is a spanning tree for m . The *left-to-right* order of pairs of unrelated vertices in τ has also a clear interpretation in terms of the algorithm: a vertex u lies (strictly) left of an unrelated vertex v if and only if u is popped before v from the *bud* stack.



Of course, τ does not yet code m : in order to be able to reconstruct the map, one needs to keep track of the edges being erased, which we shall do by appropriately selecting a bicolouring of τ .

Suppose the edge $\{u, v\}$ of m does *not* appear in τ , and suppose u is popped from the stack before v ; then v must be a *bud* at the time when u is popped from the *bud* stack. As a consequence, we have already determined the vertex $p(v)$, which has already been popped. Now, u must be a *descendant* of $p(v)$; this is because, after $p(v)$ is popped from the stack, all of its descendants are popped before any unrelated vertices: children of $p(v)$ are added to the stack, then children of children, etc. Therefore, since v is a descendant of $p(v)$ and is still a *bud*, u must be a descendant of $p(v)$ as well. Consider now the cycle in m given by the ancestor path leading from u to $p(v)$, the edge $\{p(v), v\}$ and the edge $\{u, v\}$. If $p(v)$ had a child in τ that is not an ancestor of u and lies to the *left* of u (hence a vertex unrelated to u lying left of v), then such a vertex would be within the cycle, and the map would fail to be outerplanar.

The above argument shows that any edge $\{u, v\} \in E(m) \setminus E(\tau)$, where u is popped before v from the *bud* stack, is such that v is indeed the first vertex unrelated to u to be met in a counter-clockwise contour of the face of τ ; we therefore complete the construction of τ by colouring each vertex u black or white, according to whether or not $\{u, t(u)\} \in E(m)$, and colouring vertices in the rightmost branch of τ automatically white; what we obtain is indeed a well bicoloured tree, and it is now obvious that $\Psi(\tau) = m$.



This is the first infobox in Part II

This is the last infobox in Part II

II.3 Rough localisation of geodesics

We now delve now into the central problem of the rather unclear relationship between distances on an outerplanar map and distances on its corresponding plane tree: given a well bicoloured tree τ , we wish to compute distances on the map $\Psi(\tau)$. We restrict ourselves, in this section and many of the subsequent ones, to distances from the root vertex; in Section II.7, before the proof of Theorem 1.1, we will give a way to bound

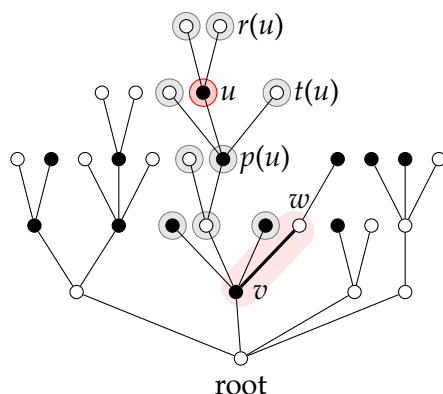


Figure II.3: (v, w) is a separating pair for u (also, it is a separating pair for $r(u)$, $t(u)$, $p(u)$, or indeed for any of the circled vertices).

distances between arbitrary vertices of an outerplanar map with a function of distances from the root. In what follows, geodesics to the root in $\Psi(\tau)$ are built in a step-by-step manner, using local information about the tree structure of τ and its colouring.

We shall refer to geodesics of $\Psi(\tau)$ as map-geodesics; since τ and $\Psi(\tau)$ have the same vertex set, any path in $\Psi(\tau)$ can be interpreted as a sequence of vertices $v_0 \dots v_n$ of τ , where for each i between 0 and $n - 1$ vertices v_i and v_{i+1} are either neighbours in τ (parent and child, in any order), or a black vertex and its target (again, a priori, in any order).

We need some additional notation: as per Section 2.1, for each vertex u of τ , if u is not the root, we write $p(u)$ for its parent; if u has children in τ , we call $r(u)$ its rightmost child; finally, if u is a black vertex, we write $t(u)$ for its target. Also, given three distinct vertices u , v and w of τ , we say that (v, w) is a *separating pair* for u (from the root of the tree) if v is an ancestor of u and w is a child of v lying to the right of u ; see Figure II.3.

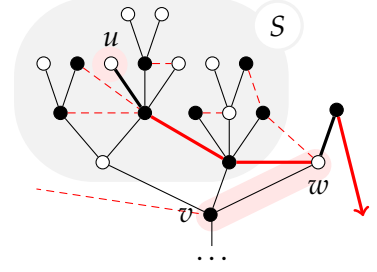
We write $d_M(u, v)$ for the graph distance between vertices u and v in the map $\Psi(\tau)$, and simply write $d_M(u)$ for $d_M(u, \emptyset)$, where \emptyset is the root of τ . We are ready to prove the following:

Proposition II.3.1. *In a well bicoloured tree τ , let (v, w) be a separating pair for u . Then any map-geodesic from u to the root of τ will pass through v or w (possibly both). Consequently, any map-geodesic from u to the root can be constructed by starting from u and iteratively applying one of the maps t , r or p , so that r or p are applied to white vertices, and p or t are applied to black vertices.*

Proof. Let S be the set of (strict) descendants of v that lie strictly to the left of w , and $u_0 u_1 \dots u_n$ a map-geodesic such that $u = u_0$ and $u_n = \emptyset$ is the root of the tree. Clearly, $u \in S$ and $u_n \notin S$; take the minimum i such that $u_i \notin S$, and consider its relation to u_{i-1} . Children of elements in S are in S , and for any pair $(x, t(x))$ in the tree (where x is a black vertex), either both vertices belong to S or neither does, except for the case where $x \in S$

and $t(x) = w$. Hence either u_i is the parent of u_{i-1} (therefore $u_i = v$) or u_i is the target of u_{i-1} , which can only be the case if $u_i = w$, and thus the first part of the proposition is established.

Let us consider what this implies in term of distances: if (v, w) is a separating pair for u , then $d_M(u) > d_M(v)$ or $d_M(u) > d_M(w)$; that is, since $|d_M(v) - d_M(w)| \leq 1$, $d_M(u) \geq \max\{d_M(v), d_M(w)\}$. Now, consider a map-geodesic from u to the root. If x is a child of u distinct from $r(u)$, then such a geodesic does not go through x , because $(u, r(u))$ is a separating pair for x , and thus $d_M(x) \geq d_M(u)$ (whereas, if there were a geodesic from u to the root that involved x , we would have $d_M(x) < d_M(u)$). If u is the target of some y , then consider $p(u)$, which must be an ancestor of y : $(p(u), u)$ is a separating pair for y , and thus $d_M(y) \geq d_M(u)$, so a map-geodesic from u to the root does not go through y . Only three possibilities remain: either the geodesic moves from u to $p(u)$, or to $t(u)$, or to $r(u)$.



Clearly, a white vertex u in a map-geodesic to the root will be followed by either $r(u)$ or $p(u)$, since it is not directly connected to any target in the map. Suppose, on the other hand, that u is a black vertex; it will be followed in a map-geodesic to the root by $p(u)$ or $t(u)$, never by a child: this is because $(p(t(u)), t(u))$ is a separating pair for u ; if the map-geodesic does not move from u to $t(u)$, then it passes through $p(t(u))$, which has map-distance at most 2 from u , and at least 2 from any child of u (it cannot be the target of one, since children of u have $t(u)$ or other children of u as targets, and is not connected to strict descendants of u in the tree); as a consequence, the map-geodesic does not go through $r(u)$. \square

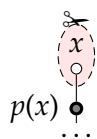
II.4 An algorithm to compute map-distances

Suppose we have a well bicoloured tree τ and a vertex x of τ of height n ; we know that $d_M(x)$, the map-distance between x and the root of τ , is no more than n . From now on, we write $d(\tau, x)$ for the map distance $d_M(x)$ between x and the root of τ . We propose to compute $d(\tau, x)$ via a recursive algorithm which takes the pair (τ, x) as input and outputs a pair (τ', x') , where x' is a vertex of τ' such that $d(\tau', x') = d(\tau, x) - 1$; this way the number of iterations needed for the algorithm to output a pair consisting of a well bicoloured tree and its root is equal to the length of a geodesic path from x to the root in τ .

Given (τ, x) , consider the path *in the tree* leading from x to the root; thanks to Proposition II.3.1 we know that a map-geodesic from x to the root cannot involve any of the vertices that lie strictly to the left of this path (parents, targets and rightmost children of vertices that are part of the path or lie to the right of it cannot lie to its left). We may thus safely erase all such vertices from τ , and we will always output pairs (τ', x') such that no vertices lie strictly to the left of the tree path leading from x' to the root of τ' .

In what follows, given a tree τ and a vertex x , we will write τ^x for the subtree of τ formed by x and its descendants; given a tree τ and a subtree $\tilde{\tau}$ (which does not include the root of τ), we will write $\tau \setminus \tilde{\tau}$ for the rooted plane tree obtained from τ by erasing all vertices of $\tilde{\tau}$ and any edges adjacent to those vertices. We will also write $|x|$ for the height of x in τ , whenever the tree τ can be inferred from the context.

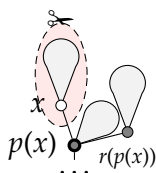
The description of the algorithm follows.



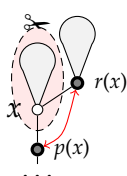
[w₀] Suppose x is a white leaf of τ ; then a map-geodesic to the root necessarily moves from x to $p(x)$ (hence $d(\tau, p(x)) = d(\tau, x) - 1$). Consider the tree $\tau' = \tau \setminus x$ and the pair $(\tau', p(x))$ (where we still write $p(x)$ for the obvious image of the original vertex of τ in τ'); it is clear that $d(\tau', p(x)) = d(\tau, p(x))$ (because the only vertex removed is x , which was further from the root than $p(x)$) and so it equals $d(\tau, x) - 1$.



[w_{>0}] If x is a white vertex of τ and has offspring, the matter is more complicated. Proposition II.3.1 ensures that a geodesic to the root moves to either $r(x)$ or $p(x)$, but it is not clear which: we need to distinguish two cases.



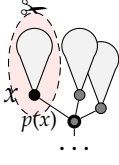
[w_{>0.1}] Suppose that $x \neq r(p(x))$, that is x has some right siblings; then $(p(x), r(p(x)))$ is a separating pair for $r(x)$, and thus $d(\tau, p(x)) \leq d(\tau, r(x))$; hence there is a geodesic moving from x to $p(x)$, and $d(\tau, p(x)) = d(\tau, x) - 1$. We choose to follow such a geodesic and define τ' to be $\tau \setminus \tau^x$, and output $(\tau', p(x))$ so that, as before, we have $d(\tau', p(x)) = d(\tau, x) - 1$.



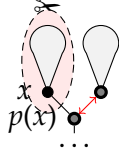
[w_{>0.2}] Suppose now that $x = r(p(x))$. We build the new tree τ' by erasing τ^x from the original tree and rerooting the subtree $\tau^{r(x)}$ onto $p(x)$, by identifying $p(x)$ with $r(x)$, thus merging them into a single vertex y ; the colour of y is set to white if and only if both $p(x)$ and $r(x)$ were white in τ . We need to show that $d(\tau', y) = d(\tau, x) - 1$: there is an obvious map sending vertices of τ that are not in $\tau^x \setminus \tau^{r(x)}$ to vertices of τ' ; the map is 1-on-1 with the exceptions of $p(x)$ and $r(x)$, which are both sent to y . Neighbours in τ are sent to neighbours in τ' , and (since $x = r(p(x))$ in τ) the target of a vertex in τ becomes the target of its image in τ' : hence $d(\tau', y) \leq \min\{d(\tau, p(x)), d(\tau, r(x))\}$. On the other hand, any map-path in τ' can be lifted to a map-path in τ (by appropriately selecting a pre-image for y as first step of the path), which gives equality.



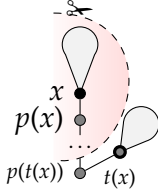
[b] If x is a black vertex of τ , then the new option of *jumping* to $t(x)$ presents itself. As by Proposition II.3.1, a geodesic will either move to $p(x)$ or to $t(x)$. We need to deal with three separate cases:



[b.1] Suppose x , $t(x)$ and $r(p(x))$ are distinct: that is to say, x has at least two right siblings; in this case, $(p(x), r(p(x)))$ is a separating pair for $t(x)$, hence there is a geodesic moving from x to $p(x)$; we thus set τ' to be $\tau \setminus \tau^x$, and output $(\tau', p(x))$.



[b.2] Suppose now that x has only one right sibling, which is therefore $t(x)$ as well as $r(p(x))$. We build the new tree τ' by simply erasing τ^x and identifying vertices $p(x)$ and $t(x)$, merging them into a single vertex y to be coloured white if and only if both of the original vertices were white in τ , and output (τ', y) . We have $d(\tau', y) = d(\tau, x) - 1$ by roughly the same argument as previously.



[b.3] The last case is that of x being the rightmost child of its parent; in this case $(p(t(x)), t(x))$ is a separating pair for $p(x)$, so $d(\tau, t(x)) \leq d(\tau, p(x))$, and we may assume a geodesic to the root does jump from x to its target. We can thus build τ' by erasing *all that lies left of $t(x)$* , and output $(\tau', t(x))$.

Notice that, in all cases listed except for the very last one, the output vertex x' has height $|x| - 1$ in τ' , whereas the jump made in the last case (the one marked [b.3]) may lead to a vertex x' of arbitrarily smaller height. Also, the information on τ that the algorithm uses to select the appropriate τ' is entirely local (child structure of x and its parent) with the exception of the last case, which requires to make changes to parts of τ that are, a priori, arbitrarily far from x .

In the spirit of making each step by the algorithm entirely determined by local information, which will in turn entail valuable independence properties as soon as we switch to a random setting, we add extra data to inputs and outputs: we let the algorithm run on triples of the form (τ, x, s) , where s is one of four *states*, and output a triple (τ', x', s') .

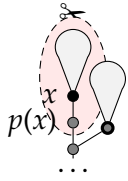
Three of the states simply mimic the cases listed above: we call them w_0 , $w_{>0}$ and b ; a fourth state, labelled j for *jump*, is devised to deal specifically with situations that fall under case [b.3]: the idea is that, instead of simply outputting an entirely different tree paired with the target of the jump, the algorithm goes into a *jump* state; it proceeds modifying the tree a little at a time until it reaches the original target, at which point it 'lands' in one of the three non-jump states.

We propose to re-define outputs according to the state of the input triple, keeping in mind that they mostly adhere to the preceding description for pairs; if the output state in the triple (τ', x', s') is known *not* to be j , then it is determined by (τ', x') . The initial state, in particular, is not jump: given τ and a vertex x , it can be determined as being

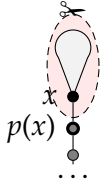
- w_0 , if x is a white leaf of τ ;
- $w_{>0}$, if x is white and it is not a leaf in τ ;
- b , if x is black.

The behaviour of the algorithm for an input triple of the form (τ, x, w_0) or $(\tau, x, w_{>0})$, and for input triples (τ, x, b) with x having one or more right siblings, is exactly that described in cases $[w_0]$, $[w_{>0.1}]$, $[w_{>0.2}]$, $[b.2]$ and $[b.1]$. Namely, the tree τ' and a vertex x' are produced, and the state s' is selected again among the three non-jump states $(w_0, w_{>0}, b)$ according to the colour and degree of the output vertex x' (white leaf, white non-leaf, black).

We now describe the behaviour of the algorithm when the input is of the form (τ, x, b) , and x is the rightmost child of its parent. As explained earlier (case $[b.3]$), the next vertex in a map-geodesic to the root would be (without loss of generality) $t(x)$. We distinguish yet two subcases.

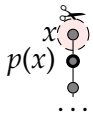


[b.3.1] If $t(x)$ has height $|x| - 1$ (that is, if $p(x)$ has a right sibling: again, a local property) then define τ' by erasing $\tau^{p(x)}$ from τ and output $(\tau', t(x), s')$, where s' is – again – one of $w_0, w_{>0}, b$, according to properties of $t(x)$ in τ' .

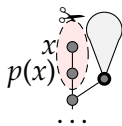


[b.3.2] If, however, $p(x)$ has no right siblings, then it is time to finally put the jump state j to use. We define τ' to be $\tau \setminus \tau^x$ and output $(\tau', p(x), j)$. Notice that now $p(x)$ has height $|x| - 1$ in τ' , and that the identity of $t(x)$ can still be recovered in τ' (even though vertex x has been erased) by the sole knowledge of $p(x)$: if $p(x)$ were black, $t(x)$ would be the target of $p(x)$.

We finally give instructions for the algorithm to follow when confronted with a jump state. Suppose we have an input (τ, x, j) ;



[j.1] if $p(x)$ has no right siblings, then output $(\tau \setminus \tau^x, p(x), j)$; this way, the vertex on which the geodesic should land is still the target of $p(x)$ (or would be if $p(x)$ were black) and its map-distance from the root remains unchanged;



[j.2] if $p(x)$ has right siblings, then the leftmost one (call it x') is the (image of the) vertex the geodesic was supposed to land on; output $(\tau \setminus \tau^{p(x)}, x', s')$, with s' being appropriately chosen among the three non-jump states.

We now summarise the key properties of the algorithm as just described: given a well bicoloured tree τ and a vertex x of height n , we can generate a sequence of $n + 1$ triples (τ_i, x_i, s_i) , with i ranging from 0 to n , where

- for each i , τ_i is a well bicoloured tree, x_i is a vertex of τ and s_i is one of four states $(w_0, w_{>0}, b, \text{ or } j)$;
- τ_0 is the tree τ deprived of all that lies left of the (tree) path from the root to x , and $x_0 = x$;

- $(\tau_{i+1}, x_{i+1}, s_{i+1})$ is obtained from (τ_i, x_i, s_i) as described, with changes of a ‘local’ nature;
- for each i , the height of x_i in τ_i is $n - i$; consequently, x_n is the root of τ_n ;
- for each i between 0 and $n - 1$ such that $s_i \neq j$, $d(\tau_{i+1}, x_{i+1}) = d(\tau_i, x_i) - 1$; therefore,

$$d(\tau, x) = \sum_{0 \leq i < n | s_i \neq j} 1 = n - |\{0 \leq i < n | s_i = j\}|; \quad (\star)$$

that is, the distance $d(\tau, x)$ is the number of non-jump states appearing in the input triples on which the algorithm runs (indeed, it is also the number of non-jump states appearing in the n output triples, because s_n cannot be j and neither can s_0). We will make frequent use of this fact in what follows.

The time has come to run our algorithm on a random tree. Ideally, one would run the algorithm on a uniformly random well bicoloured tree with n vertices; notice that the measure induced on plane trees with n vertices by forgetting the bicolouring of such a tree, however, is not the uniform measure. We shall see that, in fact, we may run a version of the algorithm on random vertices of height n in a critical geometric Galton–Watson tree, uniformly bicoloured, slightly altered so as to give it a white rightmost branch. In order to do this effectively, an especially useful tool is the standard construction of the *geometric Galton–Watson tree conditioned to survive*, which will provide us with a way of unifying results given by the algorithm for vertices of arbitrary height into a single random variable. This tool has already been introduced in Section 2.5; the next section will recall definitions and provide some additional notation needed for further progress.

II.5 The Galton–Watson tree conditioned to survive

For the purpose of the next sections, we shall use the second description provided in Section 2.5 of the *critical Galton–Watson tree conditioned to survive* with a geometric offspring distribution. We briefly recall it here in order to adjust notation to our present needs.

Build a random infinite tree, called T_∞ , in the following way: consider an infinite path $v_0 v_1 \dots v_n \dots$, called the *spine*; let $(\lambda^i)_{i \geq 0}$ be a sequence of independent critical geometric Galton–Watson trees (that is, with offspring distribution μ , where $\mu(k) = 2^{-k-1}$ for all natural numbers k), and let $(\rho^i)_{i \geq 0}$ be another such sequence, independent of the first; we consider the Galton–Watson trees as random rooted plane trees and, for each $i \geq 0$, attach λ^i to the spine by identifying its root and v_i , so that λ^i lies to the left of the spine; similarly, attach each ρ^i so that its root is identified with v_i and all of its vertices lie to the right of the spine (see Figure II.4a); finally, root the random infinite tree thus obtained in v_0 .

The relevance of critical geometric Galton–Watson trees lies in the fact that, if θ is one such tree and θ_n is the random tree obtained by conditioning θ on having exactly

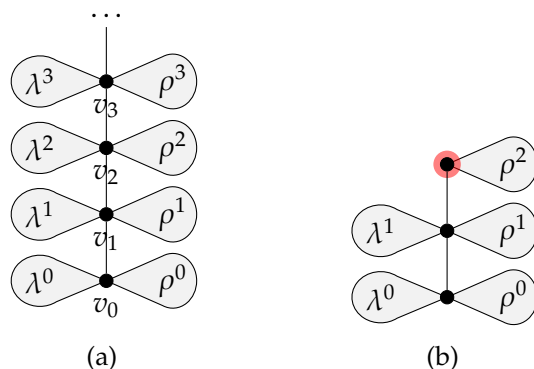


Figure II.4: Figure (a) represents the critical geometric Galton–Watson tree conditioned to survive; trees $\rho^1, \dots, \rho^n, \dots$ and $\lambda^1, \dots, \lambda^n, \dots$ are independent geometric Galton–Watson trees. Figure (b) represents $\text{cut}_2(T_\infty)$.

n vertices, then θ_n is uniformly distributed over plane trees with n vertices; as a result, the tree T_∞ itself has much to do with (uniform) random plane trees, as we shall now see.

We write $\text{cut}_n(T_\infty)$ for the pair (τ, v_n) , where τ is the (finite plane rooted) tree obtained from T_∞ by erasing every descendant of v_n which lies *strictly to the left* of v_{n+1} , together with v_{n+1} itself and all of its descendants: that is, τ consists of the path $v_0 \dots v_n$, with trees ρ^0, \dots, ρ^n attached to the right and trees $\lambda^0, \dots, \lambda^{n-1}$ attached to the left. Then we have the following standard result.

Lemma II.5.1. *Let F be a non-negative real valued function defined on pairs (τ, u) , where τ is a finite rooted plane tree and u is a vertex in τ ; let θ be a Galton–Watson tree with critical geometric offspring distribution. Then for all $n \geq 0$*

$$\mathbb{E} [F(\text{cut}_n(T_\infty))] = \mathbb{E} \left[\sum_{\substack{u \in \theta \\ |u|=n}} F(\theta, u) \right].$$

Proof. For the left hand side we have

$$\begin{aligned} \mathbb{E} [F(\text{cut}_n(T_\infty))] &= \sum_{(\tau, u)} F(\tau, u) \text{GW}(\text{cut}_n(T_\infty) = (\tau, u)) = \\ &= \sum_{\tau} \sum_{\substack{u \in \tau \\ |u|=n}} F(\tau, u) \text{GW}(\text{cut}_n(T_\infty) = (\tau, u)) \end{aligned}$$

where (τ, u) ranges among all pairs formed by a finite (rooted plane) tree and a vertex u of height n in the tree.

Thus it is enough to show that, for all such pairs (τ, u) ,

$$\text{GW}(\text{cut}_n(T_\infty) = (\tau, u)) = \text{GW}(\theta = \tau).$$

But the probability $\mathbb{GW}(\text{cut}_n(T_\infty) = (\tau, u))$ is easy to compute: consider the set formed by u and its ancestors in τ ; order them according to height, and label them u_0, \dots, u_n , so that $|u_i| = i$ (u_0 is the root and u_n is u). For $i = 0, \dots, n-1$, let τ_l^i be the subtree of τ formed by u_i and its descendants lying strictly to the left of u_{i+1} . Similarly, let τ_r^i be the subtree of τ formed by u_i and its descendants lying strictly to the right of u_{i+1} . Then

$$\begin{aligned} \mathbb{GW}(\text{cut}_n(T_\infty) = (\tau, u)) &= \left(\prod_{i=0}^{n-1} \mathbb{GW}(\lambda^i = \tau_l^i) \mathbb{GW}(\rho^i = \tau_r^i) \right) \cdot \mathbb{GW}(\rho^n = \tau^u) = \\ &= \left(\prod_{i=0}^{n-1} \mathbb{GW}(\theta = \tau_l^i) \mathbb{GW}(\theta = \tau_r^i) \right) \cdot \mathbb{GW}(\theta = \tau^u). \end{aligned}$$

Now, for each vertex x in τ , let $c(x)$ be the number of children of x in τ ; clearly,

$$\mathbb{GW}(\theta = \tau) = \prod_{x \in \tau} 2^{-c(x)-1}$$

by definition of θ .

On the other hand, for each vertex in tree τ_l^i (i between 1 and $n-1$) call $c_l(x)$ the number of its children in τ_l^i ; similarly, call $c_r(x)$ the number of children of x in τ_r^i , if x belongs to such a tree. Then

$$\mathbb{GW}(\text{cut}_n(T_\infty) = (\tau, u)) = \prod_{i=0}^{n-1} \left\{ \prod_{x \in \tau_l^i} 2^{-c_l(x)-1} \prod_{x \in \tau_r^i} 2^{-c_r(x)-1} \right\} \cdot \prod_{x \in \tau^u} 2^{-c(x)-1}.$$

Consider any vertex x of τ such that $x \notin \{u_0, \dots, u_{n-1}\}$; then x appears only once in the expression above, as part of some tree τ_l^j or τ_r^j , or possibly of τ^u . Furthermore, the number of children of x in its subtree ($c_l(x)$ or $c_r(x)$ or $c(x)$) is exactly the same as the number of children $c(x)$ that x has in τ . Now, for $i = 0, \dots, n-1$, consider u_i ; it appears inside two of the products, as part of tree τ_l^i and tree τ_r^i , therefore it contributes to $\mathbb{GW}(\text{cut}_n(T_\infty) = (\tau, u))$ with a factor $2^{-c_l(u_i)-1} 2^{-c_r(u_i)-1}$; on the other hand, u_i has $c(u_i) = c_l(u_i) + c_r(u_i) + 1$ children in τ , so that its contribution to $\mathbb{GW}(\theta = \tau)$ is a factor $2^{-c(u_i)-1} = 2^{-c_l(u_i)-c_r(u_i)-2}$.

Consequently, we have $\mathbb{GW}(\text{cut}_n(T_\infty) = (\tau, u)) = \mathbb{GW}(\theta = \tau)$, as wanted. \square

In order to adapt the notion of the critical geometric Galton–Watson tree conditioned to survive to our prior setting, we need to endow it with a random bicolouring. We do this by simply choosing the colour for each vertex of T_∞ uniformly at random with probability $1/2$. In what follows, since the context will determine whether or not trees are bicoloured, we will still write T_∞ for the object just introduced, namely the *critical geometric Galton–Watson tree conditioned to survive, uniformly bicoloured*.

Similarly, if τ is a (random) finite tree, it can be uniformly bicoloured by choosing a colour for each of its vertices independently and uniformly at random, conditionally on τ itself. This applies in particular when τ is a critical geometric Galton–Watson tree.

Finally, we remark that a bicoloured critical geometric Galton–Watson tree is not necessarily *well* bicoloured; given a finite bicoloured tree τ , we define the new tree τ° as the one obtained by adding a white leaf as rightmost child of the root of τ and recolouring the root white, so that τ° is well bicoloured; we will always think of τ as being embedded in τ° in the obvious way. One may of course consider map-distances on τ° : given a vertex u in τ , we write $d^\circ(\tau, u) = d(\tau^\circ, u)$ for the map distance between vertex u and the root in τ° . Analogously, we may consider $d^\circ(\text{cut}_n(T_\infty))$, which, if $\text{cut}_n(T_\infty) = (\tau, u)$, we take to mean $d(\tau^\circ, u)$.

II.6 The algorithm running on the infinite bicoloured tree

Let T_∞ be the critical geometric Galton–Watson tree conditioned to survive, uniformly bicoloured; call v_0, \dots, v_n, \dots the vertices on its spine (v_0 being the root). The distance $d^\circ(\text{cut}_n(T_\infty))$ is, for each positive integer n , a random variable which we wish to estimate (at least asymptotically in n).

We have described in Section II.4 an algorithm that can now be started on (τ°, x, s) , where $(\tau, x) = \text{cut}_n(T_\infty)$ and s depends on the colour and offspring of x in τ (therefore on T_∞ and n); this will yield a sequence of n states s_0, \dots, s_{n-1} , each a random variable taking values in the space of states $\Sigma = \{w_0, w_{>0}, b, j\}$, such that

$$d^\circ(\text{cut}_n(T_\infty)) = n - |\{0 \leq i < n \mid s_i = j\}|.$$

This sequence $(s_i)_{0 \leq i < n}$ is ‘almost’ a Markov Chain, in the sense clarified by the following fundamental proposition:

Proposition II.6.1. *Fix $n > 0$; take the random infinite tree T_∞ and consider the sequence s_0, \dots, s_{n-2} of the first $n - 1$ inputs for the algorithm from Section II.4, started on (τ°, x, s_0) , where $(\tau, x) = \text{cut}_n(T_\infty)$. Then such a sequence has the same law as (the first $n - 1$ steps of) a Markov chain $(X_i)_{i \geq 0}$ with transition matrix*

$$M = \left(\begin{array}{c|cccc} \text{P} & w_0 & w_{>0} & b & j \\ \hline w_0 & 1/4 & 1/4 & 1/2 & 0 \\ w_{>0} & 1/16 & 5/16 & 5/8 & 0 \\ b & 3/32 & 7/32 & 7/16 & 1/4 \\ j & 1/8 & 1/8 & 1/4 & 1/2 \end{array} \right)$$

and a random initial state distributed as $(1/4, 1/4, 1/2, 0)$.

This proposition plays a key role in finally establishing Theorem II.1.1; it is, in fact, the motivation that led to the algorithm as described in Section II.4, and its proof is nothing but a careful observation of how the various steps of the algorithm interact with the random element: in particular, some key independence properties are always

preserved, mainly thanks to the Galton–Watson structure of subtrees and the nature of the geometric law.

In order to prove Proposition II.6.1, we highlight those exact independence properties in a separate Lemma, for which some additional notation is needed. Suppose the algorithm is started on a triple (τ_0, x_0, s_0) , where x_0 has height n in τ_0 ; we write p^j for the j -th iteration of the parent function, so that $p^0(x_0) = x_0$ and $p^j(x_0)$ has height $n - j$ (in particular, $p^n(x_0)$ is the root of τ_0). We call ρ_0^j the subtree of τ_0 consisting of $p^{n-j}(x_0)$ and its descendants lying *strictly to the right* of $p^{n-j-1}(x_0)$ (so that the tree ρ_0^j is rooted in a vertex of height j in τ_0); ρ_0^n is simply $\tau_0^{x_0}$.

We repeat the same construction for all subsequent triples (τ_i, x_i, s_i) : x_i has height $n - i$; we write ρ_i^j for the subtree of τ_i consisting of $p^{n-i-j}(x_i)$ and its descendants lying *strictly to the right* of $p^{n-i-j-1}(x_i)$ (see Figure II.5); as before, the root of ρ_i^j has height j in τ_i , and $\rho_i^{n-i} = \tau_i^{x_i}$.

We wish to prove the following:

Lemma II.6.2. *Fix $n > 0$ and consider the (random) triples (τ_i, x_i, s_i) obtained from T_∞ through the algorithm for i between 0 and $n - 2$. Then for each i ,*

- if $s_i = w_0$ or $s_i = b$, then ρ_i^j , for $j = 1, \dots, n - i - 1$, is a sequence of independent uniformly bicoloured Galton–Watson trees;
- if $s_i = w_{>0}$, then ρ_i^j , for $j = 1, \dots, n - i - 1$, is a sequence of independent uniformly bicoloured Galton–Watson trees; also, $\tau_i^{r(x_i)}$ is a uniformly bicoloured Galton–Watson tree independent of the block of the ρ_i^j 's;
- if $s_i = j$, then ρ_i^j , for $j = 1, \dots, n - i - 2$, is a sequence of independent uniformly bicoloured Galton–Watson trees, whilst $\rho_i^{n-i-1} = \{p(x_i)\}$ and $\rho_i^{n-i} = \{x_i\}$.

Proof. We proceed by induction on i ; for $i = 0$, all assertions are trivial by definition of T_∞ (more precisely, by the random structure of $\text{cut}_n(T_\infty)$): with the exception of ρ_0^0 , whose root is recoloured white and has a white leaf attached as a rightmost child, $\rho_0^j = \rho^j$: all right trees attached to the spine of T_∞ are uniformly bicoloured Galton–Watson trees.

We loosely follow the original presentation of the algorithm and deal separately with each case.

Suppose $s_i = w_0$, and consider $(\tau_{i+1}, x_{i+1}, s_{i+1})$; we have $\rho_{i+1}^j = \rho_i^j$ for $j = 1, \dots, n - i - 1$, since all the algorithm does is erase x_i (that is, ρ_i^{n-i}), and the claim follows by the induction hypothesis.

If $s_i = w_{>0}$, then the output of the algorithm depends on whether ρ_i^{n-i-1} consists of only $p(x_i)$ or not. If $s_{i+1} = b$ or $s_{i+1} = w_0$, then $\rho_{i+1}^j = \rho_i^j$ for $j = 1, \dots, n - i - 2$, which is all

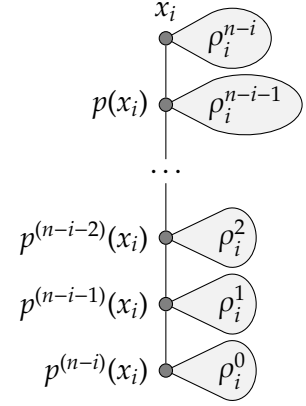


Figure II.5: Structure of τ_i .

that is required. The same is true for $s_{i+1} = w_{>0}$, but we also need to show that $\tau_{i+1}^{r(x_{i+1})}$ is Galton–Watson and independent of the ρ_{i+1}^j ’s. The subtree ρ_{i+1}^{n-i-1} is determined by the algorithm as follows. If $\rho_i^{n-i-1} = \{p(x_i)\}$ then it is isomorphic to $\tau_i^{r(x_i)}$ (we are interested only in the case of $r(x_i)$ and $p(x_i)$ being white), which has the required properties by the induction hypothesis. Otherwise we simply have $\rho_{i+1}^{n-i-1} = \rho_i^{n-i-1}$, and we are done.

If $s_i = b$, then we need to deal with a few cases separately. The most straightforward one is that of $s_{i+1} = j$; what the algorithm does in this case is merely erase $\tau_i^{x_i}$: conditions on trees ρ_{i+1}^j are automatic (including the fact that $\rho_{i+1}^{n-i-2} = \{p(x_{i+1})\}$ and $\rho_{i+1}^{n-i-1} = \{x_{i+1}\}$, or we would not have switched to jump state). If $s_{i+1} = w_0$, this may be for one of two reasons:

- x_i has only one right sibling in τ_i , which is a white leaf, and $p(x_i)$ is white (case [b.2]); there is nothing to prove here, since $\rho_{i+1}^j = \rho_i^j$ for $j = 1, \dots, n - i - 2$;
- x_i has no right sibling in τ_i , but $p(x_i)$ does, and its next sibling is a white leaf (case [b.3.1]); in this case, while trees ρ_i^j remain unchanged for $j \leq n - i - 3$, ρ_{i+1}^{n-i-2} is ρ_i^{n-i-2} with its leftmost branch erased; on the other hand, what we have done is precisely condition such a tree on having a leftmost branch made up of a white leaf, and then remove it, which leaves nothing but a Galton–Watson tree.

The case of $s_{i+1} = b$ presents no added difficulties apart for the need for more casework. One needs to deal separately with cases [b.2], [b.3.1] (same as above, with a weaker condition to check) and [b.1], which is again trivial. Finally, one has to go through essentially the same for $s_{i+1} = w_{>0}$, but with the added requirement to show that $\tau_{i+1}^{r(x_{i+1})}$ is Galton–Watson and independent of the ρ_{i+1}^j ’s. This is true in case [b.1] ($\tau_{i+1}^{r(x_{i+1})} = \tau_i^{r(p(x_i))}$), [b.2] ($\tau_{i+1}^{r(x_{i+1})} = \tau_i^{r(r(p(x_i)))}$, where $r(r(p(x_i)))$ does exist in τ_i , or we would not go to state $w_{>0}$), and [b.3.1] ($\tau_{i+1}^{r(x_{i+1})} = \tau_i^{r(r(p(p(x_i))))}$).

The very last possibility is for s_i to be j ; if s_{i+1} is j as well, there is hardly anything to prove; all other cases require arguments that are exactly the same as those used for $s_i = b$, and that we shall not repeat.

This concludes the proof by induction. □

Given Lemma II.6.2, Proposition II.6.1 is only a matter of computing transition probabilities. We refer the reader to the summary table in the next page, which covers all of the cases described in Section II.4. For the reader’s convenience, we briefly interpret the table for one of the states, as an example.

Example II.6.1 (Transition probabilities from $w_{>0}$). Consider the case where $s_i = w_{>0}$; if $p(x_i)$ is black, which happens with probability $1/2$, then, regardless of whether we are in case $[w_{>0}.1]$ or $[w_{>0}.2]$, $s_{i+1} = b$, as represented by the last panel in the first row. The panels in the second row represent all possible outcomes for s_{i+1} when $p(x_i)$ is white: if $r(p(x_i)) \neq x_i$ (case $[w_{>0}.1]$) then $x_{i+1} = p(x_i)$ and $s_{i+1} = w_{>0}$; if $x_i = r(p(x_i))$ (case $[w_{>0}.2]$) then s_{i+1} depends on the colour and offspring of $r(x_i)$, as represented by the last three

panels of the second row. One can infer that the transition probabilities from $w_{>0}$ are as follows:

- $1/16$ for w_0 (probability that $p(x_i)$ is white, $r(p(x_i)) = x_i$ and $\tau^{r(x_i)} = \{r(x_i)\}$);
- $5/16$ for $w_{>0}$ (probability that $p(x_i)$ is white and that either $r(p(x_i)) \neq x_i$, or $r(p(x_i)) = x_i$, $r(x_i)$ is white and $\tau^{r(x_i)} \neq \{r(x_i)\}$);
- $5/8$ for b (probability that $p(x_i)$ is black, or that $r(p(x_i)) = x_i$ and $r(x_i)$ is black);
- 0 for j : one can't jump from a white vertex.

Notice that the initial state of the Markov chain is not important for our purposes (since the chain is recurrent and we are only interested in asymptotics); however, one is sure to have $s_0 \neq j$; moreover, $s_0 = b$ if the $(n + 1)$ -th vertex on the spine of T_∞ (which was called x_0) is black (which has probability $1/2$, since $n > 0$), and $s_0 = w_0$ if x_0 is white and ρ_0^n only consists of x_0 (probability $1/4$); hence the initial distribution $(1/4, 1/4, 1/2, 0)$ in the statement of Proposition II.6.1.

The purpose of the algorithm was, since the very beginning, to give estimates for the map-distance of vertices from the root; we are now in a position to easily obtain asymptotics for the distance $d^\circ(\text{cut}_n(T_\infty))$. Namely, we have

Proposition II.6.3. *Let T_∞ be the geometric Galton–Watson tree conditioned to survive, uniformly bicoloured; then*

$$\lim_{n \rightarrow \infty} \frac{d^\circ(\text{cut}_n(T_\infty))}{n} = 7/9,$$

where the convergence is almost sure. More specifically, one has the following Large Deviation result: for all $\varepsilon > 0$ there exist positive n_ε, C such that, for all $n \geq n_\varepsilon$,

$$\mathbb{P}\left(\left|\frac{d^\circ(\text{cut}_n(T_\infty))}{n} - \frac{7}{9}\right| \geq \varepsilon\right) \leq e^{-Cn}.$$

Proof. We know that, for each $n > 1$, the sequence of random states s_0, \dots, s_{n-2} (from the first $n - 1$ triples that act as input for the algorithm when started on $\text{cut}_n(T_\infty)^\circ$) has the distribution described in Proposition II.6.1. Since we have $d^\circ(\text{cut}_n(T_\infty)) = |\{0 \leq i < n | s_i \neq j\}|$, we also have $|d^\circ(\text{cut}_n(T_\infty)) - |\{0 \leq i \leq n - 2 | s_i \neq j\}|| \leq 1$.

On the other hand,

$$\lim_{n \rightarrow \infty} \frac{1}{n} |\{0 \leq i \leq n - 2 | s_i \neq j\}|$$

is a constant by the law of large numbers and is easily computed via the limit distribution for a Markov chain with transition matrix M , which is $\pi = \frac{1}{9}(1, 2, 4, 2)$.

As a consequence, we have

$$\lim_{n \rightarrow \infty} \frac{1}{n} d^\circ(\text{cut}_n(T_\infty)) = \lim_{n \rightarrow \infty} \frac{1}{n} |\{0 \leq i \leq n - 2 | s_i \neq j\}| = 7/9.$$

STATE TRANSITIONS

w_0	$\mathbb{P}(\circ)\mu(0)=\frac{1}{4}$ go to w_0	$\mathbb{P}(\circ)(1-\mu(0))=\frac{1}{4}$ go to $w_{>0}$	$\mathbb{P}(\bullet) = \frac{1}{2}$ go to b	$w_{>0}$ $\mathbb{P}(\bullet) = \frac{1}{2}$ go to b
	$\mathbb{P}(\circ)(1-\mu(0))=\frac{1}{4}$ go to $w_{>0}$	$\mathbb{P}(\circ)\mathbb{P}(\bullet)\mu(0)=\frac{1}{8}$ go to b	$\mathbb{P}(\circ)^2\mu(0)(1-\mu(0))=\frac{1}{16}$ go to $w_{>0}$	$\mathbb{P}(\circ)^2\mu(0)^2=\frac{1}{16}$ go to w_0
b	$\mathbb{P}(\circ)(1-\mu(0)-\mu(1))=\frac{1}{8}$ go to $w_{>0}$	$\mathbb{P}(\bullet)(1-\mu(0)-\mu(1))=\frac{1}{8}$ go to b	$\mathbb{P}(\circ, \bullet, \bullet, \bullet)\mu(1)=\frac{3}{16}$ go to b	$\mathbb{P}(\circ)^2\mu(1)(1-\mu(0))=\frac{1}{32}$ go to $w_{>0}$
	$\mathbb{P}(\circ)^2\mu(1)\mu(0)=\frac{1}{32}$ go to w_0	$\mathbb{P}(\bullet)\mu(0)(1-\mu(0))=\frac{1}{8}$ go to b	$\mathbb{P}(\circ)\mu(0)(1-\mu(0))^2=\frac{1}{16}$ go to $w_{>0}$	$\mathbb{P}(\circ)\mu(0)^2(1-\mu(0))=\frac{1}{16}$ go to w_0
	$\mu(0)^2 = \frac{1}{4}$ go to j			
j	$\mathbb{P}(\bullet)(1-\mu(0))=\frac{1}{4}$ go to b	$\mathbb{P}(\circ)(1-\mu(0))^2=\frac{1}{8}$ go to $w_{>0}$	$\mathbb{P}(\circ)\mu(0)(1-\mu(0))=\frac{1}{8}$ go to w_0	$\mu(0) = \frac{1}{2}$ go to j

Table 3.1: Transitions from states w_0 , $w_{>0}$, b and j . Vertices enclosed within a red region get identified by the algorithm.

The second part of the proposition is a direct consequence of classical results of Large Deviation Theory about Markov chains with a finite state space, see for example Chapter 3 of [32]. The statement is true if we substitute $S_n = |\{0 \leq i \leq n-2 | s_i \neq j\}|$ for $d^\circ(\text{cut}_n(T_\infty))$, because s_0, \dots, s_{n-2} is a (recurrent) Markov chain with finite state space.

The inequality $|d^\circ(\text{cut}_n(T_\infty)) - S_n| \leq 1$ implies that $\text{GW}(d^\circ(\text{cut}_n(T_\infty)) = d) \leq \text{GW}(|S_n - d| \leq 1)$ for any natural number d , and thus

$$\text{GW}\left(\left|\frac{d^\circ(\text{cut}_n(T_\infty))}{n} - \frac{7}{9}\right| \geq \varepsilon\right) \leq \text{GW}\left(\left|\frac{S_n}{n} - \frac{7}{9}\right| \geq \varepsilon - \frac{1}{n}\right)$$

which establishes the result for $d^\circ(\text{cut}_n(T_\infty))$. \square

II.7 Final proofs

The final technical steps follow [27], but we need to bypass the rerooting argument exploited there by establishing a more practical control on all map-distances (not only map-distances from the root, as we have done so far). We will start, however, with a proposition dealing only with map-distances from the root, in order to extend the statement as soon as all of the necessary lemmas are in place.

Before we start, let us introduce a little notation: suppose $(x_n)_{n \geq 1}$ is a sequence of real numbers; we write $x_n = \text{oe}(n)$ to mean that $x_n \leq C_1 e^{-C_2 n^a}$ for some positive C_1, C_2, a . Also, in the following proposition and proof, we will write c for the constant $\frac{7}{9}$, which we obtained in Section II.6, and d for the usual graph distance on the outerplanar map obtained from a tree via the bijection Ψ , with $d(u)$ being the graph distance of u from the root vertex.

Proposition II.7.1. *Let τ_n be a uniformly random well bicoloured tree with n vertices, and let $\Delta(\tau_n)$ be its (random) diameter; then for all $\varepsilon > 0$*

$$p_n = \text{GW}\left(\exists u \in \tau_n \text{ s.t. } |d(\tau_n, u) - c|u|| \geq \varepsilon \max\{\Delta(\tau_n), \sqrt{n}\}\right) = \text{oe}(n).$$

Proof. For any positive integer k , we call τ_n^k a random well bicoloured tree with n vertices conditioned on having a rightmost branch of length exactly k . We claim that the probability of τ_n having a rightmost branch of length greater than $\varepsilon \sqrt{n}/4$ is $\text{oe}(n)$; we shall need a more general result before the end of this section, and we postpone the proof of this claim, in a stronger form, until the end of the proof (see Lemma II.7.2). Given the claim, we have that p_n is $\text{oe}(n)$ if and only if the same is true for

$$\sum_{k=1}^{\frac{\varepsilon}{4} \sqrt{n}} q_{n,k} \text{GW}\left(\exists u \in \tau_n^k \text{ s.t. } |d(\tau_n^k, u) - c|u|| \geq \varepsilon \max\{\Delta(\tau_n^k), \sqrt{n}\}\right)$$

where $q_{n,k}$ is the probability that τ_n has a rightmost branch of length exactly k .

Let us consider a single term of the sum. Notice that, for each k , τ_n^k can be seen as a random forest of k ordered trees, with $n-1$ vertices between them, such that the trees are linked by the roots with a path going from left to right, and a single extra vertex is linked to the root of the rightmost tree; each of the trees is bicoloured (not necessarily well bicoloured) with the only condition of having a white root; the rightmost vertex is white.

The number of such forests, if we ignore the bicolouring, is well known to be the generalised Catalan number $\text{Cat}(n-1-k, k)$ (see for example [14]), where

$$\text{Cat}(n, k) = \frac{k}{n+k} \binom{2n+k-1}{n},$$

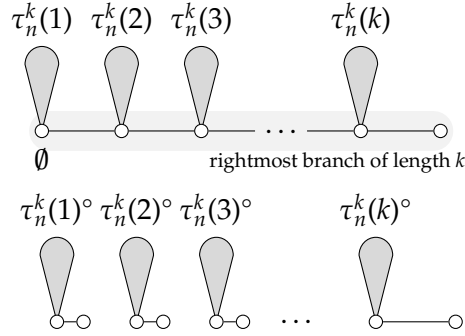


Figure II.6: The tree τ_n^k seen as a forest of k linked rooted plane trees.

whereas the number of (rooted plane) trees with $n + 1$ vertices is $\text{Cat}(n) = \text{Cat}(n, 1)$.

We label the k (random) trees in the forest τ_n^k , ordered from left to right, $\tau_n^k(1), \dots, \tau_n^k(k)$; if, for each i between 1 and k , we condition $\tau_n^k(i)$ on having a certain number n_i of vertices (with $n_i \geq 1$ and $n_1 + \dots + n_k = n - 1$), then $\tau_n^k(i)$ simply becomes a random plane tree with n_i vertices (uniformly bicoloured but with a white root), which we call θ_{n_i} .

Notice now that, for any vertex u in $\tau_n^k(i)$, $|d(\tau_n^k, u) - d^\circ(\tau_n^k(i), u)| \leq k$; also, the height of u in $\tau_n^k(i)$ differs from the height of u in τ_n^k by at most k , and we have the obvious inequality $\Delta(\tau_n^k(i)) \leq \Delta(\tau_n^k)$ between diameters. As a consequence,

$$\begin{aligned} & \text{GW}\left(\exists u \in \tau_n^k \text{ s.t. } |d(\tau_n^k, u) - c|u|| \geq \varepsilon \max\{\Delta(\tau_n^k), \sqrt{n}\}\right) \leq \\ & \leq \sum_{i=1}^k \text{GW}\left(\exists u \in \tau_n^k(i) \text{ s.t. } |d^\circ(\tau_n^k(i), u) - c|u|| \geq \varepsilon \max\{\Delta(\tau_n^k(i)), \sqrt{n}\} - 2k\right) \end{aligned}$$

where in the second expression we still write $|u|$ for the height of the vertex in $\tau_n^k(i)$.

Hence the probability above is no more than

$$\max_{\substack{n_1, \dots, n_k > 0 \\ n_1 + \dots + n_k = n-1}} \sum_{i=1}^k \text{GW}\left(\exists u \in \theta_{n_i} \text{ s.t. } |d^\circ(\theta_{n_i}, u) - c|u|| \geq \varepsilon \max\{\Delta(\theta_{n_i}), \sqrt{n}\} - 2k\right).$$

Now, we know that $k \leq \frac{\varepsilon}{4} \sqrt{n}$, and therefore we can reduce to evaluating the expression

$$\frac{\varepsilon}{4} \sqrt{n} \max_{0 < m < n} \text{GW}\left(\exists u \in \theta_m \text{ s.t. } |d^\circ(\theta_m, u) - c|u|| \geq \frac{\varepsilon}{2} \max\{\Delta(\theta_m), \sqrt{n}\}\right).$$

Let θ be a uniformly bicoloured Galton–Watson tree (see Section II.5); the probability that θ has m vertices is $2^{-2m-1} \text{Cat}(m-1)$, which is asymptotic to $m^{-\frac{3}{2}}$; we can therefore find a constant C_1 such that, for any m , $2^{-2m-1} \text{Cat}(m-1) \geq C_1 m^{-\frac{3}{2}}$. This guarantees that, for any positive integer m less than n ,

$$\text{GW}\left(\exists u \in \theta_m \text{ s.t. } |d^\circ(\theta_m, u) - c|u|| \geq \frac{\varepsilon}{2} \max\{\Delta(\theta_m), \sqrt{n}\}\right) \leq$$

$$\leq \frac{1}{C_1} m^{\frac{3}{2}} \cdot \mathbb{GW} \left(\exists u \in \theta \text{ s.t. } |d^\circ(\theta, u) - c|u|| \geq \frac{\varepsilon}{2} \max\{\Delta(\theta), \sqrt{n}\} \right).$$

If we write q_n for the probability appearing in the above expression, then (since $m \leq n$) proving $q_n = \text{oe}(n)$ would guarantee that the above – and therefore p_n – is $\text{oe}(n)$. We shall now turn to the former endeavour.

It is clear that

$$q_n \leq \mathbb{E} \left[\sum_{u \in \theta} \mathbb{1} \left(|d^\circ(\theta, u) - c|u|| \geq \frac{\varepsilon}{2} \max\{\Delta(\theta), \sqrt{n}\} \right) \right]$$

and, grouping vertices together according to height, the latter can be rewritten as

$$\mathbb{E} \left[\sum_{j \geq 1} \sum_{\substack{u \in \theta \\ |u|=j}} \mathbb{1} \left(|d^\circ(\theta, u) - cj| \geq \frac{\varepsilon}{2} \max\{\Delta(\theta), \sqrt{n}\} \right) \right] \leq \sum_{j \geq 1} \mathbb{E} \left[\sum_{\substack{u \in \theta \\ |u|=j}} \mathbb{1} \left(|d^\circ(\theta, u) - cj| \geq \frac{\varepsilon}{2} \max\{j, \sqrt{n}\} \right) \right]$$

where we have used the fact that, for each u in the sum, we have $d(\theta) \geq |u|$.

We can now use Lemma II.5.1 to turn the expression above into

$$\sum_{j \geq 1} \mathbb{GW} \left(|d^\circ(\text{cut}_j(T_\infty)) - cj| \geq \frac{\varepsilon}{2} \max\{j, \sqrt{n}\} \right)$$

where T_∞ is the critical geometric Galton–Watson tree conditioned to survive, randomly bicoloured, as presented in Section II.5.

We split the sum into two parts, which we will deal with separately: the sum for $j \leq n^{1/4}$ and that of the terms with $j > n^{1/4}$.

Suppose that $j \leq n^{1/4}$; clearly, $d^\circ(\text{cut}_j(T_\infty)) \leq j$, and $\max\{j, \sqrt{n}\} = \sqrt{n}$. This gives $|d^\circ(\text{cut}_j(T_\infty)) - cj| \leq d^\circ(\text{cut}_j(T_\infty)) + cj \leq (1+c)j \leq (1+c)n^{1/4}$. Thus it is enough to choose n so that $(1+c)n^{1/4} < \frac{\varepsilon}{2} \sqrt{n}$, that is $n^{1/4} > \frac{2+2c}{\varepsilon}$, to obtain that

$$\sum_{j=1}^{\lfloor n^{1/4} \rfloor} \mathbb{GW} \left(|d^\circ(\text{cut}_j(T_\infty)) - cj| \geq \frac{\varepsilon}{2} \max\{j, \sqrt{n}\} \right) = 0.$$

As for the sum with $j > n^{1/4}$, we have

$$\mathbb{GW} \left(|d^\circ(\text{cut}_j(T_\infty)) - cj| \geq \frac{\varepsilon}{2} \max\{j, \sqrt{n}\} \right) \leq \mathbb{P} \left(\left| \frac{d^\circ(\text{cut}_j(T_\infty))}{j} - c \right| \geq \frac{\varepsilon}{2} \right)$$

which, by choosing n appropriately according to Proposition II.6.3, can be bounded by e^{-Cn} .

This gives, for n suitably big, the bound

$$\sum_{j > n^{1/4}} e^{-Cj} = \text{oe}(n),$$

which is our aim. □

We now prove the claim from the beginning of the proof, in the form of the following Lemma:

Lemma II.7.2. *Let τ_n be a random well bicoloured plane tree with n vertices, and let $\alpha, \varepsilon > 0$ be positive real numbers; we call a path in τ_n an ancestor path if it is of the form $x_0 \dots x_l$, with $x_i = p(x_{i-1})$ for all integers i such that $1 \leq i \leq l$. Then*

$\text{GW}(\tau_n \text{ has an ancestor path of length at least } \alpha n^\varepsilon \text{ entirely made up of white vertices}) = \text{oe}(n)$;

in particular, the probability that τ_n has a rightmost branch of length at least αn^ε is $\text{oe}(n)$.

Proof. We start by showing the last, more specific assertion: that the probability of τ_n having a rightmost branch of length at least αn^ε is $\text{oe}(n)$.

For any $d > 0$, the number of bicoloured trees with n vertices and a rightmost branch of length d , as seen within the proof of Proposition II.7.1, is

$$2^{n-1-d} \text{Cat}(n-1-d, d) = 2^{n-1-d} \frac{d}{2n-2-d} \binom{2n-2-d}{n-1-d},$$

that is the number of plane trees with n vertices and a rightmost branch of length d (or, equivalently, of sequences of d plane trees with $n-1$ vertices in total, see Figure II.6), multiplied by the number of possible bicolourings (2^{n-1-d} , since $d+1$ out of the n vertices belong to the rightmost branch of the tree).

The total number of outerplanar maps with n vertices is asymptotic (up to a multiplicative constant) to $2^{3n} n^{-\frac{3}{2}}$, as can be easily obtained from Stirling estimates for the above formula (see, for detailed analogous computations, [14]); on the other hand,

$$\sum_{\alpha n^\varepsilon < d < n} 2^{n-1-d} \text{Cat}(n-1-d, d) \leq \sum_{\alpha n^\varepsilon < d < n} 2^{n-1-d} \binom{2n-2-d}{n-1-d},$$

which in turn is less than

$$2^{3n} p(n) \sum_{\alpha n^\varepsilon < d < n} 2^{-2d},$$

where $p(n)$ a polynomial in n . As a consequence, the above expression divided by the total number of outerplanar maps with n vertices is $\text{oe}(n)$.

It is now very easy to extend the result to general ancestor paths. Since the probability that τ_n has a rightmost branch of length at least $\frac{\alpha}{2} n^\varepsilon$ we have shown to be $\text{oe}(n)$, we may assume τ_n is conditioned on having a rightmost branch of length less than $\frac{\alpha}{2} n^\varepsilon$. For each vertex v of height at least αn^ε in τ_n consider the path $P_v = vp(v) \dots p^i(v) \dots p^{\lceil \alpha n^\varepsilon \rceil}(v)$. No more than $\frac{1}{2} \alpha n^\varepsilon$ of its vertices belong to the rightmost branch of τ_n , and thus the probability of P_v being entirely white is at most $2^{-\frac{\alpha}{2} n^\varepsilon}$. Hence

$$\text{GW} \left(\begin{array}{l} \tau_n \text{ has an ancestor path of length } \alpha n^\varepsilon \text{ entirely made up of white} \\ \text{vertices and the rightmost branch of } \tau_n \text{ is shorter than } \frac{\alpha}{2} n^\varepsilon \end{array} \right) < n \cdot 2^{-\frac{\alpha}{2} n^\varepsilon}$$

which is $\text{oe}(n)$ as wanted. □

Proposition II.7.1 is a substantial step toward being able to bound the Gromov–Hausdorff distance between a (rescaled) tree and its corresponding planar map, but dealing with distances from the root is not enough: we need a way to derive results of the same kind about distances between generic vertices.

To this end, we will rewrite the map-distance between two vertices in terms of the distances between each vertex and the root. This is easily done when the vertices in question are related, and the one of smaller height is black; this basic case we will use as a stepping stone, together with Lemma II.7.2, to establish the required general result.

Lemma II.7.3. *Let τ be a bicoloured tree and v a vertex in τ ; let w be a black ancestor of v in τ , \emptyset the root of τ ; call d_M the map-distance on τ and (as in Section II.3) write $d_M(u)$ for $d_M(u, \emptyset)$. Then $|d_M(v, w) - d_M(v) + d_M(w)| \leq 2$.*

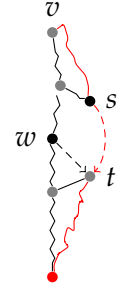
Proof. Consider a map-geodesic from v to the root; if this path goes through w , then $d_M(v) = d_M(v, w) + d_M(w)$. If it does not, then at some point it jumps from a descendant s of w onto a target t ‘below’ w , which must be the child of an ancestor of w , thus also the target of w . We have

$$d_M(v, s) \leq d_M(v, w) \leq d_M(v, s) + 2$$

$$d_M(v) = d_M(v, s) + 1 + d_M(t)$$

$$d_M(t) \leq d_M(w) \leq d_M(t) + 1$$

hence $|d_M(v) - d_M(v, w) - d_M(w)| \leq 2$ as wanted. \square



Here is a general statement analogous to Proposition II.7.1, where we write $d_T(u, v)$ for the distance of two vertices *in the tree*, and d_M for the map distance (again, with $d_M(u)$ being the map distance from the root).

Corollary II.7.4. *Let τ_n be a random well bicoloured tree with n vertices, and let $\Delta(\tau_n)$ be its (random) diameter; then for all $\varepsilon > 0$*

$$\mathbb{GW}\left(\exists u, v \in \tau_n \text{ s.t. } |d_M(u, v) - cd_T(u, v)| \geq \varepsilon \max\{\Delta(\tau_n), \sqrt{n}\}\right) = \text{oe}(n).$$

Proof. Thanks to Lemma II.7.2 (by choosing $\alpha = \frac{\varepsilon}{8}$) we may restrict ourselves to the event of τ_n having no white ancestor path of length $\frac{\varepsilon}{8} \sqrt{n}$ or greater.

Consider, given u and v vertices of τ_n , their first common ancestor w . Either $|w| > \frac{\varepsilon}{8} \sqrt{n}$, in which case there is a *black* ancestor z of w such that $d_T(w, z) \leq \frac{\varepsilon}{8} \sqrt{n}$ (otherwise there would be a long white ancestor path), or $|w| < \frac{\varepsilon}{8} \sqrt{n}$, in which case we just set z to be the root of τ_n .

Suppose without loss of generality that u lies to the left of v and let w' be the child of w that is also an ancestor of v ; then a map-geodesic from u to v goes through at least one of w and w' , thanks to an argument very similar to that employed in Proposition II.3.1. This yields that $|d_M(u, v) - d_M(u, w) - d_M(w, v)| \leq 2$ (this is trivial if the map-geodesic passes

through w ; if it goes through w' then we have $|d_M(u, v) - d_M(u, w) - d_M(w, v)| = |d_M(u, w') + d_M(w', v) - d_M(u, w) - d_M(w, v)| \leq |d_M(u, w') - d_M(u, w)| + |d_M(w', v) - d_M(w, v)| \leq 2$.

Also notice that we have $|d_M(u, w) - d_M(u, z)| \leq d_M(w, z) \leq \frac{\varepsilon}{8} \sqrt{n}$, and the same inequality is true if we substitute v for u .

Now, if z is black, then $|d_M(u, z) - d_M(u) + d_M(z)| \leq 2$ and $|d_M(v, z) - d_M(v) + d_M(z)| \leq 2$ by Lemma II.7.3; otherwise z is the root of τ_n , and the same assertions are trivial (since $d_M(u, z) = d_M(u)$ and $d_M(z) = 0$).

All of the above observations combined yield

$$\begin{aligned} |d_M(u, v) - cd_T(u, v)| &= |d_M(u, v) - c(|u| + |v| - 2|w|)| \leq \\ &\leq \frac{\varepsilon}{2} \sqrt{n} + 6 + |d_M(u) - c|u|| + |d_M(v) - c|v|| + 2|d_M(z) - c|z||. \end{aligned}$$

Hence

$$\text{GW}\left(\exists u, v \in \tau_n \text{ s.t. } |d_M(u, v) - cd_T(u, v)| \geq \varepsilon \max\{\Delta(\tau_n), \sqrt{n}\}\right) \leq$$

$$\text{GW}\left(\exists u, v, z \in \tau_n \text{ s.t. } \frac{\varepsilon}{2} \sqrt{n} + 6 + |d_M(u) - c|u|| + |d_M(v) - c|v|| + 2|d_M(z) - c|z|| \geq \varepsilon \max\{\Delta(\tau_n), \sqrt{n}\}\right) \leq$$

$$\text{GW}\left(\exists u, v, z \in \tau_n \text{ s.t. } |d_M(u) - c|u|| + |d_M(v) - c|v|| + 2|d_M(z) - c|z|| \geq \frac{\varepsilon}{4} \max\{\Delta(\tau_n), \sqrt{n}\}\right) \leq$$

$$\text{GW}\left(\exists u \in \tau_n \text{ s.t. } |d_M(u) - c|u|| \geq \frac{\varepsilon}{16} \max\{\Delta(\tau_n), \sqrt{n}\}\right)$$

which we show to be $o_\varepsilon(n)$ by invoking Proposition II.7.1. \square

The time has come for the proof of our main theorem, which is now quite straightforward:

Proof of Theorem II.1.1. Corollary II.7.4 yields that, given a random well bicoloured tree with n vertices τ_n ,

$$\text{GW}\left(d_{\text{GH}}(\Psi(\tau_n), c\tau_n) \geq \varepsilon \max\{\sqrt{n}, \Delta(\tau_n)\}\right) = o_\varepsilon(n)$$

where $\Psi(\tau_n)$ in this context is seen as the metric space made up of the vertices of τ equipped with the map-distance, and $c\tau_n$ is the set of vertices in τ_n , equipped with the graph distance of τ_n rescaled by a factor $c = \frac{7}{9}$.

This is because

$$d_{\text{GH}}(\Psi(\tau_n), c\tau_n) \leq \frac{1}{2} \left(\sup_{u, v \in \tau_n} |d_M(u, v) - cd_T(u, v)| \right),$$

as seen by considering the trivial correspondence between the vertices of τ_n and those of $\Psi(\tau_n)$ (see Infobox 1.2 and in particular Corollary 1.2.2).

Thus we have established that

$$\lim_{n \rightarrow \infty} d_{\text{GH}}\left(\frac{\Psi(\tau_n)}{\max\{\sqrt{n}, \Delta(\tau_n)\}}, \frac{c\tau_n}{\max\{\sqrt{n}, \Delta(\tau_n)\}}\right) = 0$$

in probability, where τ_n is a random rooted well bicoloured plane tree with n vertices, and – given a graph G and a real number k – we take kG to denote the rescaled metric space $(V(G), k \cdot d_{\text{gr}})$.

We now claim that

$$\lim_{n \rightarrow \infty} \left(\tau_n, \frac{d_{\text{gr}}}{\sqrt{2n}} \right) = (\mathcal{T}_e, d_e)$$

in distribution for the Gromov–Hausdorff distance, with (\mathcal{T}_e, d_e) being the CRT.

This result is a consequence of a famous theorem of Aldous [5] and would be immediate if τ_n were replaced by a uniform plane tree with n vertices or, equivalently, by a critical geometric Galton–Watson tree conditioned on having n vertices. Even though this is not the case, τ_n is not very far from the latter: indeed, we saw in Lemma II.7.2 that the length L_n of the rightmost branch of τ_n remains tight (it even converges in distribution) as $n \rightarrow \infty$, and furthermore that, conditionally on $L_n = k$, the k subtrees grafted onto the rightmost branch form a forest $\tau_n^k(1), \tau_n^k(2), \dots, \tau_n^k(k)$ whose total number of vertices is $n - 1$. It is known that such a forest has, as $n \rightarrow \infty$, a unique macroscopic tree $\tilde{\tau}_n$ of size $s_n = n - o(n)$, which is uniformly distributed over all plane trees of size s_n . The scaling limit of τ_n is thus the same as that of $\tilde{\tau}_n$, which is that of a random uniform plane tree of size n . See Section 3.3 of [52] for details.

But then the random variable

$$\frac{\max\{\sqrt{n}, \Delta(\tau_n)\}}{\sqrt{n}}$$

also converges in distribution, and to an almost surely positive random variable. That is, if we multiply by $\frac{\max\{\sqrt{n}, \Delta(\tau_n)\}}{\sqrt{n}}$ we can in fact deduce that

$$\lim_{n \rightarrow \infty} d_{\text{GH}} \left(\frac{\Psi(\tau_n)}{\sqrt{n}}, \frac{c\tau_n}{\sqrt{n}} \right) = 0.$$

Now remember that, thanks to Theorem II.2.1, $\Psi(\tau_n)$ is a random rooted simple outerplanar map with n vertices, that is it has the same distribution as \mathbf{M}_n . This finally gives

$$\lim_{n \rightarrow \infty} \left(\mathbf{M}_n, \frac{d_{\text{gr}}}{\sqrt{n}} \right) = \lim_{n \rightarrow \infty} \left(\tau_n, \frac{7d_{\text{gr}}}{9\sqrt{n}} \right) = \left(\mathcal{T}_e, \frac{7\sqrt{2}}{9} d_e \right).$$

□

Remark II.7.1. *As suggested by the referees, one might be able to extend the result to Galton–Watson trees with a more general offspring distribution, and with a non-uniform bicolouring.*

Notice, however, that there is no immediate way of adapting Proposition II.6.1 to offspring distributions more general than the geometric law. Within the proof of Lemma II.6.2, we have heavily relied upon a peculiar property of geometric Galton–Watson trees: if one conditions the root x of a geometric Galton–Watson tree θ on having at least one child and then erases the whole tree $\theta^{r(x)}$, one obtains again a geometric Galton–Watson tree. This is only true because the offspring distribution is geometric.

On the other hand, the proof should not change substantially (if not for the transition probabilities of the Markov chain and the final constant) if a generic probability $0 \leq p \leq 1$ is assigned to the event that a vertex that does not lie on the rightmost branch is white.

Part III

The geometry of the UIHPQ

where we give a new construction of the uniform infinite quadrangulation of the half-plane (or UIHPQ), analogous to the construction of the UIPQ presented by Chassaing and Durhuus [23], and proceed with a detailed study of its geometry. We show that the process of distances to the root vertex read along the boundary contour evolves as a particularly simple Markov chain and converges to a pair of independent Bessel processes of dimension 5 in the scaling limit. We study the “pencil” of infinite geodesics issued from the root vertex as in [30], and prove that it induces a decomposition of the UIHPQ into three independent submaps. Also, we have our second encounter with the constant $7/9$. Based on joint work with Nicolas Curien [21, 20].

III.1 Introduction

This third part of the present work deals with the geometry of large random quadrangulations with a boundary, and in particular their infinite local limit, an object named *the Uniform Infinite Quadrangulation of the Half-Plane* (UIHPQ for short).

The core of this final part consists in an adaptation of methods which were originally developed in [24, 30, 31, 35, 45, 53] in order to study the Uniform Infinite Planar Quadrangulation (UIPQ), an object we have introduced in Section 3.5. In order to better highlight the motivation and inspiration for our discussion of the UIHPQ, we make the point on the UIPQ in the short paragraph below, by summarising some of the points touched on in Section 3.5. The paragraphs to follow will give an overview of previous results on the UIHPQ and of the present part of this thesis.

A brief history of the UIPQ. Following pioneering work of Angel & Schramm [9] on local limits of random triangulations, Krikun [35] studies the local limit of uniform random quadrangulations of the sphere. Taking \mathcal{Q}_n to be a uniform random rooted quadrangulation of the sphere with n faces, he uses exact enumeration formulas to prove that

$$\mathcal{Q}_n \xrightarrow[n \rightarrow \infty]{(d)} \mathcal{Q}_\infty$$

for the local topology (see Section III.2.1.2); \mathcal{Q}_∞ , commonly referred to as the UIPQ, is a random infinite quadrangulation of the plane with a distinguished oriented edge.

Meanwhile, Chassaing and Durhuus [23] give a “Schaeffer-type” construction for an infinite random quadrangulation of the plane; this construction, which relies on a bijection between quadrangulations and certain trees whose vertices bear positive labels (later referred to as *positive labelled trees*), is proved to be equivalent to that of Krikun by Ménard [53], and lays the basis for much further work on the geometry of the UIPQ. Le Gall and Ménard [45] compute scaling limits for the contour functions coding the infinite positive labelled tree that Chassaing and Durhuus used to build the UIPQ; in particular, they prove [45, Theorem 6]: if $\#[\mathcal{Q}_\infty]_n$ is the number of vertices within distance n from the root vertex in the UIPQ, then we have

$$\frac{1}{n^4} \#[\mathcal{Q}_\infty]_n \xrightarrow[n \rightarrow \infty]{(d)} \mathcal{V}_p \tag{III.1}$$

for a certain explicit limiting law \mathcal{V}_p (where “ p ” stands for “plane”).

An alternative construction of the UIPQ is given in [30]: it is this time an “unconstrained” construction, in the sense that it is based on a Schaeffer-type correspondence which relates pointed, rooted quadrangulations to labelled plane trees with no positivity condition on their labels. While the positive construction of [23] encodes the UIPQ as a labelled infinite tree carrying precise information about distances between the root vertex and other vertices of the map, labels in the “unconstrained” tree carry a different set of geometric information, and can in some sense be interpreted as distances to infinity in the corresponding UIPQ, see [30, Theorem 2.8]. Such a construction is thus

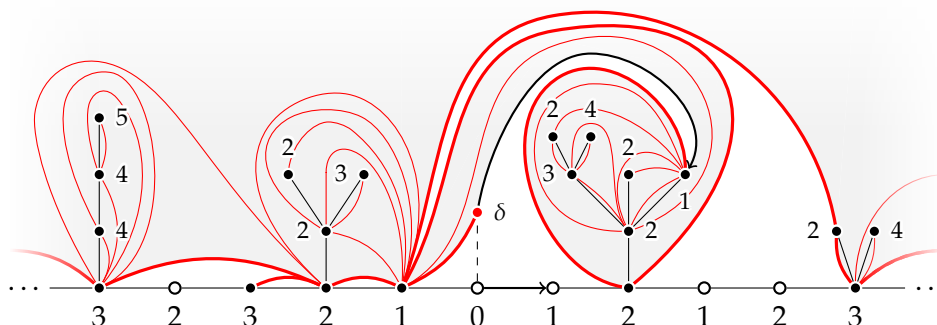


Figure III.1: The construction of the UIHPQ as $\Phi(\mathcal{B}_\infty)$.

well-suited to the study of coalescence properties of geodesic rays to infinity, which is treated in detail in [30]; furthermore, it underlies the proof of the fact that the UIPQ admits a scaling limit in the local Gromov–Hausdorff sense: a scale invariant locally compact random metric space that is homeomorphic to the plane and has Hausdorff dimension 4, known as *the Brownian plane*, see [28, 29].

Previous results on the UIHPQ. A *quadrangulation with a boundary* is a rooted planar map whose faces are all quadrangles, except for the face adjacent to the root edge and lying to its right (called the external face, or outerface), which can be of arbitrary (even) degree (and, like other faces, is not necessarily simple); all of the relevant definitions and enumeration results are given in Section III.2.1.2.

If we denote by $\mathcal{Q}_{n,p}$ a uniformly random quadrangulation with n inner quadrangular faces and a boundary of perimeter $2p$, then – as shown in [31] – we have the following convergences in distribution for the local metric:

$$\mathcal{Q}_{n,p} \xrightarrow[n \rightarrow \infty]{(d)} \mathcal{Q}_{\infty,p} \xrightarrow[p \rightarrow \infty]{(d)} \mathcal{H}_\infty. \tag{III.2}$$

The random map $\mathcal{Q}_{\infty,p}$ is the Uniform Infinite Planar Quadrangulation with a boundary of perimeter $2p$, while \mathcal{H}_∞ , our object of interest, is the aforementioned UIHPQ. The proof of [31] relies on a Schaeffer construction of the “unconstrained” type, roughly analogous to that of [30] for the UIPQ.

Our first goal is to give an equivalent construction of the UIHPQ, modelled on that of [23], which employs a treed bridge bearing positive labels (see Section III.2.1.3), thus rendering information about the profile of distances from the root vertex readily available for further study.

The positive construction of \mathcal{H}_∞ . Let us describe this new construction in some detail. We first consider a random process $(X_i)_{i \in \mathbb{Z}}$ indexed by \mathbb{Z} such that $(X_i)_{i \geq 0}$ and $(X_{-i})_{i \geq 0}$ are two independent, identically distributed, nearest-neighbour random walks

on $\mathbb{N} = \{0, 1, 2, \dots\}$, issued from $X_0 = 0$, with transition probabilities given by

$$\mathbf{p}(n, n-1) = \frac{n}{2(n+2)}, \quad \mathbf{p}(n, n+1) = \frac{n+4}{2(n+2)} \quad \text{for } n \geq 0. \quad (\text{III.3})$$

The process $(X_i)_{i \in \mathbb{Z}}$ can be seen as a non-negative labelling of the vertices of a doubly infinite path, indexed by \mathbb{Z} .

This path acts as a baseline on which we graft a sequence of random positive labelled plane trees: each tree is finite, its vertices labelled with (strictly) positive integers so that labels assigned to neighbouring vertices differ by 0, 1 or -1 . For each $i \geq 0$, we denote by ρ_i^+ the probability measure that gives weight proportional to 12^{-n} to any positive labelled tree with n edges such that the label of the root vertex is i (ρ_i^+ is the *Boltzmann distribution on positive labelled trees* with root labelled i , see Section III.2.1.1 and [23, 45]).

We construct a random “infinite treed bridge” \mathcal{B}_∞ as follows: conditionally on $(X_i)_{i \in \mathbb{Z}}$, on each vertex j of the baseline path such that $X_{j+1} < X_j$ (such indices j will be dubbed *down-steps*) we graft an independent random plane tree of law $\rho_{X_j}^+$ (see Section III.3). Through a variant of the Schaeffer construction, \mathcal{B}_∞ corresponds to a (random) infinite quadrangulation with an infinite boundary, denoted $\Phi(\mathcal{B}_\infty)$ (see Figure III.1). Our first result (Theorem III.3.4) consists in showing that such a construction yields the UIHPQ with general boundary, that is to say

$$\Phi(\mathcal{B}_\infty) = \mathcal{H}_\infty \quad \text{in distribution.} \quad (\text{III.4})$$

This new construction provides precious insight into the geometry of the UIHPQ, since vertices of $\Phi(\mathcal{B}_\infty)$ (with the exception of the root vertex) correspond to vertices of the trees in \mathcal{B}_∞ , and their respective distances from the root vertex in $\Phi(\mathcal{B}_\infty)$ are encoded by their labels in \mathcal{B}_∞ . The process $(X_i)_{i \in \mathbb{Z}}$ has an especially simple geometric interpretation: it corresponds to the process of distances to the root vertex read along the left-to-right contour of the boundary of the UIHPQ. An immediate consequence is the fact (nontrivial at first glance) that the two processes of distances from the root vertex read along the boundary of the UIHPQ, starting with the root vertex and proceeding to the right or to the left, are independent.

Although the construction of the UIHPQ given via the positive treed bridge \mathcal{B}_∞ is more involved than that of [31], we shall see that it still leads to simple computations, delivering a substantial amount of geometric information not readily accessible from [31].

Study of the geodesic pencil. A geodesic ray in \mathcal{H}_∞ is a one-ended infinite geodesic issued from the root vertex of \mathcal{H}_∞ . Thanks to our new construction (III.4), we are able to characterise geodesic rays as sequences of corners in \mathcal{B}_∞ and prove (Theorem III.4.6) that the “geodesic pencil” consisting of all geodesic rays has infinitely many cut-points: in order words, there almost surely exists an infinite set of vertices that all geodesic rays must pass through in order to go to infinity. This result is the exact analogue of the confluence of discrete geodesics established in [30] for the case of the UIPQ.

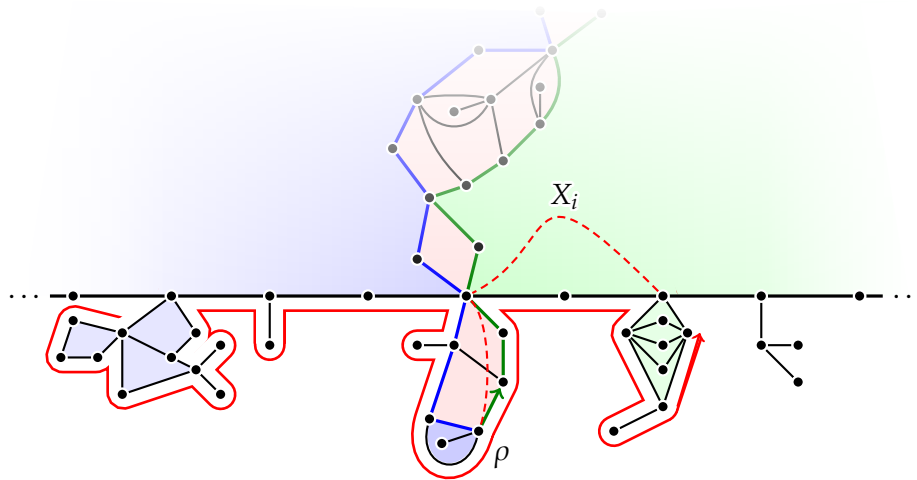


Figure III.2: The drawing illustrates the pencil decomposition of the UIHPQ; the blue and green paths are the leftmost and rightmost geodesic rays, while ρ is the root vertex and the red arrow represents the boundary contour.

We also prove that the geodesic pencil splits the UIHPQ into two independent submaps (whose distributions mirror one another) giving an additional explanation of the fact that the processes of distances to the root vertex read along the left and right halves of the boundary are independent. This study of geodesics also yields an answer to an open question of [31] about the geometric interpretation of labels in the construction of [31], which proves similar to [30, Theorem 2.8].

Scaling limits for \mathcal{B}_∞ . Our description of \mathcal{H}_∞ as $\Phi(\mathcal{B}_\infty)$ also yields scaling limit results for the UIHPQ: combining the explicit transition probabilities (III.3) with a well known result of Lamperti, we obtain

$$\left(\frac{X_{[nt]}}{\sqrt{n}} \right)_{t \in \mathbb{R}} \xrightarrow[n \rightarrow \infty]{(d)} (Z_t)_{t \in \mathbb{R}},$$

where $(Z_t)_{t \geq 0}$ and $(Z_{-t})_{t \geq 0}$ are two independent Bessel processes of dimension 5 started from 0 (see Proposition III.5.1). It is also possible to describe the scaling limit of the contour functions coding \mathcal{B}_∞ , in the spirit of the work of Le Gall and Ménard [45], see Section III.5.1 for details.

Such results yield scaling limits for various geometric quantities associated with the UIHPQ: if $\#[\mathcal{H}_\infty]_n$ is the number of vertices within distance n from the root vertex in \mathcal{H}_∞ , then (Proposition III.5.3) we have

$$\frac{1}{n^4} \#[\mathcal{H}_\infty]_n \xrightarrow[n \rightarrow \infty]{(d)} \mathcal{V}_h \tag{III.5}$$

for a certain explicit limiting law \mathcal{V}_h (where “ h ” stands for “half-plane”). We can compare the expectations of \mathcal{V}_h and of the random variable \mathcal{V}_p from (III.1), thus obtaining

$$\frac{\mathbb{E}[\mathcal{V}_h]}{\mathbb{E}[\mathcal{V}_p]} = \frac{7}{9}; \quad (\text{III.6})$$

that is, large balls in the UIHPQ are on average $7/9$ times as large as balls of the same radius in the UIPQ. The factor $7/9$ should be universal (i.e. independent of the specific combinatorics of the class of maps being considered) as it can be interpreted directly in terms of the scaling limit.

Finally, by mimicking the Schaeffer construction on the continuous processes describing the scaling limit of \mathcal{B}_∞ (in a way similar to the construction of the Brownian map [43] or the Brownian plane [28, 29] from labelled continuous trees) we construct a random locally compact metric space that we name the *Brownian half-plane* and conjecture it to be the scaling limit of the UIHPQ in the local Gromov–Hausdorff sense.

The UIHPQ with a simple boundary. All of the scaling limit results obtained for the UIHPQ can be adapted to the case of the *UIHPQ with a simple boundary*. Consider the set $\tilde{\mathcal{Q}}_{n,p} \subseteq \mathcal{Q}_{n,p}$ of (rooted) quadrangulations having area n , perimeter $2p$ and a *simple* boundary (i.e. the quadrangulations of the $2p$ -gon with n internal faces). If $\tilde{\mathcal{Q}}_{n,p}$ is a quadrangulation chosen uniformly at random within $\tilde{\mathcal{Q}}_{n,p}$, then we have the following convergence in distribution for the local distance, shown by Angel [8]:

$$\tilde{\mathcal{Q}}_{n,p} \xrightarrow[n \rightarrow \infty]{(d)} \tilde{\mathcal{Q}}_{\infty,p} \xrightarrow[p \rightarrow \infty]{(d)} \tilde{\mathcal{H}}_\infty, \quad (\text{III.7})$$

where $\tilde{\mathcal{Q}}_{\infty,p}$ is the uniform infinite quadrangulation of the $2p$ -gon and $\tilde{\mathcal{H}}_\infty$ is the Uniform Infinite Half-Planar Quadrangulation with a simple boundary (abbreviated here by $\text{UIHPQ}^{(s)}$). The second author and Miermont [31] have given a construction of the $\text{UIHPQ}^{(s)}$ via a pruning procedure applied to the UIHPQ, which consists in erasing the finite quadrangulations hanging from the (simple) boundary of its infinite core (see Figure III.14). We use this construction to extend all of our scaling limit results for the UIHPQ to the simple boundary case, mainly thanks to the fact that the extra finite quadrangulations do not contribute to the mass of balls of large radius, and simply dilate the contour process by a constant factor when considered at large scales.

Part of the interest of the $\text{UIHPQ}^{(s)}$ lies in the fact that one can perform surgery operations by glueing its boundary in various ways: glueing the left half of the boundary to the right half yields a random infinite quadrangulation of the plane endowed with a one-ended self-avoiding walk, while glueing the boundaries of two independent copies of the $\text{UIHPQ}^{(s)}$ to one another gives a random infinite quadrangulation of the plane with a two-ended SAW. Thanks to the results on the $\text{UIHPQ}^{(s)}$ obtained here, we are at present investigating models of self-avoiding walks on random infinite quadrangulations; a brief overview of the results we intend to accomplish on this front is given in Section III.7.

III.2 Schaeffer-type constructions

This section will recall two constructions of quadrangulations with a general boundary via Schaeffer-type bijections. Most of the necessary notation is contained within Sections 2.1, 3.1, 3.2 and 3.3, but the crucial notions will be recalled here, and more specific references will be given.

III.2.1 Trees, bridges and treed bridges

We start by introducing the combinatorial objects we shall employ and some necessary notation.

III.2.1.1 Trees

Given a plane tree τ as in Definition 2.1.1, again we write $|\tau|$ for the number of edges in τ , also called the *size* of τ . Note that, as opposed to [31] (and to other parts of the present work), we shall not need to deal with any infinite trees throughout our discussion of the UIHPQ; thus all trees mentioned from here onwards will be implicitly considered finite.

We consider the set \mathbb{T} of all finite plane trees as endowed with the local metric and use the same notation as in Section 2.5: given a plane tree τ and a non-negative integer h we denote by $[\tau]_h$ the tree one obtains by erasing from τ all vertices having graph distance strictly greater than h from the root (and any edges involving such vertices) so that only the first h generations (the 0-th being the root) remain. We then define, for each pair of plane trees τ, τ' in \mathbb{T} ,

$$d_{\text{tree}}(\tau, \tau') = \left(1 + \sup\{h \geq 0 : [\tau]_h = [\tau']_h\}\right)^{-1}.$$

Our trees will often be endowed with labellings; a (finite) *labelled plane tree* is, as per Definition 3.2.1, given by

- a plane tree τ ;
- a function l from the vertex set of τ to the integers such that, if u and v are neighbours in τ , then $|l(u) - l(v)| \leq 1$.

For each integer k , we call LT_k the set of all *finite* labelled plane trees whose root has label k , and LT the set $\cup_{k \in \mathbb{Z}} \text{LT}_k$ of all finite labelled plane trees. The distance d_{tree} can still be defined on LT by declaring equality of labelled trees to imply equality of labels as well as equality of underlying plane trees.

Many considerations from Section 3.3 will be crucial for what follows; remember in particular that one may define a probability measure ρ_k on LT_k in such a way that, for each $\tau \in \rho_k$, we have $\rho_k(\{\tau\}) = 12^{-|\tau|}/2$. The probability measure ρ_k is the law of a critical geometric Galton–Watson tree for which (conditionally on its shape) a uniform random integer $i_e \in \{1, 0, -1\}$ is selected independently for each edge e ; its labels are computed

as $l(u) = k + \sum_{e \in P_u} i_e$, where P_u is the unique non-backtracking path leading from the root to the vertex u .

We will also work with *positive* versions of labelled plane trees: for each $k > 0$, we define sets $\text{LT}_k^+ \subset \text{LT}_k$ and $\text{LT}^+ \subset \text{LT}$ by requiring each label to be a (strictly) positive integer.

As discussed in Section 3.3 and shown in [23, 16], we have

$$\sum_{\tau \in \text{LT}_k^+} 12^{-|\tau|} = \frac{2k(k+3)}{(k+1)(k+2)} =: w_k, \quad (\text{III.8})$$

which justifies the definition of the Boltzmann probability measure ρ_k^+ on LT_k^+ by $\rho_k^+(\{\tau\}) = 12^{-|\tau|}/w_k$. Again, this is the law of a multi-type Galton–Watson tree (see [23, Theorem 4.6]), in a sense that has already been made precise at the end of Section 3.3, to which we refer for further details.

III.2.1.2 Quadrangulations

A quadrangulation with a boundary is a locally finite planar map whose faces are all quadrangles, except for one finite or infinite face which we call the *outerface*, and whose boundary (which is a path, not necessarily simple) we see as the boundary of the map; the map is rooted by choosing an edge of the boundary, oriented so that the outerface lies to its right. Please note that this convention is actually the opposite of the one adopted throughout Part I and II of this thesis.

We say a quadrangulation with a boundary has area n if it has $n + 1$ faces (outerface included); it has perimeter $2p$ if such is the length of its boundary. We call $\mathbb{Q}_{n,p}$ the set of all quadrangulations of area n and perimeter $2p$, and \mathbb{Q} the set of all rooted quadrangulations with a boundary, which may have finite or infinite area and perimeter (though they are always, as per our definition, locally finite). Notice that the set $\mathbb{Q}_{n,1}$ can be identified with the set of all “standard” quadrangulations with n faces (where this time we mean rooted maps all of whose faces are quadrangles) by collapsing the two edges of the boundary of each of its elements. The word “quadrangulation” will, from this moment onwards, always stand for “rooted quadrangulation with a boundary” unless otherwise stated.

We can define a local distance on the set \mathbb{Q} : given a quadrangulation $q \in \mathbb{Q}$, let $[q]_r$ (for $r \geq 1$) be the (rooted) map obtained from q by erasing all vertices at (graph) distance strictly greater than r from the root vertex of q (i.e. the tail of the root edge) and all edges involving such vertices; for any pair of quadrangulations q, q' in \mathbb{Q} we define

$$d_{\text{loc}}(q, q') = \left(1 + \max(0, \sup\{r \geq 1 : [q]_r = [q']_r\})\right)^{-1}.$$

Furthermore, for $g, z \geq 0$ let $W(g, z)$ be the bi-variate generating function of $\mathbb{Q}_{n,p}$ with weight g per internal face and \sqrt{z} per edge on the boundary, that is

$$W(g, z) := \sum_{n,p \geq 0} \#\mathbb{Q}_{n,p} g^n z^p.$$

A closed form for W can be found in [17]; the radius of convergence of W in g can be seen to be $1/12$, and in particular we have

$$W_c(z) = W(1/12, z) = \frac{(1 - 8z)^{3/2} - 1 + 12z}{24z^2}. \quad (\text{III.9})$$

Via singularity analysis, one can deduce that

$$[z^p]W_c(z) \underset{p \rightarrow \infty}{\sim} \frac{2}{\sqrt{\pi}} 8^p p^{-5/2}. \quad (\text{III.10})$$

As before we define the Boltzmann measure ν_p on the set \mathcal{Q}_p of all quadrangulations with perimeter $2p$: we set $\nu_p(\{q\}) = \frac{1}{[z^p]W_c(z)} 12^{-n}$ for each quadrangulation q having perimeter $2p$ and area n ; notice that $\nu_p|_{\mathcal{Q}_{n,p}}$ is the uniform probability measure. Throughout this thesis we shall write \mathcal{Q}_p^B for a random quadrangulation of perimeter $2p$ distributed according to ν_p .

III.2.1.3 Treed bridges

A *bridge of length $2p$* is a sequence of integers $b = (x_0, \dots, x_{2p-1})$ such that $x_0 = 0$ and $|x_{i+1} - x_i| = 1$ for $i = 0, \dots, 2p-1$, where indices are considered modulo $2p$ (so that $x_{2p} = 0$). Notice that, given a bridge $b = (x_0, \dots, x_{2p-1})$, there are p indices $d_1 \leq \dots \leq d_p$ such that $x_{d_i+1} = x_{d_i} - 1$ (again, consider indices modulo $2p$); we call these indices *down-steps* for b and denote their set by $\text{DS}(b)$.

Analogously, we define an *infinite bridge* (and declare its length to be ∞) to be a doubly infinite sequence $b = (x_i)_{i \in \mathbb{Z}}$ of integers such that $x_0 = 0$ and that $|x_{i+1} - x_i| = 1$ for each $i \in \mathbb{Z}$; again, we denote by $\text{DS}(b)$ the set of its down-steps, which may be finite or infinite.

A bridge of length $2p$ will be seen as a simple $2p$ -cycle embedded in the plane, with a distinguished edge oriented so that the infinite face lies to its right; labels are assigned to its vertices so that the tail of the root edge has label $x_0 = 0$, and labels x_1, \dots, x_{2p-1} are assigned to subsequent vertices in the cycle according to the orientation given by the direction of the root edge. The same interpretation can be given to an infinite bridge, using a doubly infinite path (giving rise to two infinite faces in its planar embedding, which we see as the upper and lower half-planes) instead of a cycle; we order labels left-to-right (so that the tail of the root edge lies left of its head).

Remark III.2.1. Notice that, while labels in a labelled tree can vary by $\{-1, 0, 1\}$ between neighbouring vertices, they can only vary by $\{-1, +1\}$ along a bridge.

We introduced the notion of *bridge* in order to discuss that of a *treed bridge*, which we define as follows:

Definition III.2.1. For $p \in \{1, 2, \dots\} \cup \{\infty\}$, a treed bridge of length $2p$ (or of infinite length in the case where $p = \infty$) is a pair $(b; T)$ such that $b = (x_0, \dots, x_{2p-1})$ is a bridge of length $2p$ (or $b = (x_i)_{i \in \mathbb{Z}}$ is an infinite bridge if $p = \infty$) and T is a function from $\text{DS}(b)$ to LT , such

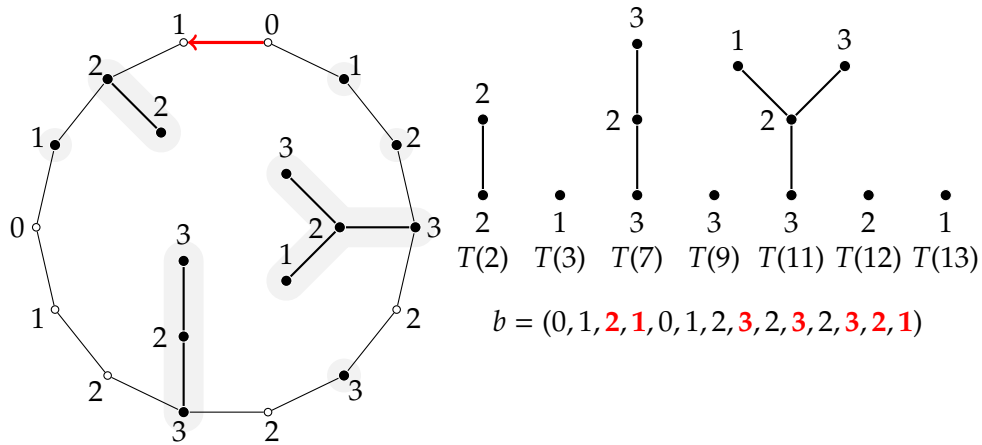


Figure III.3: A positive treed bridge $(b; T)$ of length 14 seen as a map.

that $T(i)$ is in LT_{x_i} . The size of a treed bridge $(b; T)$ is computed as $\sum_{i \in \text{DS}(b)} |T(i)|$, i.e. as the sum of the sizes of its trees.

Treed bridges – like bridges – have a clear geometric interpretation (see Figure III.3): each tree $T(i)$, for $i \in \text{DS}(b)$, may be seen as being grafted on the i -th vertex of the cycle (or infinite path) which represents b ; we embed each tree $T(i)$ inside the cycle (or within the upper half-plane) so as to preserve its planar structure.

We call TB_p the set of all treed bridges of length $2p$ (TB_∞ is the set of all treed bridges of infinite length); $\text{TB}_{n,p}$ is the set of all treed bridges of length $2p$ and size n . As we did for trees and labelled trees, we may define a local distance on the set $\cup_{p \in \mathbb{Z}^+ \cup \{\infty\}} \text{TB}_p$. Given a bridge $(b; T)$ and a non-negative integer k , we shall write $[(b; T)]_k$ for the pointed map obtained from the treed bridge by erasing all trees $T(i)$ for $i \in \text{DS}(b) \setminus [-k, k]$ (where elements of $\text{DS}(b)$ are considered modulo $2p$ if $(b; T)$ is a finite treed bridge of length $2p$) and all vertices and edges of the bridge except for the path of length $2k$ centred in the 0-th vertex. Given a pair of treed bridges $B = (b; T)$ and $B' = (b'; T')$, we set

$$d_{\text{loc}}((b; T), (b'; T')) = \left(1 + \sup\{0, h \geq 0 : [(b; T)]_h = [(b'; T')]_h\}\right)^{-1}.$$

As we did with labelled trees, we also define subsets TB_p^+ for each TB_p (where $p \in \mathbb{Z}^+$): a *positive treed bridge* is a treed bridge $(b; T)$, where $b = (x_0, \dots, x_{2p-1})$, such that for each i in $\text{DS}(b)$ we have $x_i > 0$ (that is, the bridge has no negative labels, though it may have more than one null label) and $T(i) \in \text{LT}^+$.

Our interest in these objects lies in the following constructions, variants of the classical Schaeffer bijection and based on [16, 17] and described within Section 3.2. In the sections that follow we briefly describe the parts of the constructions that will be useful for our purposes; for the reader interested in how such constructions came about and why they work, we provide some answers within Infobox III.1, where the strong link between them and the BDFG bijection from Section 3.2.3 is highlighted.

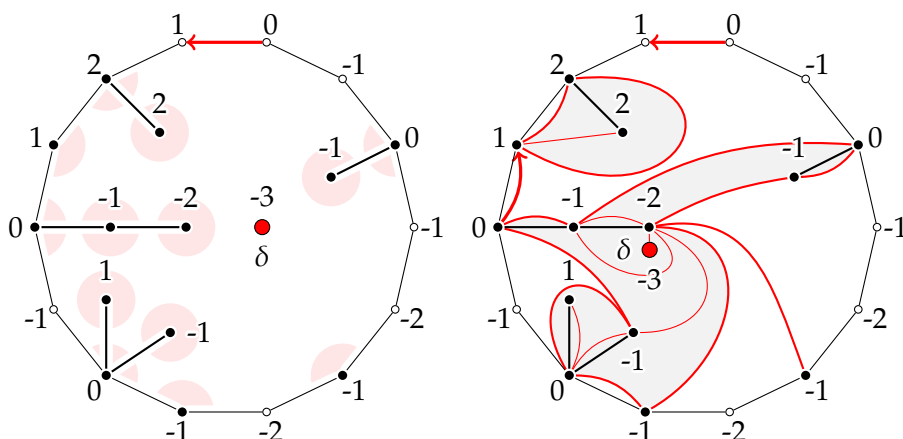


Figure III.4: A treed bridge with 19 corners and the construction of its corresponding quadrangulation via Φ^\bullet .

III.2.2 Finite construction with unconstrained labels

Proposition III.2.1. *There is an explicit bijection Φ^\bullet between the set $\text{TB}_{n,p}$ of all treed bridges of length $2p$ and size n , and the set $\mathcal{Q}_{n,p}^\bullet$ of all pointed quadrangulations with a boundary having perimeter $2p$ and area n , that is*

$$\mathcal{Q}_{n,p}^\bullet = \{(q, \delta) \mid q \in \mathcal{Q}_{n,p}, \delta \text{ is a vertex of } q\}.$$

The construction is described in [17, 31]; we briefly go through it here, referring the reader to Infobox III.1 (or [31]) for a description of its inverse.

Consider the geometric interpretation of a treed bridge $(b; T) \in \text{TB}_{n,p}$ as described in the previous section: $(b; T)$ is seen as a rooted map with two faces, one of which is unbounded; the root is oriented counterclockwise. Consider the *counterclockwise contour* of the bounded face, which contains the trees: it defines a (cyclic) sequence of corners, a corner being the angular region corresponding to a pair of edges sharing a vertex (see Figure III.4); notice that each vertex may be adjacent to more than one corner. Since they will be preserved by the construction we are about to describe, we call vertices belonging to the trees in $T(\text{DS}(b))$ *real vertices*; other vertices, which belong to the $2p$ -cycle but do not correspond to down-steps, are called *phantom vertices*. The classification naturally extends to corners; we also consider corners as being labelled, by having them inherit the label of their vertex.

Call k the minimum label appearing on *real vertices* of $(b; T)$, and add a vertex labelled $k - 1$, which we call δ , within the bounded face of the treed bridge. Now apply the standard Schaeffer construction to the labelled map at hand: link each real corner c bearing label $h > k$ to the next real corner labelled $h - 1$ in the counterclockwise contour of the bounded face; each real corner labelled k is then linked to the added vertex δ ; notice that all new edges can be drawn in such a way that they do not cross each other.

Finally, all phantom vertices, all labels and all original edges of the treed bridge are erased.

What one obtains (see [31]) is a quadrangulation with a boundary pointed in the vertex δ . It is not hard to see that the boundary has length $2p$ and that each edge of the $2p$ -cycle can be made to correspond to an edge of the boundary; we root the map in the edge corresponding to the original root of the treed bridge (preserving its original orientation) to obtain $\Phi^\bullet((b; T))$: see Figure III.4.

Remark III.2.2. *The construction Φ^\bullet is such that:*

- *one may identify the real vertices of $(b; T)$ with the vertices of $\Phi^\bullet((b; T))$, if one excludes the vertex δ in which the map is pointed;*
- *for each real vertex x of $(b; T)$, if we call $l(\delta)$ the label the construction gives to the additional vertex δ , we have $d_{\text{gr}}(x, \delta) = l(x) - l(\delta)$, where the graph distance d_{gr} is taken in the map $\Phi^\bullet((b; T))$;*
- *the edges of the embedded cycle representing b correspond to the edges on the boundary of $\Phi^\bullet((b; T))$.*

The map Φ^\bullet is naturally defined on the whole set $\cup_{p>0} \text{TB}_p$ of finite treed bridges, and takes values in the set \mathbf{Q}^\bullet of (rooted) pointed quadrangulations with a boundary. Composing with the forgetful map from \mathbf{Q}^\bullet to \mathbf{Q} (which simply takes elements of \mathbf{Q}^\bullet and forgets their pointing) we get a mapping Φ which sends treed bridges in $\cup_{p>0} \text{TB}_p$ to the set \mathbf{Q} of rooted quadrangulations with a boundary.

III.2.3 Finite construction with positive labels

Consider the restriction of Φ (as defined above) to the set $\cup_{p>0} \text{TB}_p^+$ of finite positive treed bridges.

Notice that, if we apply Φ^\bullet to a positive treed bridge $(b; T)$, the label of the added vertex δ is 0: the trees in $T(\text{DS}(b))$ are in LT^+ , so their vertices bear only strictly positive labels; furthermore, $2p - 1$ is always a down-step for any positive bridge of length $2p$; the root of the tree $T(2p - 1)$ is thus always labelled 1, hence the minimum label that does not appear on real vertices is 0. Since the root vertex of the quadrangulation $\Phi^\bullet((b; T))$ corresponds to the root vertex of the treed bridge $(b; T)$ and thus has the same (null) label, the added vertex δ in which $\Phi^\bullet((b; T))$ is pointed must also be its root vertex; hence no information is lost by forgetting the pointing and taking $\Phi((b; T))$ instead of $\Phi^\bullet((b; T))$.

As a consequence we have the following:

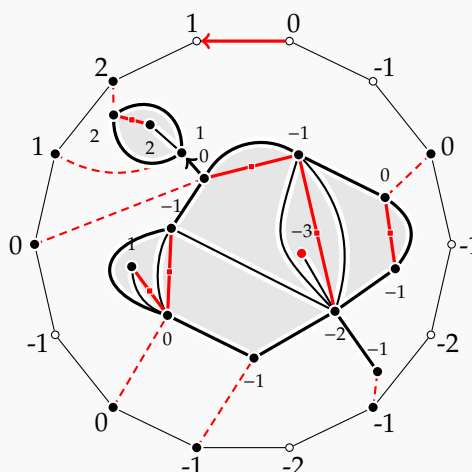
Proposition III.2.2. *The restriction of Φ to the set $\text{TB}_{n,p}^+$ of all positive treed bridges of length $2p$ and size n is a bijection with the set $\mathbf{Q}_{n,p}$ of rooted quadrangulations with a boundary of length $2p$ and area n .*

Remark III.2.2 is updated as follows:

BDFG and quadrangulations with a boundary iii.1

Quadrangulations with a boundary are naturally bipartite (because all of their faces have even degree), so we may perform on them the BDFG construction from Section 3.2.3. Given $(q, \delta) \in \mathcal{Q}_{n,p}^*$, the construction will build a mobile whose $n + 1$ unlabelled vertices all have degree 2 except for (possibly) one, which corresponds to the unbounded face of q and has degree p .

Consider the unlabelled vertex of the mobile that corresponds to the unbounded face; its p neighbours are the p vertices adjacent to down-step corners of the (clockwise) contour of the outerface of q . If we ignore all other unlabelled vertices, simply seeing labelled vertices as neighbours when they are adjacent to the same unlabelled vertex of degree two, the rest of the mobile consists of p labelled trees (possibly of size 0), each attached to one of the p neighbours of the outerface-vertex.



Notice that the rooting of the mobile and the choice of ε , which would normally follow in the BDFG construction, only serve to encode the root of the map q : all but the root edge can be recovered with the first steps of the inverse construction, which only involves the cyclic contour of the mobile (hence does not depend on its root!). In the special case of quadrangulations with a boundary, we will find it convenient to skip the last steps of the construction and simply keep track of which oriented edge of the boundary is the root of q .

We do this by encoding (q, δ) not by a mobile, but by a pair $(b; T)$: the first element, b , represents the label contour of the boundary; corners of the unbounded face are represented by $\mathbb{Z} \pmod{2p}$, corner 0 being the corner adjacent to the root vertex of q that lies directly to the right of the root edge, and their labels are recorded as $b = (x_i)_{0 \leq i \leq 2p-1}$ (x_i being the label of corner i). The second element in the pair is the sequence of p labelled trees we built from the mobile; since each tree can be paired with one down-step corner of the unbounded face, we see T as a function from the set $\text{DS}(b)$ of down-steps of b to the set LT , such that $T(i)$ is in LT_{x_i} . In other words, the pair $(b; T)$ is a treed bridge of length $2p$ whose size is the number of unlabelled vertices of the original mobile, minus 1, that is n .

Recovering (q, δ) from $(b; T)$ can indeed be done as described in Section III.2.2: arranging the trees in $T(\text{DS}(b))$ within the simple cycle that represents b and taking the counterclockwise contour of the inner face is equivalent to just taking the contour of the original mobile; the steps performed are then exactly those of the original BDFG bijection (see Section 3.2.3), and the root edge is reconstructed by taking the (oriented) edge of the boundary that corresponds to the one between the 0th and 1st vertex of the “artificial” simple cycle.

This is the first infobox in Part III

Next infobox: III.2 \leftrightarrow

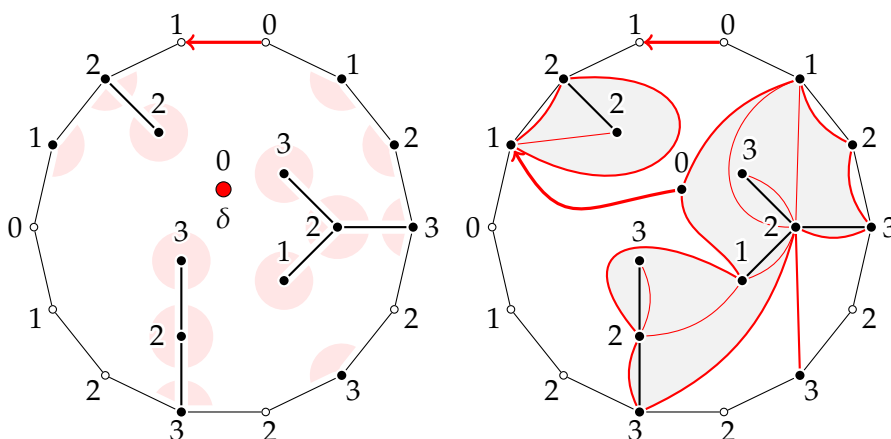


Figure III.5: The positive treed bridge $(b; T)$ from Figure III.3 is depicted with its 19 corners, which become the 19 edges of $\Phi((b; T))$; notice that the quadrangulation is the same as that of Figure III.4.

Remark III.2.3. When applying the construction Φ to a (finite) positive treed bridge,

- there is a correspondence between real vertices of the positive treed bridge $(b; T)$ and vertices of its image $\Phi((b; T))$, if one excludes its root vertex;
- the label of each real vertex of $(b; T)$ represents its distance from the root vertex in the quadrangulation $\Phi((b; T))$;
- the edges of the embedded cycle representing b correspond to the edges on the boundary of $\Phi((b; T))$; as a consequence, the bridge labels (x_0, \dots, x_{2p-1}) correspond to the distances from the root vertex of vertices on the boundary of $\Phi((b; T))$, read counterclockwise along its contour.

III.2.4 Infinite construction

Notice that the construction Φ can easily be extended to certain classes of treed bridges with an infinite boundary in such a way that it still yields elements of \mathcal{Q} .

Let $\text{TB}^{-\infty}$ be the set of all infinite treed bridges $(b; T)$, with $b = (x_i)_{i \in \mathbb{Z}}$, such that $\liminf_{i \rightarrow \pm\infty} x_i = -\infty$. Given such a bridge $(b; T)$, we may order its real corners according to the left-to-right contour of the upper face (similarly to how we took the counterclockwise contour of the inner face in the finite case). We can list real corners of $(b; T)$, in this order, as a sequence $(c_i)_{i \in I}$, where I is either \mathbb{Z} (the sequence is two-ended if there is an infinite number of real corners on each side of the root vertex, as will essentially be the case for all “unconstrained” treed bridges within this work) or \mathbb{N} (which covers the case where only a finite number of real corners lie left of the root vertex). Notice that $\liminf_{i \rightarrow \infty} x_i = -\infty$ implies that there is always an infinite number of real corners lying right of the root vertex, since $\text{DS}(b) \cap \mathbb{N}$ must be infinite.

We now define $\Phi((b; T))$ by analogy with the construction performed on finite treed bridges: for each i , set $j = \min\{h > i \mid l(c_h) = l(c_i) - 1\}$ (such a minimum always exists, since the requirement on bridge labels implies $\liminf_{i \rightarrow +\infty} l(c_i) = -\infty$); link the real corner c_i to the real corner c_j , which we shall call the *successor* of c_i and denote by $s(c_i)$. The map obtained after erasing all phantom vertices and all edges of the original treed bridge is then rooted as in Section III.2.2 to obtain $\Phi((b; T))$, which is a locally finite (rooted) quadrangulation with an infinite boundary.

Remark III.2.4. Notice that the mapping $\Phi : \cup_{p>0} \text{TB}_p \cup \text{TB}^{-\infty} \rightarrow \mathcal{Q}$ is continuous. This is stated in [31] and exploited in order to construct the uniform infinite quadrangulation with an infinite general boundary from an infinite labelled treed bridge (see Section III.3.1 and [31, Section 6]). Since the (simple) proof was left as an exercise for the reader in [31], in the interest of completeness we include one within Infobox III.2.

The bijection presented in Section III.2.3 induces us to also consider an extension of Φ to the set of all positive treed bridges of infinite length where each label appears a finite number of times, which we call TB_{∞}^+ . Given a treed bridge $(b; T)$ in TB_{∞}^+ , we list its real corners as a sequence $(c_i)_{i \in I}$ ordered according to the left-to-right contour of the upper face, where this time I is either \mathbb{Z} or $\mathbb{Z}_{\leq 0}$ (the fact that each label appears a finite number of times implies divergence to $+\infty$ of labels along the boundary, hence $\text{DS}(b) \cap \mathbb{Z}_{\leq 0}$ is infinite). Note that, while we shall mostly consider positive treed bridges for which we can take $I = \mathbb{Z}$, we will see some examples of positive treed bridges whose sequence of real corners is one-ended in Sections III.4.1 and III.4.2 (see Corollary III.4.2 and Proposition III.4.5).

We build $\Phi((b; T))$ exactly as described above (joining each corner to its successor), except that this time the set $\{h > i \mid l(c_h) = l(c_i) - 1\}$ might very well be empty; when this is the case and $l(c_i) > 1$, we consider $j' = \min\{h \mid l(c_h) = l(c_i) - 1\}$ and set $s(c_i) = c_{j'}$; finally, we add an extra vertex labelled 0 within the upper face of the treed bridge, setting its one corner to be the successor of every real corner labelled 1. Joining each real corner to their successor, erasing phantom vertices and original edges of the treed bridge and rooting appropriately yields a quadrangulation with an infinite boundary $\Phi((b; T))$; notice that all properties from Remark III.2.3 still hold: in particular, labels of real vertices in $(b; T)$ represent distances from the root vertex, so that the condition on the number of appearances of each label entails local finiteness of $\Phi((b; T))$, which thus belongs to the set \mathcal{Q} .

Let $\text{TB}^+ = \cup_{p \in \mathbb{Z}^+ \cup \{\infty\}} \text{TB}_p^+$ be the set of all positive treed bridges with a finite or infinite perimeter, such that each label appears a finite number of times. The question of whether Φ is continuous (for the local metric) as a function from TB^+ to \mathcal{Q} will be very relevant (continuity would allow us to proceed as in [31], whose proofs of convergence rely on Remark III.2.4); we have the following:

Remark III.2.5. The mapping Φ is not continuous (for the local metric) on TB^+ ; in fact, it is discontinuous at every point of TB_{∞}^+ .

The main problem comes from the possible occurrence of small labels far from the root of a treed bridge: two treed bridges B and B' may be very near for the local metric, in the sense that

Continuity of Φ *iii.2*

We prove Remark III.2.4, that is that for each treed bridge $B \in \cup_{p>0} \text{TB}_p \cup \text{TB}^{-\infty}$ and positive real number ε , there is $\delta > 0$ such that, if $B' \in \cup_{p>0} \text{TB}_p \cup \text{TB}^{-\infty}$ is such that $d_{\text{loc}}(B, B') < \delta$, then $d_{\text{loc}}(\Phi(B), \Phi(B')) < \varepsilon$ (where the d_{loc} denotes the local distance in the appropriate sets, as defined in Section III.2.1.2 and III.2.1.3).

Equivalently, we shall show that, given a treed bridge $B \in \cup_{p>0} \text{TB}_p \cup \text{TB}^{-\infty}$ and a positive integer k , there is a positive integer $r(k)$ such that, whenever $[B]_{r(k)} = [B']_{r(k)}$ for $B' \in \text{TB}_p \cup \text{TB}^{-\infty}$, we also have $[\Phi(B)]_k = [\Phi(B')]_k$.

Since if $B \in \text{TB}_p$ one can always take $r(k) = 2p$, we shall suppose that $B = (b; T) \in \text{TB}^{-\infty}$. Consider the ball of radius k in $\Phi(B)$; since the construction Φ allows us to identify vertices of a treed bridge with those of the corresponding quadrangulation, we may see the set finite set S of vertices of $[\Phi(B)]_k$ as contained within the set of real vertices of B , and in particular within $\cup_{i \in \text{DS}(b) \cap [-t, t]} V(T(i))$ for some $t > 0$. Let ℓ be the minimum label appearing on vertices in $\cup_{i \in \text{DS}(b) \cap [-t, t]} V(T(i))$; suppose $b = (x_i)_{i \in \mathbb{Z}}$ and take z and w such that $z < -t$, $w > t$, $x_z < \ell$ and $x_w < \ell - 1$; set $r(k) = \max\{|z|, w\}$.

We claim that, if B' is a treed bridge in $\text{TB}_p \cup \text{TB}^{-\infty}$ such that $[B]_{r(k)} = [B']_{r(k)}$, then $[\Phi(B)]_k = [\Phi(B')]_k$. Consider the set of corners in B adjacent to vertices in S ; since such corners are within $[B]_{r(k)}$, we may identify them with certain corners of B' , and it is sufficient to show that those are not joined by an edge to anything outside $[B']_{r(k)}$.

But this is true: for one thing, corner adjacent to vertices of S have their successors (which bear label at least $\ell - 1$) within $[B']_{r(k)}$ (in particular in trees $T'(i)$ with $-t \leq i \leq w$), since $x_w < \ell - 1$. On the other hand, consider any corner c of B' that is not within $[B']_{r(k)}$; if $l(c) \leq \ell$, then its successor has label at most $\ell - 1$, hence is not adjacent to a vertex in S ; if $l(c) > \ell$, on the other hand, the successor of c is on the same side of $[B']_{|z|}$ as c itself, thanks to the fact that $x_z < \ell$.

This completes the proof.

↔ **Previous infobox:** III.1

This is the last infobox in Part III

their bridges and trees coincide up to a great distance from the root (say $[B]_r = [B']_r$ for some large r); if, however, a (real) vertex labelled 1 appears in $B \setminus [B]_r$ and does not appear in $B' \setminus [B']_r$, then $[\Phi(B)]_1 \neq [\Phi(B')]_1$, so the two images are far apart.

This problem is exactly the same as that arising for the definition of the UIPQ via the positive bijection from [23], and needs to be addressed as Ménard did in [53] by giving bounds for the probability that small labels appear very far from the root, a statement which will be made precise in Section III.3.4.

III.3 The new construction

Before introducing our new construction based on the bijection from Section III.2.3, we shall briefly review the construction of the UIHPQ given in [31]. We will then

prove that the UIHPQ can alternatively be obtained as the local limit of Boltzmann quadrangulations with a boundary whose perimeter is sent to infinity, without the need for a double limit such as that of (III.2), which will render our new construction of the UIHPQ considerably simpler.

III.3.1 Convergences to the UIHPQ

The construction of the UIHPQ given in [31] is illustrated by the following commutative diagram (see [31] for the proof), where the second line is obtained by applying the (unpointed) Schaeffer mapping Φ to the first one:

$$\begin{array}{ccccc}
 \mathcal{B}_{n,p}^{\pm} & \xrightarrow[n \rightarrow \infty]{(d)} & \mathcal{B}_{\infty,p}^{\pm} & \xrightarrow[p \rightarrow \infty]{(d)} & \mathcal{B}_{\infty}^{\pm} \\
 \Phi \downarrow & & \Phi \downarrow & & \Phi \downarrow \\
 \mathcal{Q}_{n,p} & \xrightarrow[n \rightarrow \infty]{(d)} & \mathcal{Q}_{\infty,p} & \xrightarrow[p \rightarrow \infty]{(d)} & \mathcal{H}_{\infty}
 \end{array} \tag{III.11}$$

In this diagram, $\mathcal{B}_{n,p}^{\pm}$ is a uniform treed bridge of length $2p$ and size n (with no positivity constraint on the labels). As per Proposition III.2.1, its image via Φ^{\bullet} is $\mathcal{Q}_{n,p}^{\bullet}$, a uniformly random pointed quadrangulation with a boundary of perimeter $2p$ and area n (i.e. a uniform element of $\mathcal{Q}_{n,p}^{\bullet}$); forgetting the pointing of $\mathcal{Q}_{n,p}^{\bullet}$ yields the random quadrangulation with a boundary $\mathcal{Q}_{n,p} = \Phi(\mathcal{B}_{n,p}^{\pm})$. Notice now that, since each quadrangulation in $\mathcal{Q}_{n,p}$ has exactly $n + p + 1$ vertices by Euler's formula, the law of $\mathcal{Q}_{n,p}$ is uniform on the set $\mathcal{Q}_{n,p}$.

We shall not describe the intermediate bridge $\mathcal{B}_{\infty,p}^{\pm}$ or its image $\mathcal{Q}_{\infty,p}$, since they are irrelevant for our purpose; we will, however, recall the definition of $\mathcal{B}_{\infty}^{\pm}$, which will be used below and again in Section III.4.3:

Definition III.3.1. The random treed bridge $\mathcal{B}_{\infty}^{\pm}$ is the pair $((X_i^{\pm})_{i \in \mathbb{Z}}; T^{\pm})$, where $(X_i^{\pm})_{i \geq 0}$ and $(X_{-i}^{\pm})_{i \geq 0}$ are two independent uniform simple random walks issued from $X_0^{\pm} = 0$ and, conditionally on the bridge X^{\pm} , the trees $T^{\pm}(i)$, for $i \in \text{DS}(X^{\pm})$, are independent and distributed according to $\rho_{X_i^{\pm}}$.

Notice that we have $\liminf_{i \rightarrow \pm\infty} X_i^{\pm} = -\infty$ almost surely, hence $\mathcal{B}_{\infty}^{\pm}$ almost surely belongs to the set $\text{TB}^{-\infty}$ as defined in Section III.2.4. Given the first line of the diagram (III.11) (that is the convergence of random treed bridges) one can thus invoke the continuity of Φ on $\bigcup_{p>0} \text{TB}_p \cup \text{TB}^{-\infty}$ (see Remark III.2.4) to produce the convergences from the second line, thus deducing that

$$\Phi(\mathcal{B}_{\infty}^{\pm}) = \mathcal{H}_{\infty}, \tag{III.12}$$

which is how the UIHPQ \mathcal{H}_{∞} was introduced in [31].

We now use the same argument to prove that the UIHPQ can alternatively be seen as the local limit in p of the random Boltzmann quadrangulations \mathcal{Q}_p^B from Section III.2.1.2:

Proposition III.3.1. *The UIHPQ is the local limit of Boltzmann quadrangulations with a boundary of perimeter p , when p is sent to infinity:*

$$\mathcal{Q}_p^B \xrightarrow[p \rightarrow \infty]{(d)} \mathcal{H}_\infty.$$

Proof. For each $p > 0$, we shall denote by $\mathcal{Q}_p^{B, \bullet}$ the random pointed map obtained by selecting a vertex of \mathcal{Q}_p^B uniformly at random (conditionally on the quadrangulation itself). Consider now the random treed bridge obtained by taking the pre-image of $\mathcal{Q}_p^{B, \bullet}$ via the pointed Schaeffer construction Φ^\bullet from Section III.2.3: set $\mathcal{B}_p^\pm := (\Phi^\bullet)^{-1}(\mathcal{Q}_p^{B, \bullet})$.

We claim that \mathcal{B}_p^\pm converges in law to \mathcal{B}_∞^\pm , when p is sent to infinity, for the local distance on the set of treed bridges; as above, by Remark III.2.4 this entails the convergence of $\Phi(\mathcal{B}_p^\pm)$ to $\Phi(\mathcal{B}_\infty^\pm) = \mathcal{H}_\infty$; since $\Phi(\mathcal{B}_p^\pm) = \mathcal{Q}_p^B$ by construction, this would establish the proposition.

Recall that quadrangulations in $\mathcal{Q}_{n,p}$ have $n+p+1$ vertices, so that for any treed bridge $(b; T)$ of length $2p$ the definition of the Boltzmann law (see Section III.2.1.2) implies

$$\mathbb{P}(\mathcal{B}_p^\pm = (b; T)) = \mathbb{P}(\mathcal{Q}_p^{B, \bullet} = \Phi^\bullet((b; T))) = \frac{12^{-\sum_{i \in \text{DS}(b)} |T(i)|}}{[z^p] W_c(z) (\sum_{i \in \text{DS}(b)} |T(i)| + p + 1)}. \quad (\text{III.13})$$

Notice that bridges in TB_p can be represented as $(p+1)$ -tuples $(b, \tau_1, \dots, \tau_p)$, where $b = (x_0, \dots, x_{2p-1})$ is any bridge of length $2p$ and τ_1, \dots, τ_p are labelled trees in LT_0 : one recovers the treed bridge as presented in Section III.2.1.3 by grafting tree τ_i on the i -th down-step $d \in \text{DS}(b)$ and shifting all of its labels by x_d .

It is clear from (III.13) that, if we see $\mathcal{B}_p^\pm = (X^{p, \pm}, T_1^\pm, \dots, T_p^\pm)$ as being presented this way, the trees T_i^\pm (for $i = 1, \dots, p$) are independent of the random bridge $X^{p, \pm}$, which is distributed uniformly over all bridges of length $2p$. Similarly, one can present \mathcal{B}_∞^\pm as $((X_i^\pm)_{i \in \mathbb{Z}}, (\theta_i)_{i \in \mathbb{Z}})$, where $(X_i^\pm)_{i \in \mathbb{Z}}$ is as in Definition III.3.1, and θ_i is distributed according to ρ_0 ; one recovers $T^\pm(j)$, for $j \in \text{DS}(X^\pm)$, by shifting labels of θ_j by X_j^\pm .

The fact that the local limit of $X^{p, \pm}$ is the infinite two-sided simple random walk X^\pm is a classical result; all we need in order to prove local convergence of \mathcal{B}_p^\pm to \mathcal{B}_∞^\pm is thus the fact that the trees T_i^\pm are asymptotically independent and distributed according to ρ_0 .

Take any non-negative continuous function f on p -tuples in LT_0^p ; let T_1^\pm, \dots, T_p^\pm be the p -tuple of random trees of \mathcal{B}_p^\pm and let $\theta_1, \dots, \theta_p$ be p independent trees of law ρ_0 ; notice that by combining the fact that $\rho_0(\{\tau\}) = 12^{-|\tau|}/2$ with (III.13) we get

$$\begin{aligned} \mathbb{E}[f(T_1^\pm, \dots, T_p^\pm)] &= \frac{2^p}{[z^p] W_c(z)} \sum_{\tau_1, \dots, \tau_p \in \text{LT}_0} \frac{f(\tau_1, \dots, \tau_p)}{\sum_{i=1}^p |\tau_i| + p + 1} \prod_{i=1}^p \frac{12^{-|\tau_i|}}{2} = \\ &= \frac{2^p}{[z^p] W_c(z)} \mathbb{E} \left[\frac{f(\theta_1, \dots, \theta_p)}{\sum_{i=1}^p |\theta_i| + p + 1} \right]. \end{aligned}$$

Since the above expected value must be 1 when f is taken to be the constant 1, we have

$$1 = \frac{2^p}{[z^p]W_c(z)} \mathbb{E} \left[\frac{1}{\sum_{i=1}^p |\theta_i| + p + 1} \right], \text{ and we can write}$$

$$\mathbb{E}[f(T_1^\pm, \dots, T_p^\pm)] = \mathbb{E} \left[\frac{f(\theta_1, \dots, \theta_p)}{\sum_{i=1}^p |\theta_i| + p + 1} \right] \mathbb{E} \left[\frac{1}{\sum_{i=1}^p |\theta_i| + p + 1} \right]^{-1}.$$

Choose any $k > 0$; by renumbering trees T_1^\pm, \dots, T_p^\pm appropriately, we may suppose that, in addition to them being grafted in counterclockwise order within the bridge, the root vertex lies between the trees $T_{\lfloor k/2 \rfloor}^\pm$ and $T_{\lfloor k/2 \rfloor + 1}^\pm$ (possibly coinciding with the root of $T_{\lfloor k/2 \rfloor}^\pm$). Suppose that f is a bounded non-negative function that only depends on T_1^\pm, \dots, T_k^\pm ; we want to investigate $\lim_{p \rightarrow \infty} \mathbb{E}[f(T_1^\pm, \dots, T_k^\pm)]$, which can be rewritten as

$$\lim_{p \rightarrow \infty} \mathbb{E} \left[\frac{f(\theta_1, \dots, \theta_k)}{\sum_{i=1}^p |\theta_i| + p + 1} \right] \mathbb{E} \left[\frac{1}{\sum_{i=1}^p |\theta_i| + p + 1} \right]^{-1} \quad (\text{III.14})$$

where the trees $(\theta_i)_{i>0}$ are independent and distributed according to ρ_0 .

Using the fact that $\lim_{p \rightarrow \infty} \mathbb{P} \left(\frac{\sum_{i=k+1}^p |\theta_i| + p + 1}{\sum_{i=1}^p |\theta_i| + p + 1} < 1 - \varepsilon \right) = 0$ for all $\varepsilon > 0$, straightforward computations lead to the identity

$$\lim_{p \rightarrow \infty} \mathbb{E} \left[\frac{f(\theta_1, \dots, \theta_k)}{\sum_{i=1}^p |\theta_i| + p + 1} \right] = \lim_{p \rightarrow \infty} \mathbb{E} \left[\frac{f(\theta_1, \dots, \theta_k)}{\sum_{i=k+1}^p |\theta_i| + p + 1} \right];$$

since numerator and denominator are now independent, by splitting the expected value and applying the identity again to the constant function 1 two copies of the expression $\mathbb{E} \left[\left(\sum_{i=k+1}^p |\theta_i| + p + 1 \right)^{-1} \right]$ cancel out from (III.14), thus proving that

$$\lim_{p \rightarrow \infty} \mathbb{E}[f(T_1^\pm, \dots, T_k^\pm)] = \mathbb{E}[f(\theta_1, \dots, \theta_k)].$$

The above identity, together with the convergence of bridges, implies the convergence in law for the local topology of the random treed bridges \mathcal{B}_p^\pm to the random treed bridge \mathcal{B}_∞^\pm , which was our claim; this completes the proof of the proposition. \square

III.3.2 The Boltzmann positive treed bridges

Our aim is to present \mathcal{H}_∞ as the image via Φ of the random infinite positive treed bridge \mathcal{B}_∞ mentioned in the Introduction. In view of Proposition III.3.1, we start by describing the law of the finite positive treed bridge that corresponds to a Boltzmann quadrangulation of perimeter $2p$. Recall the transition probabilities \mathbf{p} from (III.3):

$$\forall n \geq 0, \quad \mathbf{p}(n, n-1) = \frac{n}{2(n+2)}; \quad \mathbf{p}(n, n+1) = \frac{n+4}{2(n+2)}. \quad (\text{III.15})$$

We will occasionally call \mathbb{P}_x the law of a nearest neighbour random walk with transition probabilities given by \mathbf{p} , issued from x . The following property of \mathbf{p} , relating it to the quantity w_n as defined in (III.8), shall be especially useful: we have

$$w_n = 8\mathbf{p}(n, n-1)\mathbf{p}(n-1, n) \quad (\text{III.16})$$

as can be easily checked by substituting the expression $\frac{2n(n+3)}{(n+1)(n+2)}$ for w_n .

This being said, we can now prove the following:

Proposition III.3.2. *Given $p > 0$, consider the bijection $\Phi|_{\text{TB}_p^+} : \text{TB}_p^+ \rightarrow \mathbf{Q}_p$ between the set of all positive treed bridges of length $2p$ and the set of all finite rooted quadrangulations with a boundary of perimeter $2p$; write Φ^{-1} for its inverse. Let \mathbf{Q}_p^B be a Boltzmann quadrangulation with a boundary of length $2p$ (which is a random variable taking values in \mathbf{Q}_p), and set $\mathcal{B}_p := \Phi^{-1}(\mathbf{Q}_p^B)$. Then the random positive treed bridge $\mathcal{B}_p = (X^p, T^p)$ can be described as follows:*

- the random bridge $X^p = (X_0^p, \dots, X_{2p-1}^p)$ has the same law as the initial segment of a nearest neighbour random walk with transition probabilities given by \mathbf{p} , issued from 0 and conditioned on hitting 0 at time $2p$;
- conditionally on the bridge X^p , the random trees $T^p(i)$, for $i \in \text{DS}(X^p)$, are independent and distributed according to $\rho_{X_i^p}^+$.

Proof. Suppose $(b; T)$ is a given positive treed bridge with $b = (x_0, \dots, x_{2p-1})$; using the fact that $\Phi|_{\text{TB}_{n,p}^+}$ is a bijection with the set $\mathbf{Q}_{n,p}$ and that the size of a treed bridge is the sum of the sizes of its trees, we have

$$\begin{aligned} \mathbb{P}(\mathcal{B}_p = (b; T)) &= \mathbb{P}(\mathbf{Q}_p^B = \Phi((b; T))) = \\ &= \frac{1}{[z^p]W_c(z)} \prod_{i \in \text{DS}(b)} 12^{-|T(i)|} = \frac{1}{[z^p]W_c(z)} \prod_{i \in \text{DS}(b)} w_{x_i} \prod_{i \in \text{DS}(b)} \rho_{x_i}^+({T(i)}). \end{aligned}$$

It is clear from the rightmost expression that the random trees $T^p(i)$ (for $i \in \text{DS}(X^p)$) are independent and distributed according to $\rho_{X_i^p}^+$ conditionally on the labels of their roots. As for the law of the bridge, it follows from (III.16) that

$$\prod_{i \in \text{DS}(b)} w_{x_i} = 8^p \prod_{i \in \text{DS}(b)} \mathbf{p}(x_i, x_i - 1)\mathbf{p}(x_i - 1, x_i);$$

notice now that, in order for the bridge to “close” (i.e. to attain the value 0 at time $2p$), there must be a bijection f between $\text{DS}(b)$ and $\{0, \dots, 2p-1\} \setminus \text{DS}(b)$ such that $x_{f(i)} = x_i - 1$ (each down-step from a label x must have a corresponding up-step from $x - 1$), hence

$$8^p \prod_{i \in \text{DS}(b)} \mathbf{p}(x_i, x_i - 1)\mathbf{p}(x_i - 1, x_i) = 8^p \prod_{i \in \text{DS}(b)} \mathbf{p}(x_i, x_i - 1) \prod_{i \notin \text{DS}(b)} \mathbf{p}(x_i, x_i + 1) = 8^p \prod_{i=0}^{2p-1} \mathbf{p}(x_i, x_{i+1}),$$

and this completes the proof of the proposition. \square

As a byproduct of the proof of the preceding proposition one may compute the probability that $X_{2p} = 0$ for a nearest neighbour random walk $(X_i)_{i \geq 0}$, issued from 0 and with transition probabilities \mathbf{p} ; we have obtained that $\mathbb{P}_0(X_{2p} = 0) = 8^{-p}[z^p]W_c(z)$; hence, using (III.10), we have

$$\mathbb{P}_0(X_{2p} = 0) \underset{p \rightarrow \infty}{\sim} \frac{2}{\sqrt{\pi}} p^{-5/2}, \quad (\text{III.17})$$

which will be useful later.

Remark III.3.1. Notice that, since the bridge labels may be interpreted as distances between boundary vertices and the root vertex of \mathcal{Q}_p^B , read along the contour of the map, invariance of their law by time-reversal is clear (though it is not evident in the description of the process given above). In other words, $(0, X_1^p, \dots, X_{2p-1}^p)$ has the same law as $(0, X_{2p-1}^p, \dots, X_1^p)$.

As we have seen with Proposition III.3.1, the UIHPQ is the local limit in p of Boltzmann quadrangulations \mathcal{Q}_p^B ; we wish to show that it has the same law as the image via Φ of the local limit \mathcal{B}_∞ of the random treed bridges \mathcal{B}_p from Proposition III.3.2, when p is sent to infinity. We give now a description of \mathcal{B}_∞ , whose validity we shall prove in the following section:

Proposition III.3.3. *The local limit (in law) of the sequence of random positive treed bridges \mathcal{B}_p , for $p \rightarrow \infty$, is the random positive treed bridge $\mathcal{B}_\infty = (X; T)$ such that:*

- *the two process $(X_i)_{i \geq 0}$ and $(X_{-i})_{i \geq 0}$ are independent nearest neighbour random walks with transition probabilities given by \mathbf{p} , issued from $X_0 = 0$;*
- *conditionally on the bridge X , the random trees $T(i)$, for $i \in \text{DS}(X)$, are independent and distributed according to $\rho_{X_i}^+$.*

We then claim that the UIHPQ can be constructed from \mathcal{B}_∞ via Φ as claimed in (III.4):

Theorem III.3.4 (The new construction of the UIHPQ). *We have $\mathcal{H}_\infty = \Phi(\mathcal{B}_\infty)$ in distribution.*

Establishing such a theorem given Proposition III.3.3 and Proposition III.3.1 would be straightforward if Φ were continuous on TB^+ , which – as we have seen in Remark III.2.5 – is not the case, even if we restrict ourselves to a set of probability 1 under the law of \mathcal{B}_∞ . As anticipated, we need the same kind of computation that Ménard used in [53] to show that the two constructions of the UIPQ (from [23] and [35]) are equivalent; we shall set it up in Section III.3.4.

III.3.3 \mathcal{B}_∞ is the local limit of the \mathcal{B}_p 's

This section is devoted to showing Proposition III.3.3. Since the trees in \mathcal{B}_p and \mathcal{B}_∞ are conditionally independent given the bridges, with laws independent of p , all we need to show is that the local limit of the bridge $X^p = (X_0^p, \dots, X_{2p-1}^p)$, which is distributed as the initial segment of a nearest neighbour random walk with law \mathbb{P}_0 conditioned on hitting 0 after time $2p$, is simply an infinite bridge $(X_i)_{i \in \mathbb{Z}}$, where $(X_i)_{i \geq 0}$ and $(X_{-i})_{i \geq 0}$ are independent nearest neighbour random walks with law \mathbb{P}_0 . In order to show this, we first prove a lemma giving an estimate for the probability that such a random walk transitions from i to j in time p .

Lemma III.3.5. *Let i, j and p be non-negative integers such that $i + j$ has the same parity as p ; call $\mathbf{p}^{(p)}(i, j)$ the probability that a walk with transition probabilities given by \mathbf{p} moves from i to j in time p , that is*

$$\mathbf{p}^{(p)}(i, j) = \sum \prod_{k=0}^{p-1} \mathbf{p}(x_k, x_{k+1})$$

where the sum is taken over all sequences (x_0, \dots, x_p) of non-negative integers such that $x_0 = i$, $x_p = j$ and $|x_{k+1} - x_k| = 1$ (for $k = 0, \dots, p-1$). Then, when p is sent to infinity (along values having the same parity as $i + j$), we have

$$\mathbf{p}^{(p)}(i, j) \sim \frac{1}{6\sqrt{\pi}}(j+1)(j+2)^2(j+3)p^{-5/2}. \quad (\text{III.18})$$

Proof. Notice that the right hand side of (III.18) only depends on j , and that we have already dealt with the case $i = j = 0$, see (III.17). For $\mathbf{p}^{(p)}(i, 0)$, one has the recursive decomposition

$$\mathbf{p}^{(p)}(i, 0) = \mathbf{p}^{(p-1)}(i+1, 0)\mathbf{p}(i, i+1) + \mathbf{p}^{(p-1)}(i-1, 0)\mathbf{p}(i, i-1)\mathbf{1}_{i \geq 1}$$

which inductively yields that for all $i \geq 0$ we have $\mathbf{p}^{(p)}(i, 0) \sim \mathbf{p}^{(p)}(0, 0) \sim \frac{2}{\sqrt{\pi}}p^{-5/2}$ as $p \rightarrow \infty$ along values with the right parity.

An analogous expression can be written for $\mathbf{p}^{(p)}(i, j)$, using recurrence in j :

$$\mathbf{p}^{(p)}(i, j) = \mathbf{p}^{(p-1)}(i, j+1)\mathbf{p}(j+1, j) + \mathbf{p}^{(p-1)}(i, j-1)\mathbf{p}(j-1, j)\mathbf{1}_{j \geq 1};$$

this time, one obtains by induction on j that $\mathbf{p}^{(p)}(i, j) \sim \frac{2}{\sqrt{\pi}}C(j)p^{-5/2}$ (along values of p having the same parity as $i + j$), where $C(j)$ only depends on j and satisfies $C(0) = 1$, as well as $C(j) = \mathbf{p}(j+1, j)C(j+1) + \mathbf{p}(j-1, j)C(j-1)$ for $j \geq 1$. The solution for $C(j)$ is indeed

$$C(j) = \frac{1}{12}(j+1)(j+2)^2(j+3)$$

as can be checked by induction. □

In fact, all that we shall use from the above lemma is a property of the quantity $C(j)$ that is easily deduced from the recursion $C(j) = \mathbf{p}(j+1, j)C(j+1) + \mathbf{p}(j-1, j)C(j-1)$

shown within the proof of the lemma, even without the explicit expression for $C(j)$: dividing both terms of the equality by $C(j)$ yields $\mathbf{p}(j+1, j) \frac{C(j+1)}{C(j)} = 1 - \mathbf{p}(j-1, j) \frac{C(j-1)}{C(j)}$, which by induction (using the fact that $C(0) = 1$) implies

$$\mathbf{p}(j, j-1) \frac{C(j)}{C(j-1)} = \mathbf{p}(j-1, j). \quad (\text{III.19})$$

Proof of Proposition III.3.3. Let $(l_{-r}, \dots, l_0, \dots, l_r)$ be a sequence of non-negative integers such that $l_0 = 0$, $l_{-r} = i$, $l_r = j$ and $|l_{h+1} - l_h| = 1$ for all h such that $-r \leq h < r$; we wish to compute the limit in p of the probability that $(X_i^p)_{-r \leq i \leq r} = (l_i)_{-r \leq i \leq r}$, where as usual indices in the sequence X^p are read modulo $2p$.

We can express such a probability, thanks to the description of X^p given in Proposition III.3.2, as the probability that $X_i = l_i$ and that $X_{2p-i} = l_{-i}$ for $i = 0, \dots, r$, conditioned on the fact that $X_{2p} = 0$; since the probability that $X_{2p} = 0$ is $\mathbf{p}^{(2p)}(0, 0)$, the limit of $\mathbb{P}\left((X_i^p)_{-r \leq i \leq r} = (l_i)_{-r \leq i \leq r}\right)$ as $p \rightarrow \infty$ can be expressed as

$$\lim_{p \rightarrow \infty} \left(\prod_{i=-r}^{r-1} \mathbf{p}(l_i, l_{i+1}) \right) \frac{\mathbf{p}^{(2p-2r)}(l_r, l_{-r})}{\mathbf{p}^{(2p)}(0, 0)} = C(l_{-r}) \prod_{i=-r+1}^0 \mathbf{p}(l_{i-1}, l_i) \prod_{i=0}^{r-1} \mathbf{p}(l_i, l_{i+1}). \quad (\text{III.20})$$

We know that $\frac{C(l_{i-1})}{C(l_i)} \mathbf{p}(l_{i-1}, l_i) = \mathbf{p}(l_i, l_{i-1})$ from (III.19); hence

$$C(l_{-r}) \prod_{i=-r+1}^0 \mathbf{p}(l_{i-1}, l_i) = \prod_{i=-r+1}^0 \frac{C(l_{i-1})}{C(l_i)} \prod_{i=-r+1}^0 \mathbf{p}(l_{i-1}, l_i) = \prod_{i=-r+1}^0 \mathbf{p}(l_i, l_{i-1}) = \prod_{i=0}^{r-1} \mathbf{p}(l_{-i}, l_{-(i+1)}).$$

Substituting in (III.20) yields

$$\begin{aligned} \lim_{p \rightarrow \infty} \mathbb{P}\left((X_i^p)_{-r \leq i \leq r} = (l_i)_{-r \leq i \leq r}\right) &= \\ &= \mathbb{P}(X_0 = l_0, X_1 = l_1, \dots, X_r = l_r) \mathbb{P}(X_0 = l_0, X_{-1} = l_{-1}, \dots, X_{-r} = l_{-r}), \end{aligned}$$

which proves the proposition. \square

III.3.4 Control on small labels and proof of Theorem III.3.4

In order to complete the proof of Theorem III.3.4 and to overcome the obstructions on the continuity of Φ on TB^+ that we discussed in Section III.2.4 we must ensure that, *uniformly in p* , the probability that there are small labels far from the root of the treed bridges \mathcal{B}_p is small (Proposition III.3.8). Once that is done, the proof of Theorem III.3.4 can proceed in a way analogous to [53].

Our first estimate bounds the rate of growth of labels along the bridge $(X_i)_{i \in \mathbb{Z}}$ of \mathcal{B}_∞ . Since the right and left half of the bridge behave as nearest neighbour random walks with transition probabilities given by \mathbf{p} , one can invoke general results for such random walks (see [26]); in particular, the processes $(X_i)_{i \geq 0}$ and $(X_{-i})_{i \geq 0}$ are transient [26, Theorem A]; more precisely, by [26, Theorem 6.1], we have:

Proposition III.3.6. *Let $\mathcal{B}_\infty = ((X_i)_{i \in \mathbb{Z}}; T)$ be the random infinite treed bridge defined in Proposition III.3.3; then for every $\varepsilon > 0$ we have*

$$X_{|i|} \geq |i|^{\frac{1}{2}-\varepsilon}$$

almost surely, for all i large enough.

We shall need an analogous result for finite bridges, which reads as follows:

Lemma III.3.7. *We have*

$$\limsup_{k \rightarrow \infty} \sup_{p \geq 1} \mathbb{P}_0(\exists i : k \leq i \leq p, X_i < i^{1/2-\varepsilon} \mid X_{2p} = 0) = 0.$$

Proof. Introduce the stopping time $\tau_k = \inf\{i \geq k : X_i < i^{1/2-\varepsilon}\}$. We have

$$\begin{aligned} \mathbb{P}_0(\exists i : k \leq i \leq p, X_i < i^{1/2-\varepsilon} \mid X_{2p} = 0) &= \mathbb{P}_0(\{\tau_k \leq p\} \mid X_{2p} = 0) \\ &= (\mathbb{P}_0(X_{2p} = 0))^{-1} \mathbb{P}_0(\{\tau_k \leq p\} \cap \{X_{2p} = 0\}) \\ &\stackrel{\text{Markov}}{=} (\mathbb{P}_0(X_{2p} = 0))^{-1} \mathbb{E}_0[\mathbf{1}_{\{\tau_k \leq p\}} \mathbb{P}_{X_{\tau_k}}(\tilde{X}_{2p-\tau_k} = 0)], \end{aligned}$$

where $(\tilde{X}_i)_{i \geq 0}$ is an independent copy of $(X_i)_{i \geq 0}$.

Now notice that by an easy coupling argument we have $\mathbb{P}_i(X_n = 0) \leq \mathbb{P}_j(X_n = 0)$ if $j \leq i$ have the same parity. Hence we can bound $\mathbb{P}_{X_{\tau_k}}(\tilde{X}_{2p-\tau_k} = 0)$ from above by $\mathbb{P}_{0/1}(\tilde{X}_{2p-\tau_k} = 0)$, where $0/1$ depends on the parity of X_{τ_k} and τ_k . Using (III.17) and Lemma III.3.5 together with the fact that $2p - \tau_k \geq p$ we deduce that there exists a constant $C > 0$ (which does not depend on p) such that $\mathbb{P}_{X_{\tau_k}}(\tilde{X}_{2p-\tau_k} = 0) \leq Cp^{-5/2}$. Coming back to the last display and using (III.17) again, we obtain the following expression, where the constant C is not necessarily the same as above:

$$\mathbb{P}_0(\{\tau_k \leq p\} \mid X_{2p} = 0) \leq C\mathbb{P}_0(\{\tau_k \leq p\}).$$

We have found that for all p we have $\mathbb{P}_0(\exists i : k \leq i \leq p, X_i < i^{1/2-\varepsilon} \mid X_{2p} = 0) \leq C\mathbb{P}_0(\{\tau_k \leq p\}) \leq C\mathbb{P}_0(\{\tau_k < \infty\})$. Proposition III.3.6 then clearly entails that $\mathbb{P}_0(\{\tau_k < \infty\}) \rightarrow 0$ as $k \rightarrow \infty$, which implies the desired result. \square

We now use the above bounds on the rate of growth of labels along the bridge to prove that labels in the random treed bridges \mathcal{B}_p , provided they do not belong to trees grafted near the root, are unlikely to be small (see [53, Section 4.3] for analogous results in the case of the UIPQ).

Proposition III.3.8. *Consider the random treed bridges $\mathcal{B}_p = (X^p; T^p)$ as defined in Proposition III.3.2. For each $i \in \text{DS}(X^p)$, call L_i^p the minimum label appearing in $T^p(i)$. For any $\varepsilon > 0$ and $m \geq 0$ we can find $k > 0$ such that for all p , assuming we see i modulo $2p$,*

$$\mathbb{P}\left(\min_{i \in \text{DS}(X^p) \setminus [-k, k]} L_i^p \leq m\right) \leq \varepsilon.$$

Proof. Fix $m \geq 0$ and $\varepsilon > 0$. Throughout this proof we shall write the random bridge X^p as

$$(X_0^p, X_1^p, \dots, X_p^p, X_{-(p-1)}^p, X_{-(p-2)}^p, \dots, X_{-1}^p)$$

and see $\text{DS}(X^p)$ as a subset of $\{-(p-1), -(p-2), \dots, 0, 1, \dots, p\}$. This way Lemma III.3.7 (together with a symmetry argument) ensures that

$$\lim_{k \rightarrow \infty} \sup_{p \geq 1} \mathbb{P}(\exists i \in \text{DS}(X^p) \setminus [-k, k] : X_i^p \leq |i|^{1/2-\varepsilon}) = 0.$$

That is, we can assume k is such that $\mathbb{P}(\exists i \in \text{DS}(X^p) \setminus [-k, k] : X_i^p \leq |i|^{1/2-\varepsilon}) \leq \varepsilon/2$ for all p .

Therefore we can write

$$\mathbb{P}\left(\min_{i \in \text{DS}(X^p) \setminus [-k, k]} L_i^p \leq m\right) \leq \frac{\varepsilon}{2} + \mathbb{P}\left(\min_{i \in \text{DS}(X^p) \setminus [-k, k]} L_i^p \leq m \mid \forall i \in \text{DS}(X^p) \setminus [-k, k], X_i^p > |i|^{1/2-\varepsilon}\right).$$

Since the trees grafted on the bridge are conditionally independent given $(X_i^p)_{i \geq 0}$, the second term on the right hand side of the inequality is at most

$$\sum_{i \in \text{DS}(X^p) \setminus [-k, k]} \mathbb{P}(L_i^p \leq m \mid X_i^p > |i|^{1/2-\varepsilon}).$$

Let now $\text{LT}_x^{>m} \subset \text{LT}_x^+$ be the set of all positive labelled plane trees such that their root is labelled x and the minimum label appearing in the tree is strictly greater than m . For each index i in $\text{DS}(X^p) \setminus [-k, k]$, we have

$$\mathbb{P}(L_i^p \leq m \mid X_i^p > |i|^{1/2-\varepsilon}) \leq \sup_{x > |i|^{1/2-\varepsilon}} \mathbb{P}(L_i^p \leq m \mid X_i^p = x) = \sup_{x > |i|^{1/2-\varepsilon}} 1 - \rho_x^+(\text{LT}_x^{>m}).$$

Since m is fixed, we may assume that $k > m^{1/(1/2-\varepsilon)}$; we know that $|i| > k$, so we may assume that the supremum is taken over values of x greater than m . If $x > m$, it's quite clear that there is a bijection between $\text{LT}_x^{>m}$ and LT_{x-m}^+ (given by simply subtracting m from all labels), hence $\rho_x^+(\text{LT}_x^{>m}) = \frac{w_{x-m}}{w_x}$. This shows that the probability $\mathbb{P}(L_i^p \leq m \mid X_i^p = x)$ is

$$1 - \frac{w_{x-m}}{w_x} = 1 - \frac{(x-m)(x-m+3)(x+1)(x+2)}{x(x+3)(x-m+1)(x-m+2)}$$

which is less than Cx^{-3} for some constant C only depending on m .

As a consequence,

$$\sup_{x > |i|^{1/2-\varepsilon}} \mathbb{P}(L_i^p \leq m \mid X_i^p = x) \leq \mathbb{P}(L_i^p \leq m \mid X_i^p = \lceil |i|^{1/2-\varepsilon} \rceil) < C|i|^{-3/2-3\varepsilon}$$

for some constant C (only depending on m). Now, summing over i in $\text{DS}(X^p) \setminus [-k, k]$, one gets

$$\sum_{i \in \text{DS}(X^p) \setminus [-k, k]} \mathbb{P}(L_i^p \leq m \mid X_i^p > |i|^{-1/2-\varepsilon}) < 2 \sum_{i=k}^p C i^{-3/2-3\varepsilon} < 2C \sum_{i=k}^{\infty} i^{-3/2-3\varepsilon}.$$

Since the last sum is infinitesimal for $k \rightarrow \infty$ and does not depend on p , we can choose k such that the original expression

$$\mathbb{P}\left(\min_{i \in \text{DS}(X^p) \setminus [-k, k]} L_i^p \leq m \mid \forall i \in \text{DS}(X^p) \setminus [-k, k] \ X_i^p > |i|^{1/2-\varepsilon}\right)$$

is at most $\varepsilon/2$ for all p , and thus establish the proposition. \square

Finally, we shall give the last ingredients needed in order to incorporate our estimates into a proof of Theorem III.3.4. The following lemma (analogous to [53, Proposition 4]) gives the property of Φ that will act as a surrogate for continuity; immediately after, we give a corollary of Proposition III.3.8 that relates Lemma III.3.9 to the previous estimates for the growth of labels.

Lemma III.3.9. *Let $\text{TB}(k, r)$ be the set of all (finite or infinite) positive treed bridges B such that the minimum label appearing on vertices in $B \setminus [B]_k$ is at least $r + 1$. Then for any pair of treed bridges B, B' in $\text{TB}(k, r)$, the equality $[B]_k = [B']_k$ implies $[\Phi(B)]_r = [\Phi(B')]_r$.*

Proof. The argument is similar to that of Infobox III.2. Suppose B is a treed bridge in $\text{TB}(k, r)$; the ball $[\Phi(B)]_r$ is the submap of $\Phi(B)$ spanned by vertices of $\Phi(B)$ having label at most r in B (its edges are those that the construction Φ draws between such vertices). Notice that, if $(c_i)_{i \in I}$ is the sequence of real corners of B , ordered according to the left-to-right contour of the upper face (or counterclockwise contour of the inner face), then $[\Phi(B)]_r$ is determined by the subsequence $(c_{i_j})_{j=1}^N$ of corners bearing labels not exceeding r . Such a subsequence is in turn determined by $[B]_k$ if B is in $\text{TB}(k, r)$, since all corners whose vertices bear label r or smaller are within trees in $[B]_k$, and hence can be recovered (along with their ordering) from $[B]_k$ alone. As a consequence, $[B]_k = [B']_k$ implies $[\Phi(B)]_r = [\Phi(B')]_r$ for any pair of treed bridges B, B' in $\text{TB}(k, r)$. \square

Proposition III.3.8 then gives rise to the following obvious corollary, obtained by setting $m = r + 1$:

Corollary III.3.10. *Given $r \geq 0$ and $\varepsilon > 0$, there is an integer $k > 0$ such that, for each p in $\mathbb{Z}^+ \cup \{\infty\}$, we have $\mathbb{P}(\mathcal{B}_p \notin \text{TB}(k, r)) \leq \varepsilon$.*

We now proceed to show Theorem III.3.4.

Proof of Theorem III.3.4. We shall show that, for each $r > 0$ and for each q , where $q = [Q]_r$ for some rooted quadrangulation Q with an infinite boundary,

$$\lim_{p \rightarrow \infty} \mathbb{P}([\Phi(\mathcal{B}_p)]_r = q) = \mathbb{P}([\Phi(\mathcal{B}_\infty)]_r = q);$$

this will prove that the law of the ball $[\Phi(\mathcal{B}_\infty)]_r$ is the limit in p of the laws of $[\Phi(\mathcal{B}_p)]_r$ for every $r \geq 0$, hence that $\Phi(\mathcal{B}_\infty)$ is the local limit of the random quadrangulations $\Phi(\mathcal{B}_p)$, that is to say the Boltzmann quadrangulations \mathcal{Q}_p^B , for $p \rightarrow \infty$. By Proposition III.3.1, this implies that $\Phi(\mathcal{B}_\infty)$ is indeed distributed as the UIHPQ \mathcal{H}_∞ .

Fix $\varepsilon > 0$; by Corollary III.3.10, we can find k such that for all p we have $\mathbb{P}(\mathcal{B}_p \notin \text{TB}(k, r)) \leq \varepsilon$, and also $\mathbb{P}(\mathcal{B}_\infty \notin \text{TB}(k, r)) \leq \varepsilon$. Consider the set \mathbf{A} of bridges B' in $\text{TB}(k, r)$ such that $[\Phi(B')]_r = q$, and define the set \mathbf{A}_k to be the set of maps $[B']_k$ for B' in \mathbf{A} ; by Lemma III.3.9 a bridge B'' in $\text{TB}(k, r)$ is such that $[\Phi(B'')]_r = q$ if and only if $[B'']_k \in \mathbf{A}_k$. Now consider

$$\left| \lim_{p \rightarrow \infty} \mathbb{P}([\Phi(\mathcal{B}_p)]_r = q) - \mathbb{P}([\Phi(\mathcal{B}_\infty)]_r = q) \right|;$$

by taking intersections with the events $\mathcal{B}_p \in \text{TB}(k, r)$ and $\mathcal{B}_\infty \in \text{TB}(k, r)$, whose complements have probability at most ε , the above can be bounded by

$$2\varepsilon + \left| \lim_{p \rightarrow \infty} \mathbb{P}([\Phi(\mathcal{B}_p)]_r = q \text{ and } \mathcal{B}_p \in \text{TB}(k, r)) - \mathbb{P}([\Phi(\mathcal{B}_\infty)]_r = q \text{ and } \mathcal{B}_\infty \in \text{TB}(k, r)) \right|$$

that is to say

$$2\varepsilon + \left| \lim_{p \rightarrow \infty} \mathbb{P}([\mathcal{B}_p]_k \in \mathbf{A}_k \text{ and } \mathcal{B}_p \in \text{TB}(k, r)) - \mathbb{P}([\mathcal{B}_\infty]_k \in \mathbf{A}_k \text{ and } \mathcal{B}_\infty \in \text{TB}(k, r)) \right|.$$

Up to losing another 2ε , one can add terms of the kind $\mathbb{P}([\mathcal{B}_p]_k \in \mathbf{A}_k \text{ and } \mathcal{B}_p \notin \text{TB}(k, r))$ and $\mathbb{P}([\mathcal{B}_\infty]_k \in \mathbf{A}_k \text{ and } \mathcal{B}_\infty \notin \text{TB}(k, r))$ within the absolute value, thus finally bounding the quantity in question by

$$4\varepsilon + \left| \lim_{p \rightarrow \infty} \mathbb{P}([\mathcal{B}_p]_k \in \mathbf{A}_k) - \mathbb{P}([\mathcal{B}_\infty]_k \in \mathbf{A}_k) \right|,$$

which is 4ε by Proposition III.3.3 (since the law of $[\mathcal{B}_\infty]_k$ is the limit of the laws of $[\mathcal{B}_p]_k$ when p is sent to infinity). Since ε is arbitrary, we have shown the initial desired equality. \square

III.4 A study of geodesic rays in \mathcal{H}_∞

Recall that a geodesic γ in a planar map is a path, finite or infinite, that visits a sequence of vertices $(\gamma(i))_{i \in I}$, where I may be \mathbb{Z} , \mathbb{N} or the set $\{0, 1, \dots, n\}$ (in which case we say the geodesic has length n), such that for each $i, j \in I$ we have $d_{\text{gr}}(\gamma(i), \gamma(j)) = |i - j|$. Notice that, since the maps we consider are not necessarily simple and since γ is formally seen as a sequence of concatenated edges, it is *not* determined by the sequence $(\gamma(i))_{i \in I}$ of the vertices it visits.

Given a vertex x_0 in an infinite map we call a geodesic γ a *geodesic ray issued from x_0* if it is one-ended and starts with x_0 (that is, if it visits a sequence of vertices $(\gamma(i))_{i \in \mathbb{N}}$, with $\gamma(0) = x_0$). In a rooted infinite map, we simply say “geodesic ray” for geodesic

rays issued from the root vertex, as all geodesic rays in Sections III.4.1 and III.4.2 will be.

We shall investigate the (random) set of geodesic rays in the UIHPQ \mathcal{H}_∞ ; in order to do this, given a quadrangulation with a boundary $q \in \mathbf{Q}$ that is the image via Φ of a positive treed bridge $(b; T)$ in \mathbf{TB}^+ , we reconstruct geodesics issued from the root vertex in q as coded by $(b; T)$. A path in q can be expressed in $(b; T)$ as a sequence of corners, since real corners of $(b; T)$ correspond to edges of $q = \Phi((b; T))$. Given a real corner c in $(b; T)$, we shall write $s(c)$ for its successor (as defined in Section III.2.4) and $v(c)$ for its corresponding vertex (which, as remarked in Section III.2.3, can be seen both as a vertex of $(b; T)$ and as a vertex of q). Thanks to the properties that Φ displays when applied to positive treed bridges, a sequence $(c_i)_{i \in I}$ of real corners in $(b; T)$ encodes a geodesic γ issued from the root vertex in q provided that:

- I is either the set $\{1, \dots, n\}$ (for a geodesic of length n) or $\mathbb{N}^+ = \{1, 2, 3, \dots\}$ (for a geodesic ray);
- for each $i \in I$, we have $l(c_i) = i$;
- for each $i \in I \setminus \{1\}$, we have $v(s(c_i)) = v(c_{i-1})$.

The geodesic γ is the path obtained by concatenating the edges drawn by Φ between each corner c_i and its successor $s(c_i)$; in particular, the first edge of γ joins corner c_1 to the corner around the added vertex δ (that is the root vertex in $\Phi((b; T))$).

We shall make this identification implicitly in all that follows: we suppose that the UIHPQ is constructed as $\mathcal{H}_\infty = \Phi(\mathcal{B}_\infty)$, thus reducing the problem of studying geodesic rays in the UIHPQ to that of investigating geodesic rays in the infinite random treed bridge \mathcal{B}_∞ .

III.4.1 The pencil decomposition

Given two geodesic rays γ, γ' in a rooted (infinite) quadrangulation with a boundary $q \in \mathbf{Q}$ we write $\gamma \leq \gamma'$ if γ lies *to the left* of γ' ; that is, if γ lies within the quadrangulation $q|\gamma'$ obtained from q by erasing all vertices that lie strictly to the right of γ' and all edges involving such vertices; equivalently, $\gamma \leq \gamma'$ if γ' lies within $\gamma|q$, the quadrangulation obtained by erasing all vertices and edges of q lying strictly to the left of γ . Notice it is easy to prove existence and uniqueness of maximal and minimal elements for the partial order $>$: we call such elements the *rightmost* and *leftmost* geodesic rays, denoted by γ^{right} and γ^{left} (where dependence on q is implicit). Given any treed bridge $(b; T) \in \mathbf{TB}_\infty^+$, we shall speak of γ^{right} and γ^{left} in $(b; T)$ (as the sequences of corners corresponding to the rightmost and leftmost geodesic rays of $\Phi((b; T))$).

In this section we shall investigate the three random quadrangulations with a boundary one obtains by “cutting up” the UIHPQ along its leftmost and rightmost geodesic rays.

To start with, we shall give a description of the rightmost geodesic ray γ^{right} in an infinite positive treed bridge from \mathbf{TB}_∞^+ .

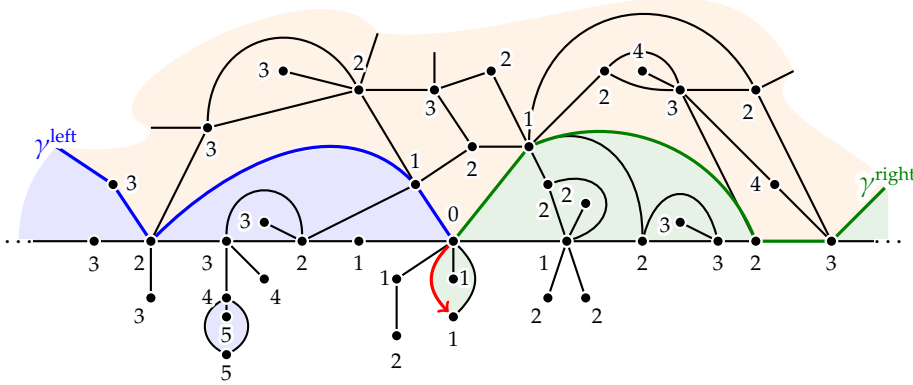


Figure III.6: A neighbourhood of the root vertex in a quadrangulation with an infinite boundary, with its leftmost and rightmost geodesic rays. Any geodesic ray is contained in the orange zone between them. Notice that in this case the root vertex belongs to the infinite “core”; for a more general situation, see Figure III.2.

Lemma III.4.1. *The rightmost geodesic ray γ^{right} in a treed bridge $(b; T) \in \text{TB}_\infty^+$ is the sequence of corners $(c_i^r)_{i \in \mathbb{N}^+}$ such that for each $i > 0$ corner c_i^r is the leftmost real corner labelled i to be found in $(b; T)$ (which is well defined since each label appears a finite number of times in $(b; T)$).*

Proof. The sequence of corners $(c_i^r)_{i \in \mathbb{N}^+}$ is indeed a geodesic ray, since for $i > 0$ we have $l(c_i^r) = i$ by definition, and c_i^r is the successor of c_{i+1}^r (hence $v(s(c_{i+1}^r)) = v(c_i^r)$).

Now consider any geodesic ray $\gamma = (c_i)_{i \in \mathbb{N}^+}$ in $(b; T)$; we shall see that all corners of γ belong to trees lying left of the root vertex.

Notice that, for any real corner c of $(b; T)$ such that $v(c)$ belongs to a tree $T(j)$ with $j < 0$, $v(s(c))$ belongs to a tree $T(j')$, again with $j' < 0$. Now suppose by contradiction that some corner c_k in $\gamma = (c_i)_{i \in \mathbb{N}^+}$ belongs to a tree $T(n_k)$, with $n_k > 0$; since we know that $v(s(c_{k+1})) = v(c_k)$, the vertex $v(c_{k+1})$ must belong to a tree $T(n_{k+1})$ with $0 < n_{k+1} \leq n_k$; inductively, the same result applies to all corners c_i with $i > k$. This, however, is in contradiction with the fact that there is only a finite number of corners whose vertices belong to $\cup_{i \in \text{DS}(b) \cap [0, n_k]} T(i)$.

Consider now any edge $(c, s(c))$ of γ : c belongs to a tree $T(i)$ with $i < 0$, hence there must be two corners c_a^r and c_{a-1}^r in $(c_i^r)_{i \in \mathbb{N}^+}$, such that c is between c_a^r and c_{a-1}^r in the (left-to-right) contour (and c is not c_{a-1}^r); since $s(c_a^r) = c_{a-1}^r$ as remarked, c must have label at least a , and $s(c)$ must be a corner between c and c_{a-1}^r ; as a consequence, the edge $(c, s(c))$ of γ is drawn below the edge (c_a^r, c_{a-1}^r) , and the geodesic ray γ is contained in the portion of $\Phi((b; T))$ lying left of the geodesic $(c_i^r)_{i \in \mathbb{N}^+}$, which is therefore the rightmost geodesic ray. \square

Consider the portion of the UIHPQ that lies to the right of the rightmost geodesic ray γ^{right} ; this is a rooted quadrangulation with a boundary (we consider any “bubbles” attached to the root vertex lying to the right of the root edge as being part of such a quadrangulation, so that it also contains the root edge of the UIHPQ, see Figure III.7),

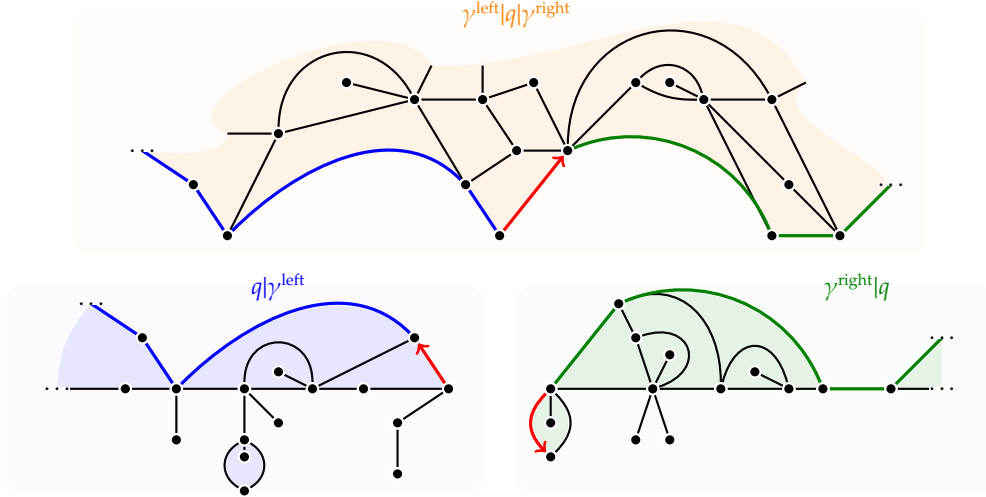


Figure III.7: The three quadrangulations in the pencil decomposition of q ; notice that the root of $\gamma^{\text{right}}|q$ is the root of q , while $q|\gamma^{\text{left}}$ and $\gamma^{\text{left}}|q|\gamma^{\text{right}}$ are rooted in the first edge of the leftmost and rightmost geodesic rays respectively.

which we call $\gamma^{\text{right}}|\mathcal{H}_\infty$. It is now easy to describe it in terms of a random positive treed bridge built from \mathcal{B}_∞ :

Corollary III.4.2. Consider the random infinite treed bridges $\mathcal{B}_\infty^r = ((X_i^r)_{i \in \mathbb{Z}}; T^r)$ and $\mathcal{B}_\infty^l = ((X_i^l)_{i \in \mathbb{Z}}; T^l)$ obtained from $\mathcal{B}_\infty = ((X_i)_{i \in \mathbb{Z}}; T)$ as follows:

- for all $i < 0$, $X_i^r = |i|$ and $T(i)$ is the labelled tree which consists of only a root vertex labelled $|i|$; on the other hand, $X_i^l = X_i$ and $T^l(i) = T(i)$;
- for all $i > 0$, $X_i^r = X_i$ and $T^r(i) = T(i)$; on the other hand, $X_i^l = i$ and $T^l(i)$ consists of only a root vertex labelled i .

Notice that \mathcal{B}_∞^r and \mathcal{B}_∞^l belong to TB_∞^+ almost surely. If we consider \mathcal{H}_∞ as being $\Phi(\mathcal{B}_\infty)$, then we have $\gamma^{\text{right}}|\mathcal{H}_\infty = \Phi(\mathcal{B}_\infty^r)$ and $\mathcal{H}_\infty|\gamma^{\text{right}} = \Phi(\mathcal{B}_\infty^l)$. In particular, the two random variables $\gamma^{\text{right}}|\mathcal{H}_\infty$ and $\mathcal{H}_\infty|\gamma^{\text{right}}$ are independent.

Consider now, given $q \in \mathcal{Q}$, the “flip” (Figure III.8) performed by applying a reflection to q and then rerooting the map thus obtained in the following way: consider the image of the root edge; reroot on the next edge to be found by rotating around the (image of) the root vertex counterclockwise. We call the image of q via this flip q^{\leftrightarrow} .

The flip is an involution on the set \mathcal{Q} , and is easily seen to be continuous for the local distance. Notice that the rightmost and leftmost geodesic rays become exchanged in q^{\leftrightarrow} ; it is easy to see that $(\gamma^{\text{right}}|q)^{\leftrightarrow} = q^{\leftrightarrow}|\gamma^{\text{left}}$, where $\gamma^{\text{right}}|q$ is the quadrangulation obtained by taking what lies to the right of the rightmost geodesic ray of q (including bubbles lying to the right of the root edge, as before), and $q^{\leftrightarrow}|\gamma^{\text{left}}$ the part of q^{\leftrightarrow} that lies left of the leftmost geodesic ray (rooted on the first edge of γ^{left}). This, since $\mathcal{H}_\infty^{\leftrightarrow}$ has the same law as \mathcal{H}_∞ , implies that $\mathcal{H}_\infty|\gamma^{\text{left}}$ has the same law as $(\gamma^{\text{right}}|\mathcal{H}_\infty)^{\leftrightarrow}$.

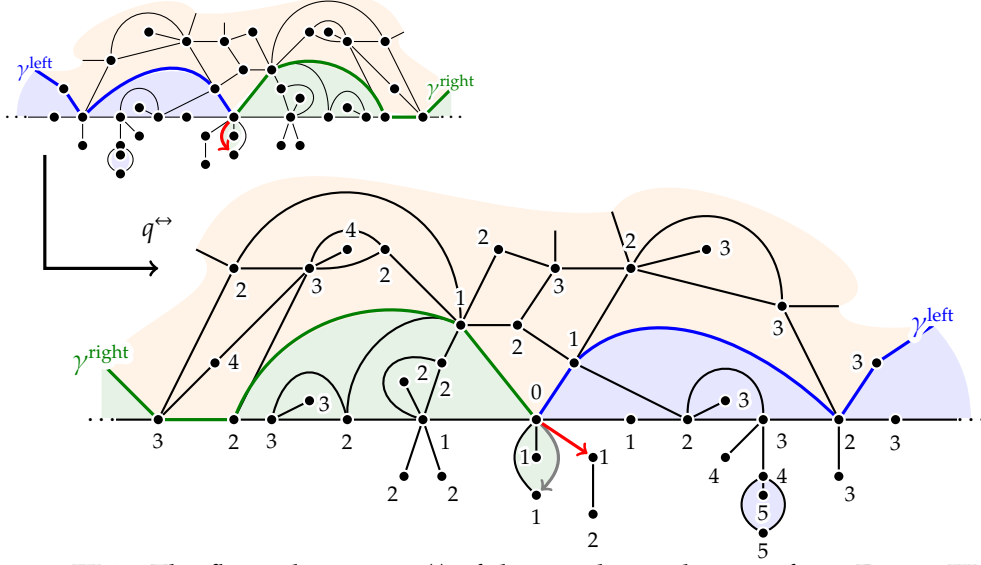


Figure III.8: The flipped version q^{\leftrightarrow} of the quadrangulation q from Figure III.6; notice how the rightmost and leftmost geodesic rays are exchanged, and the root is rotated so as to be oriented clockwise with respect to the outerface.

Using the notation $\gamma^{\text{left}}|\mathcal{H}_\infty|\gamma^{\text{right}}$ for the random quadrangulation $(\gamma^{\text{left}}|\mathcal{H}_\infty)|\gamma^{\text{right}}$ (which is the same as $\gamma^{\text{left}}|(\mathcal{H}_\infty|\gamma^{\text{right}})$), this yields:

Proposition III.4.3 (Pencil decomposition). *Let \mathcal{H}_∞ be the UIHPQ; then the random variables $\mathcal{H}_\infty|\gamma^{\text{left}}$, $\gamma^{\text{right}}|\mathcal{H}_\infty$, $\gamma^{\text{left}}|\mathcal{H}_\infty|\gamma^{\text{right}}$ defined as above (see Figure III.7) are independent.*

Proof. Notice that $\gamma^{\text{left}}|\mathcal{H}_\infty$ and $\gamma^{\text{left}}|\mathcal{H}_\infty|\gamma^{\text{right}}$ are Borel-measurable functions of the whole $\mathcal{H}_\infty|\gamma^{\text{right}}$, which is independent of $\gamma^{\text{right}}|\mathcal{H}_\infty$ by Corollary III.4.2.

Let f_l, f_c, f_r be bounded Borel-measurable functions on the space \mathcal{Q} ; then thanks to the above observation we have

$$\begin{aligned} & \mathbb{E}[f_l(\mathcal{H}_\infty|\gamma^{\text{left}})f_c(\gamma^{\text{left}}|\mathcal{H}_\infty|\gamma^{\text{right}})f_r(\gamma^{\text{right}}|\mathcal{H}_\infty)] = \\ & = \mathbb{E}[f_l(\mathcal{H}_\infty|\gamma^{\text{left}})f_c(\gamma^{\text{left}}|\mathcal{H}_\infty|\gamma^{\text{right}})]\mathbb{E}[f_r(\gamma^{\text{right}}|\mathcal{H}_\infty)]. \end{aligned}$$

On the other hand, since $\mathcal{H}_\infty|\gamma^{\text{left}} = (\gamma^{\text{right}}|\mathcal{H}_\infty^{\leftrightarrow})^{\leftrightarrow}$ and $\gamma^{\text{left}}|\mathcal{H}_\infty|\gamma^{\text{right}} = (\gamma^{\text{left}}|\mathcal{H}_\infty^{\leftrightarrow}|\gamma^{\text{right}})^{\leftrightarrow}$, we have

$$\mathbb{E}[f_l(\mathcal{H}_\infty|\gamma^{\text{left}})f_c(\gamma^{\text{left}}|\mathcal{H}_\infty|\gamma^{\text{right}})] = \mathbb{E}[f_l((\gamma^{\text{right}}|\mathcal{H}_\infty^{\leftrightarrow})^{\leftrightarrow})f_c((\gamma^{\text{left}}|\mathcal{H}_\infty^{\leftrightarrow}|\gamma^{\text{right}})^{\leftrightarrow})];$$

since \mathcal{H}_∞ has the same law as $\mathcal{H}_\infty^{\leftrightarrow}$, the above is the same as

$$\begin{aligned} & \mathbb{E}[f_l((\gamma^{\text{right}}|\mathcal{H}_\infty^{\leftrightarrow})^{\leftrightarrow})f_c((\gamma^{\text{left}}|\mathcal{H}_\infty^{\leftrightarrow}|\gamma^{\text{right}})^{\leftrightarrow})] = \mathbb{E}[f_l((\gamma^{\text{right}}|\mathcal{H}_\infty^{\leftrightarrow})^{\leftrightarrow})]\mathbb{E}[f_c((\gamma^{\text{left}}|\mathcal{H}_\infty^{\leftrightarrow}|\gamma^{\text{right}})^{\leftrightarrow})] = \\ & = \mathbb{E}[f_l(\mathcal{H}_\infty|\gamma^{\text{left}})]\mathbb{E}[f_c(\gamma^{\text{left}}|\mathcal{H}_\infty|\gamma^{\text{right}})], \end{aligned}$$

which proves the proposition. \square

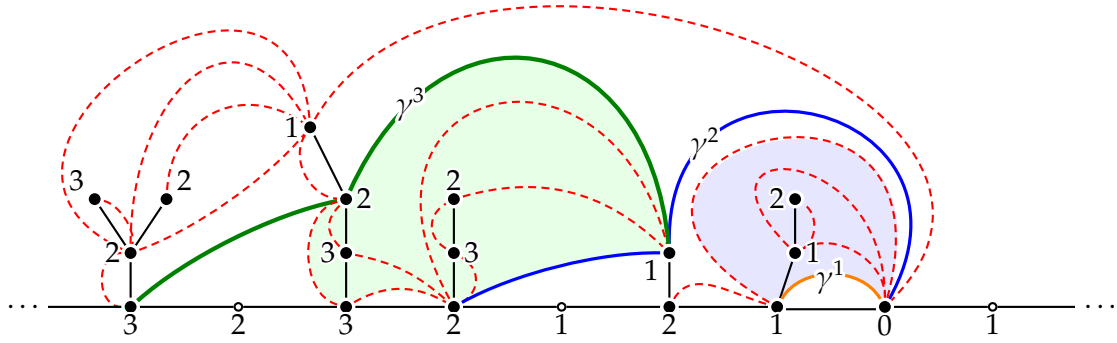


Figure III.9: The sequence of increasing geodesics $\gamma^1, \gamma^2, \gamma^3, \dots$

In this pencil decomposition, the quadrangulations $\gamma^{\text{right}}|\mathcal{H}_\infty$ and $\mathcal{H}_\infty|\gamma^{\text{left}}$ have boundaries that are “free” on one side of the root vertex (the right and left side respectively), while the other half of the boundary is a strict geodesic, in the sense that there is no way to join any two of its vertices by a geodesic other than following the boundary itself. This boundary condition is reminiscent of the works by Bouttier & Guitter [18] and Le Gall [44] on quadrangulations with geodesic boundaries involved in the “slice decomposition”.

We shall now study the geometry of the quadrangulation $\gamma^{\text{left}}|\mathcal{H}_\infty|\gamma^{\text{right}}$ and show that it does look like a “pencil” at large scales; in order to do this, we need a more detailed description of γ^{left} .

III.4.2 The leftmost geodesic ray

Proposition III.4.4. *Given a treed bridge $(b; T) \in \text{TB}_\infty^+$, define a sequence of (finite) geodesics $(\gamma^n)_{n \geq 1}$ so that $\gamma^n = (c_i^n)_{1 \leq i \leq n}$, where $v(c_n^n)$ is the root of the leftmost tree in $T(\text{DS}(b))$ having root label n , c_n^n is its rightmost corner, and for each $i = 1, \dots, n - 1$ the corner c_i^n is the rightmost among those such that $v(c_i^n) = v(s(c_{i+1}^n))$. Then γ^n converges to γ as $n \rightarrow \infty$, where γ is the leftmost geodesic ray in $\Phi((b; T))$, monotonically with respect to the left-to-right order \prec .*

Proof. The sequence of geodesics $(\gamma^n)_{n \geq 1}$ is indeed increasing for \prec , in the sense that γ^n lies left of γ^{n+1} for each $n > 0$. As a consequence, finite initial segments stabilise after finite time: for each k there is n_k such that, for $n \geq n_k$, we have $c_j^n = c_j^{n_k}$ for $j = 1, \dots, k$ (that is, the geodesics γ^n , for $n \geq n_k$, coincide up to distance k from the root).

Consider now the sequence of corners $\gamma = (c_k^{n_k})_{k > 0}$; such a sequence is a geodesic ray (since for any $k > 1$ we must have $v(s(c_k^{n_k})) = v(c_{k-1}^{n_k}) = v(c_{k-1}^{n_{k-1}})$), lies to the right of each geodesic in the sequence $(\gamma^n)_{n \geq 1}$ and is the leftmost geodesic with this property.

We now claim that γ is the leftmost geodesic ray in $(b; T)$; all we need to show is that there cannot be a geodesic ray lying left of γ . Equivalently, we show that for each geodesic γ^n , all geodesic rays lie to the right of γ^n . Suppose $\gamma' = (c'_i)_{i \in \mathbb{N}^+}$ is a geodesic ray, and suppose part of it lies strictly to the left of γ^n for some $n > 0$. Since the region of $\Phi((b; T))$ lying left of γ^n is finite, by following γ' away from the root vertex, we must

eventually leave it. This amounts to saying that we can take

$$m = \max \left\{ i \in \{1, \dots, n\} \mid v(c'_i) = v(c_i^n) \text{ and the edge } (c'_i, s(c'_i)) \text{ lies strictly left of } \gamma^n \right\},$$

since if the set above is empty, then γ' lies to the right of γ^n . This, however, is a contradiction: c_i^n is defined as the rightmost corner of $v(c_i^n)$, hence there is no edge issued from $v(c_i^n)$ lying strictly to the left of the edge $(c_i^n, s(c_i^n))$, which belongs to γ^n . \square

Proposition III.4.5. *Let $\mathcal{B}_\infty^c = ((X_i^c)_{i \in \mathbb{Z}}; T^c)$ be a random treed bridge such that*

- $X_i^c = |i|$ for all $i \in \mathbb{Z}$;
- the trees $T^c(i)$ are independent and distributed according to $\rho_{|i|}^+$ for all $i < 0$.

Notice that \mathcal{B}_∞^c belongs to \mathbf{TB}_∞^+ almost surely. Then $\gamma^{\text{left}}|\mathcal{H}_\infty|\gamma^{\text{right}}$ has the same law as $\Phi(\mathcal{B}_\infty^c)$.

Proof. Let $(\gamma^n)_{n \geq 1}$ be the (random) sequence of geodesics in \mathcal{B}_∞ defined within Proposition III.4.4, and $\gamma^{\text{left}} = (c_i)_{i \in \mathbb{N}^+}$ be the leftmost geodesic ray in \mathcal{B}_∞ . Call $T'(-i)$, for $i > 0$, the tree of descendants of $v(c_i)$ that lie “above” the geodesic ray; then $\gamma^{\text{left}}|\Phi(\mathcal{B}_\infty)|\gamma^{\text{right}}$ is the image via Φ of the treed bridge $(b; T')$, where $b = (|i|)_{i \in \mathbb{Z}}$. All we need to show is, therefore, that for each $i > 0$ the tree $T'(-i)$ has law ρ_i^+ , and that all such trees are independent.

Given any fixed $n > 0$, consider the trees t_1^n, \dots, t_n^n lying above the geodesic γ^n , rooted in $v(c_1^n), \dots, v(c_n^n)$; we show they are independent and distributed according to $\rho_1^+, \dots, \rho_n^+$. This is essentially a consequence of the fact, remarked upon in Section III.2.1.1, that ρ_i^+ is the law of a multi-type Galton–Watson tree. Consider the part of \mathcal{B}_∞ that lies below γ^n and notice that it is independent of trees t_1^n, \dots, t_n^n (given an instance of \mathcal{B}_∞ , substituting such trees for another n -tuple t_1^n, \dots, t_n^n would still yield the same geodesic γ^n , since $s(c_i^n)$, for $i = 1, \dots, n$ only depends on corners which lie below γ^n). From this observation the claim easily follows.

Now, given any positive integer k , consider the trees $T'(-1), \dots, T'(-k)$ and let f_1, \dots, f_k be measurable bounded functions on \mathbf{LT}^+ . We have

$$\mathbb{E} \left[\prod_{i=1}^k f_i(T'(-i)) \right] = \lim_{n \rightarrow \infty} \mathbb{E} \left[\prod_{i=1}^k f_i(t_i^n) \right] = \lim_{n \rightarrow \infty} \prod_{i=1}^k \mathbb{E} [f_i(t_i^n)],$$

where the first equality holds by dominated convergence and for the second we use independence of the trees t_1^n, \dots, t_n^n . Now, since $\lim_{n \rightarrow \infty} \mathbb{E} [f_i(t_i^n)] = \mathbb{E} [f_i(T'(-i))]$ for each $i = 1, \dots, k$, one obtains that the trees $T'(-1), \dots, T'(-k)$ are independent and distributed according to $\rho_1^+, \dots, \rho_k^+$, as wanted. \square

The following result is analogous to [30]:

Corollary III.4.6. *The quadrangulation $\gamma^{\text{left}}|\mathcal{H}_\infty|\gamma^{\text{right}}$ almost surely has an infinite number of pinch points; in other words, the leftmost and rightmost geodesic rays in the UIHPQ \mathcal{H}_∞ almost surely have an infinite number of vertices in common (through which all geodesic rays in \mathcal{H}_∞ must pass).*

Proof. The two rays meet in a vertex labelled k if the leftmost corner labelled k in the treed bridge $\mathcal{B}_\infty^c = ((X_i^c)_{i \in \mathbb{Z}}, T^c)$ is actually the vertex X_{-k}^c of the bridge of \mathcal{B}_∞^c , which corresponds to the leftmost geodesic ray.

Since the bridge of \mathcal{B}_∞^c is geodesic, the leftmost tree whose root is labelled k is $T^c(-k)$; the above event thus corresponds to the intersection of events

$$\cap_{i>k} \{T^c(-i) \text{ has no vertices labelled } k\},$$

which (by Proposition III.4.5) has probability

$$p_k = \prod_{i>k} \mathbb{P}(T^c(-i) \text{ has no vertices labelled } k) = \prod_{i>k} w_{i-k}/w_i = 2^{-k} \prod_{i=1}^k w_i = \frac{1}{3} \frac{k+3}{k+1}.$$

Hence the probability that the two geodesics have an infinite number of vertices in common is at least $\liminf_{k \rightarrow \infty} p_k$, which is $1/3$ (thus strictly positive). As a consequence, since the event is a tail event for the sequence of independent random variables $(T^c(-i))_{i \geq 1}$, such a probability is 1 by Kolmogorov's 0-1 law. \square

III.4.3 Extension of results from [30]

As remarked in Section III.3.2, the UIHPQ can be presented as $\Phi(\mathcal{B}_\infty^\pm)$, where \mathcal{B}_∞^\pm is the uniform infinite treed bridge from Definition III.3.1.

Notice that, while in the construction $\mathcal{H}_\infty = \Phi(\mathcal{B}_\infty)$ labels in the treed bridge have a clear geometric interpretation (as distances to the root vertex in \mathcal{H}_∞), interpreting labels of \mathcal{B}_∞^\pm as a function of \mathcal{H}_∞ is less immediate. The following result is analogous to what one obtains in the case of the UIPQ [30]; it is stated as an open question in [31], and this section will be devoted to providing a proof.

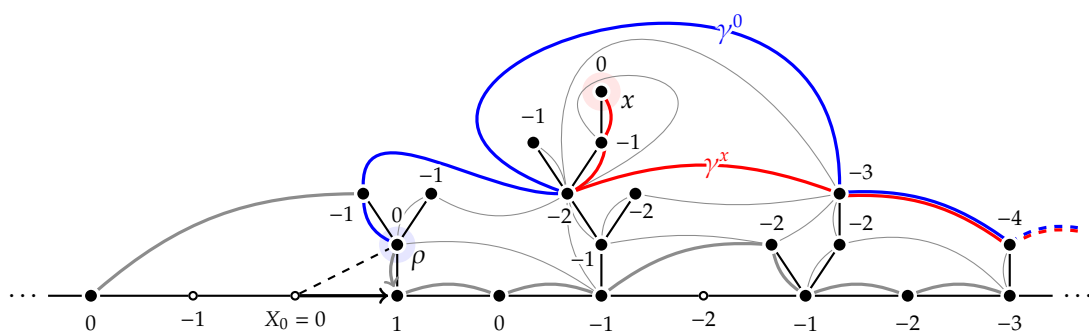
Theorem III.4.7. *Consider the UIHPQ as $\mathcal{H}_\infty = \Phi(\mathcal{B}_\infty^\pm)$ (where \mathcal{B}_∞^\pm is as in Definition III.3.1); then almost surely, for each pair of vertices x, y of \mathcal{H}_∞ , writing $l(x)$ and $l(y)$ for the labels they bear in \mathcal{B}_∞^\pm , we have*

$$l(x) - l(y) = \lim_{z \rightarrow \infty} d_{\text{gr}}(x, z) - d_{\text{gr}}(y, z), \quad (\text{III.21})$$

where by $z \rightarrow \infty$ we mean that z leaves any finite region of \mathcal{H}_∞ .

In order to prove this result we work along the same lines as in [30]; one of the ingredients that were missing in [31] in order to obtain Theorem III.4.7 is the coalescence of geodesic rays implied by our new construction of the UIHPQ.

To begin with, we need to have a look at how geodesic rays appear in \mathcal{B}_∞^\pm ; we call a *proper geodesic ray issued from x in \mathcal{B}_∞^\pm* , where x is a (real) vertex, a sequence of corners $\gamma = (c_i)_{i \geq 0}$ such that $v(c_0) = x$ and that $v(s(c_i)) = v(c_{i+1})$ for all $i \geq 0$, so that $l(c_i) = l(x) - i$. Notice that, while proper geodesic rays issued from a vertex in \mathcal{B}_∞^\pm do correspond to geodesics in \mathcal{H}_∞ (because $d_{\text{gr}}(x, y) \geq |l(x) - l(y)|$ for all vertices in \mathcal{H}_∞), it is not clear that every geodesic ray issued from a vertex in \mathcal{H}_∞ corresponds to a proper geodesic ray issued from that vertex in \mathcal{B}_∞^\pm ; we know thanks to Corollary III.4.6, however, that this is the case for geodesic rays issued from the root vertex:


 Figure III.10: The proper geodesic rays γ^0 and γ^x .

Proposition III.4.8. *Every geodesic ray (issued from the root vertex) in $\mathcal{H}_\infty = \Phi(\mathcal{B}_\infty^\pm)$ is proper.*

Proof. This follows from Corollary III.4.6 by the same argument as in [30]: we know that there is (almost surely) an infinite set I of vertices in \mathcal{H}_∞ such that every geodesic ray visits all of the vertices in the set. Notice that there exists a proper geodesic ray in \mathcal{H}_∞ , since one is obtained by simply iterating the successor function starting from a corner adjacent to the root vertex; call such a geodesic ray γ , and call $\gamma(i)$, for $i \in \mathbb{N}$, the i -th vertex visited by γ . We have $I \subseteq \{\gamma(i) \mid i \geq 0\}$, so for every vertex v in I we have $v = \gamma(j)$ (where j is the graph distance between v and the root vertex) hence $l(v) = -j$. Now take any geodesic ray γ' ; we know all vertices in I belong to γ' , hence the set $\{i \mid l(\gamma'(i)) = -i\}$ is infinite; but then, since labels vary by at most one along a geodesic ray (indeed, along any path), $l(\gamma'(i)) = -i$ for all $i \geq 0$, and γ' is proper. \square

Considering the UIHPQ as $\mathcal{H}_\infty = \Phi(\mathcal{B}_\infty^\pm)$, we shall call γ^0 the proper geodesic ray described within the above proof, which we obtain by taking the leftmost corner around the real vertex in \mathcal{B}_∞^\pm which corresponds to the root vertex ρ of \mathcal{H}_∞ and iterating the successor function, thereby generating a geodesic ray along which labels decrease strictly at each step. Notice that one may do the same for every real vertex: pick the leftmost corner adjacent to a real vertex x in \mathcal{B}_∞^\pm and iterate the successor function, building an infinite path γ^x in \mathcal{H}_∞ along which labels decrease strictly at each step, which is therefore a proper geodesic ray (issued from x).

Also notice that for any real vertex x the two proper geodesic rays $\gamma^0 = (c_i^0)_{i \geq 0}$ and $\gamma^x = (c_i^x)_{i \geq 0}$ (which is issued from x) must eventually meet (and, indeed, coincide from a certain point onwards, see Figure III.10).

We now prove a simple lemma about a property of confluence to the root that geodesic rays display in the UIHPQ; the statement is presented in terms of γ^0 , but any geodesic ray issued from the root could be used as reference.

Lemma III.4.9. *For each positive integer r there is a positive integer R such that, if z is a vertex of \mathcal{H}_∞ for which $d_{\text{gr}}(z, \rho) > R$ (where ρ is the root vertex), then there is a (finite) geodesic γ^{0z} joining ρ to z that coincides with γ^0 up to the r -th step (hence in particular $\gamma^{0z}(i) = \gamma^0(i)$ for $i = 0, \dots, r$).*

Proof. Consider $k = \min\{i \geq r \mid \gamma^0(i) \in I\}$, where I is the set of vertices at which the leftmost and rightmost geodesic rays in \mathcal{H}_∞ meet (which is infinite by Corollary III.4.6, so that k is well defined). Consider then the (finite) set of all vertices at distance k from the root vertex, with the exception of vertex $\gamma^0(k)$; since all geodesic rays issued from ρ go through $\gamma^0(k)$, no vertex in the set belongs to a geodesic ray issued from ρ . By local finiteness, this implies that there is $R \geq 0$ such that no finite geodesic issued from ρ having length more than R can go through any of the vertices in the set. Hence, if a vertex z is such that $d_{\text{gr}}(z, \rho) > R$, then any geodesic γ joining ρ to z must go through $\gamma^0(k)$. It is therefore enough to build γ^{0z} by following γ^0 from ρ to $\gamma^0(k)$, then γ from $\gamma^0(k)$ to z ; since $k \geq r$, γ^{0z} satisfies the requirement of the lemma. \square

From here we can prove a key confluence property of all “long” geodesics: given any vertex x , geodesics issued from x which reach far enough must eventually intersect γ^0 ; more precisely:

Lemma III.4.10. *Given a vertex x in $\mathcal{H}_\infty = \Phi(\mathcal{B}_\infty^\pm)$ there are positive integers r and R such that for any vertex z for which $d_{\text{gr}}(z, \rho) > R$, all geodesics joining x to z meet γ^0 before its r -th step.*

Proof. We start by showing that all geodesic rays issued from x meet γ^0 . Let γ be any such geodesic ray; since the sequence $d_{\text{gr}}(\gamma(n), \rho) - n$ is decreasing in n (for each n one has $d_{\text{gr}}(\gamma(n+1), \rho) - d_{\text{gr}}(\gamma(n), \rho) \leq 1$), it must be constant from some n_0 onwards. Thus replacing the part of γ that joins x to $\gamma(n_0)$ with a finite geodesic joining ρ to $\gamma(n_0)$ yields a geodesic ray issued from the root. By Corollary III.4.6, this implies that γ meets γ^0 an infinite number of times.

Suppose now by contradiction that for all positive integers r and n there is a vertex $z_{n,r}$ such that $d_{\text{gr}}(z_{n,r}, \rho) > n$ and that there is a geodesic $\gamma_{n,r}$ joining x to $z_{n,r}$ that does not visit any vertex in the sequence $\gamma^0(0), \dots, \gamma^0(r)$. Then for each $k > 0$ we can build a geodesic ray γ_k issued from x that does not go through $\gamma^0(0), \dots, \gamma^0(k)$ (since for every i there is, by local finiteness, an infinite subsequence of $(\gamma_{n,k})_{n>0}$ such that all of its members coincide up to the i -th step). Similarly, for each r there is an infinite subsequence of $(\gamma_k)_{k>0}$ consisting of geodesic rays that coincide up to the r -th step, hence a geodesic ray issued from x that never meets γ^0 . The lemma is thus proven by contradiction. \square

The lemmas presented above are enough to establish Theorem III.4.7:

Proof of Theorem III.4.7. Without loss of generality, we can prove the required equality for pairs involving the root vertex ρ of the UIHPQ; the statement for a pair of vertices (x, y) trivially follows by applying (III.21) to (x, ρ) and (ρ, y) .

Consider a vertex x of \mathcal{H}_∞ ; build the geodesic rays γ^0 and γ^x , and suppose they coincide from $\gamma^0(k)$ onwards for some k . By Lemma III.4.10 there are positive integers r and R_1 such that, if $d_{\text{gr}}(z, \rho) > R_1$, then any geodesic joining x to z must meet γ^0 before its r -th step (and, clearly, we may assume $r \geq k$). On the other hand, by Lemma III.4.9 one can find $R \geq R_1$ such that, if $d_{\text{gr}}(z, \rho) > R$, then there is a geodesic γ^{0z} joining ρ to z which coincides with γ^0 up to $\gamma^0(r)$.

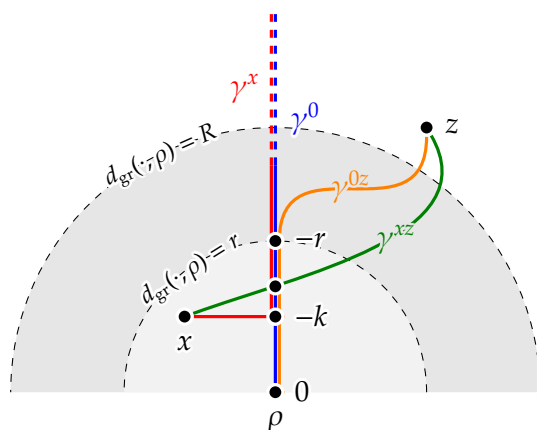


Figure III.11: The geodesics and geodesic rays from the proof of Theorem III.4.7: note that γ^x and γ^0 are proper, and that γ^{xz} is a generic geodesic joining x to z .

Take z such that $d_{\text{gr}}(z, \rho) > R$ and consider a geodesic γ^{xz} joining x to z . Notice that there is a geodesic joining x to z that goes through $\gamma^0(r)$: suppose that γ^{xz} meets γ^0 at $\gamma^0(i)$, with $i < r$; then we may follow the geodesic γ^{xz} from x up to $\gamma^0(i)$, and then follow the geodesic γ^{0z} between $\gamma^0(i)$ and z , thus obtaining a geodesic path from x to z that goes through $\gamma^0(r)$ (see Figure III.11).

As a consequence, we can compute the distance between x and z as $d_{\text{gr}}(z, x) = d_{\text{gr}}(z, \gamma^0(r)) + d_{\text{gr}}(\gamma^0(r), x)$, while we have $d_{\text{gr}}(z, \rho) = d_{\text{gr}}(z, \gamma^0(r)) + r$ (since the geodesic γ^{0z} joins ρ to z and goes through $\gamma^0(r)$). Subtracting the two expressions yields

$$d_{\text{gr}}(z, x) - d_{\text{gr}}(z, \rho) = d_{\text{gr}}(\gamma^0(r), x) - r.$$

Now, since γ^0 and γ^x are proper and they both go through $\gamma^0(r)$, we must have $l(\gamma^0(r)) = -r = l(x) - d_{\text{gr}}(\gamma^0(r), x)$, hence

$$d_{\text{gr}}(z, x) - d_{\text{gr}}(z, \rho) = l(x)$$

as wanted. □

III.5 Scaling limits

In this section we compute the scaling limit of the infinite positive treed bridge \mathcal{B}_∞ introduced in Proposition III.3.3, which encodes the UIHPQ. The definitions, results and proofs in this section are very close to those of [45]; we thus use the same notation and presentation so that the reader may easily compare the relevant sections in the two papers. From the scaling limit of \mathcal{B}_∞ we derive the limiting law for the volume of balls, suitably rescaled, in the UIHPQ. We then extend such results to the UIHPQ with a simple boundary, using the pruning operation from [31]; they shall be used in a paper now in preparation (some of whose main ideas are presented in Section III.7)

to study the model of a self-avoiding walk on the UIPQ. Finally, as a byproduct of the computation of these scaling limits we construct a new random locally compact metric space, the *Brownian half-plane*, which – we believe – describes the scaling limit of the UIHPQ in the local Gromov–Hausdorff topology.

III.5.1 Scaling limits for \mathcal{B}_∞

Let $\mathcal{B}_\infty = ((X_i)_{i \in \mathbb{Z}}; T)$ be the positive infinite treed bridge from Proposition III.3.3. Recall that the bridge X is given by the concatenation of two independent walks with step distribution \mathbf{p} , issued from 0, and that in the construction of \mathcal{H}_∞ as $\Phi(\mathcal{B}_\infty)$ the process X encodes distances between the root vertex and vertices found along the boundary of \mathcal{H}_∞ .

Proposition III.5.1 (Scaling limit for distances along the boundary). *We have the following convergence in distribution, uniformly on every compact subset of \mathbb{R} :*

$$\left(\frac{X_{[nt]}}{\sqrt{n}} \right)_{t \in \mathbb{R}} \xrightarrow[n \rightarrow \infty]{(d)} (Z_t)_{t \in \mathbb{R}},$$

where $(Z_t)_{t \geq 0}$ and $(Z_{-t})_{t \geq 0}$ are two independent Bessel processes of dimension 5.

Proof. This is a direct consequence of a well known result of Lamperti [38] (see also [10, Section 5.2]), if one uses the explicit expression for the transition probabilities \mathbf{p} given by (III.15). \square

In order to compute the scaling limit of the full infinite positive treed bridge \mathcal{B}_∞ we encode it by a pair of processes (C, V) defined on \mathbb{Z} , built by reading labels along the contour. Heuristically, imagine that a particle follows the contour of the treed bridge \mathcal{B}_∞ from left to right, meeting all corners $(c_i)_{i \in \mathbb{Z}}$ of the treed bridge (adjacent to both real and phantom vertices, in left-to-right order, so that c_0 is the corner adjacent to the root vertex of the treed bridge); we define $C(i)$ to be the distance in the treed bridge between $v(c_i)$ and the root vertex, and $V(i)$ to be the label of $v(c_i)$.

We now proceed to describe the scaling limit for the pair (C, V) . In order to introduce the limiting processes we shall need some notation: we refer the reader to [45, Section 2.4] for details. In particular we need \mathbb{N}_x , the excursion measure of the Brownian snake started at x and driven by an excursion of the Brownian motion under the standard Itô excursion measure. For our purposes, we can see this object as a sigma-finite measure on the space Ω of all pairs of continuous paths

$$\omega = (\mathbf{e}_t, \widehat{\mathbf{w}}_t)_{0 \leq t \leq \sigma}$$

where $\sigma = \sigma(\omega)$ is the lifetime of the path ω and is “distributed” according to the measure $d\sigma / (2\sqrt{2\pi\sigma^3})$. Roughly speaking, conditionally on σ , the process $(\mathbf{e}_t)_{0 \leq t \leq \sigma}$ is a Brownian excursion of length σ and $\widehat{\mathbf{w}}$ is the head of the Brownian snake started at x and driven by \mathbf{e} . We denote by $\mathcal{R}(\omega)$ the range of the path $\widehat{\mathbf{w}}$.

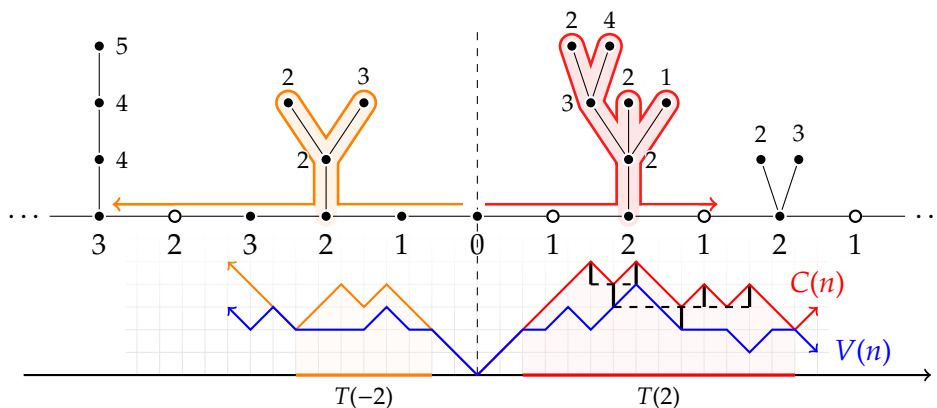


Figure III.12: The processes C and V as produced by a particle visiting the treed bridge along its contour. Notice that V may remain constant on intervals corresponding to trees $T(i)$, and may only increase or decrease when the particle is moving along the bridge; intervals corresponding to trees may be retrieved from the values of C , since the last time the i -th bridge vertex is visited corresponds to the point where C takes the value i for the last time.

Recall from Proposition III.5.1 that Z is a two-sided Bessel process of dimension 5. Conditionally given Z , let $\mathcal{N} = \sum_{i \in I} \delta_{(r_i, \omega_i)}$ be a Poisson process on $\mathbb{R} \times \Omega$ with intensity

$$dt \mathbb{N}_0(d\omega) \mathbf{1}_{\min \mathcal{R}(\omega) > -\sqrt{\frac{3}{2}} Z_t}. \quad (\text{III.22})$$

Note that, in contrast with [45, Eq. (7)], there is no multiplicative factor of 2 in the above display, and that the Bessel process has been multiplied by a factor of $\sqrt{3/2}$. From this Poisson process we build two continuous functions ζ and \widehat{W} as follows (see [45, Section 3.1] for details). For each $i \in I$ we set

$$\sigma_i = \sigma(\omega_i), \quad \omega_i = (\mathbf{e}_s^i, \widehat{\mathbf{w}}_s^i)_{0 \leq s \leq \sigma_i}.$$

Then the two functions ζ and \widehat{W} needed to describe the scaling limit of (C, V) are obtained by concatenating (in the order given by the r_i) the functions

$$\left(r_i + \mathbf{e}_s^i, \sqrt{\frac{3}{2}} Z_{r_i} + \widehat{\mathbf{w}}_s^i \right)_{0 \leq s \leq \sigma_i}.$$

More formally, for $u \in \mathbb{R}$ we set

$$\tau_u = \sum_{i \in I} \mathbf{1}_{\{r_i \in [0, u]\}} \cdot \sigma_i;$$

then clearly $u \mapsto \tau_u$ is right-continuous and increasing on \mathbb{R}_+ , left-continuous and decreasing on \mathbb{R}_- . For all $s \in \mathbb{R}$ there is a unique u with the same sign as s such that $|s|$ is between τ_{u-} and τ_{u+} , and we have exactly one of the following:

- there is a unique $i \in I$ such that $u = r_i$; in this case, we set

$$\begin{aligned}\zeta_s &= |u| + \mathbf{e}_{\|s|-\tau_{u-}|}^i \\ \widehat{W}_s &= \sqrt{\frac{3}{2}}Z_u + \widehat{\mathbf{w}}_{\|s|-\tau_{u-}|}^i\end{aligned}$$

- there is no such i (this happens if $\tau_{u-} = s = \tau_{u+}$); in this case, we set

$$\zeta_s = |u| \quad \text{and} \quad \widehat{W}_s = \sqrt{\frac{3}{2}}Z_u.$$

It is easy to see that both ζ and \widehat{W} are continuous processes over \mathbb{R} ; an easy adaptation of the argument yielding [45, Eq. (8)] (replacing the Bessel process of dimension 9 by $\sqrt{3/2}$ times a Bessel process of dimension 5) shows that \widehat{W} is transient in the sense that $\lim_{s \rightarrow \pm\infty} \widehat{W}_s = +\infty$ almost surely.

Theorem III.5.2 (Scaling limit for the contour functions). *We have the following convergence in distribution uniformly on every compact subset of \mathbb{R} :*

$$\left(\frac{1}{n}C(n^2s), \sqrt{\frac{3}{2n}}V(n^2s) \right)_{s \in \mathbb{R}} \xrightarrow[n \rightarrow \infty]{(d)} (\zeta_s, \widehat{W}_s)_{s \in \mathbb{R}}.$$

Proof. A proof of this result can be obtained with the methods developed in [45] to prove Theorem 5; since all that is needed is a series of marginal adjustments, we shall not repeat here the rather long and technical argument in full, but simply highlight the differences between our model and that of [45]. In [45], finite trees are grafted on both sides of a semi-infinite spine; they are, exactly as in our case, conditionally independent given the labels $(Y_i)_{i \geq 0}$, and distributed according to $\rho_{Y_i}^+$. The fact that in our case trees are grafted on only one side of the infinite bridge simplifies the situation slightly (we only have to account for one process \widehat{W} coding the labels instead of two correlated processes). As in [45], the fact that the labels in the contour of random positive labeled trees evolve roughly like random walks with increments uniformly chosen in $\{-1, 0, +1\}$ justifies the rescaling of the label process by $\sqrt{2n/3}$ in space and n in time, see [45, Proposition 3]. Contrary to what happens in [45], however, labels along the bridge itself can vary only by $+1$ or -1 ; because of this, rescaling (by $\sqrt{\frac{2n}{3}}$ in space and n in time) and taking the limit results in $\sqrt{3/2}$ times a standard Bessel process of dimension 5. This modification has no bearing at all on the arguments of the proof, since the rough estimates needed are also valid for multiples of Bessel 5 processes. Finally, finite trees in [45] are grafted at every vertex of the spine; here, trees are only grafted on down-steps of our infinite bridge; this has been taken into account by having the intensity measure in (III.22) lose a factor of 2 with respect to the analogue [45, Eq. (7)]. More precisely, if one considers the counting measure on down-steps then it is easy to see that

$$\frac{1}{n} \sum_{i \in \text{DS}(X)} \delta_{i/n} \xrightarrow[n \rightarrow \infty]{a.s.} \frac{1}{2} \cdot \text{Leb},$$

where Leb is the Lebesgue measure. With these remarks at hand, it is easy to adapt the proof of [45, Theorem 5] to obtain the desired result. \square

III.5.2 Volume estimates

We can now use Theorem III.5.2 to deduce the limiting law of the profile of distances in the UIHPQ exactly as in [45, Section 4]. Here we shall focus on a simpler quantity than the full distance profile, namely the volume of the ball of radius r in the UIHPQ.

Proposition III.5.3. *Let $\#[\mathcal{H}_\infty]_n$ denote the volume of the ball of radius n in the UIHPQ (that is, the number of its vertices). Then we have the following convergence in distribution:*

$$\frac{1}{n^4} \#[\mathcal{H}_\infty]_n \xrightarrow[n \rightarrow \infty]{(d)} \frac{9}{8} \int_{\mathbb{R}} ds \mathbf{1}_{\widehat{W}_s \leq 1}.$$

Again we do not provide a full proof of the proposition, since all that is needed is a simple adaptation of [45, Proof of Theorem 6] using Theorem III.5.2. We shall, however, sketch the chain of approximate equalities in order to highlight the role of the scaling constants.

To begin with, note that for large $r \geq 0$ we have

$$\frac{1}{r^4} \#[\mathcal{H}_\infty]_r \approx \frac{1}{2r^4} \int_{\mathbb{R}} \mathbf{1}_{V(s) \leq r} ds.$$

The reason for the factor $\frac{1}{2}$ is that every edge of each tree is visited twice by the contour process, and that there are roughly as many real vertices in \mathcal{B}_∞ as edges visited by the contour process on large scales. Next we use Theorem III.5.2 to argue that

$$\begin{aligned} \frac{1}{2r^4} \int_{\mathbb{R}} \mathbf{1}_{V(s) \leq r} ds &= \frac{1}{2} \int_{\mathbb{R}} \mathbf{1}_{V(r^4 s) \leq r} ds \\ &= \frac{1}{2} \int_{\mathbb{R}} \mathbf{1}_{\sqrt{\frac{3}{2^2}} V(r^4 s) \leq \sqrt{3/2}} ds \\ &\stackrel{(d)}{\approx} \frac{1}{2} \int_{\mathbb{R}} \mathbf{1}_{\widehat{W}_s \leq \sqrt{3/2}} ds \\ &\stackrel{(d)}{\stackrel{\text{scaling}}{=}} \frac{1}{2} \left(\sqrt{\frac{3}{2}} \right)^4 \int_{\mathbb{R}} \mathbf{1}_{\widehat{W}_s \leq 1} ds. \end{aligned}$$

For later use, let us adapt the calculation of [45, Proposition 5] (see [46] for an amended version) and compute the mean of the limiting law that appears in the proposition. By the Poissonian construction of (ζ, \widehat{W}) and the fact that Z_t is a five-dimensional Bessel process we have

$$\mathbb{E} \left[\int_{\mathbb{R}} ds \mathbf{1}_{\widehat{W}_s \leq 1} \right] = 2 \cdot \mathbb{E} \left[\int_0^\infty dt \mathbb{N}_{\sqrt{3/2} Z_t} \left[\mathbf{1}_{\mathcal{R} \subset (0, \infty)} \int_0^\sigma ds \mathbf{1}_{\widehat{w}_s \leq 1} \right] \right].$$

By a standard calculation, the expected value of the total local time accumulated at level $x \geq 0$ for a d -dimensional Bessel process is $x \frac{2}{d-2}$. Consequently, the expected total local time at level $x \geq 0$ for $(\sqrt{3/2}Z_t)_{t \geq 0} \stackrel{(d)}{=} (Z_{3t/2})_{t \geq 0}$ is equal to $\frac{4x}{9}$. The function $x \mapsto \mathbb{N}_x \left[\mathbf{1}_{\mathcal{R} \subset (0, \infty)} \int_0^\sigma ds \mathbf{1}_{\widehat{W}_s \leq 1} \right]$ has also been computed in [45, 46], and is equal to $\frac{2}{35x^3} \mathbf{1}_{x \geq 1} + (\frac{x^2}{5} - \frac{x^4}{7}) \mathbf{1}_{x < 1}$. Hence we have

$$\frac{9}{8} \mathbb{E} \left[\int_{\mathbb{R}} ds \mathbf{1}_{\widehat{W}_s \leq 1} \right] = \int_0^\infty dx x \left(\frac{2}{35x^3} \mathbf{1}_{x \geq 1} + \left(\frac{x^2}{5} - \frac{x^4}{7} \right) \mathbf{1}_{x < 1} \right) = \frac{1}{12}. \quad (\text{III.23})$$

III.5.3 The Brownian half-plane

To conclude this section, we use the previous scaling limit result for the contour functions to define the *Brownian half-plane*, which should be the scaling limit of the UIHPQ in the local Gromov–Hausdorff sense. The construction is similar to the construction of the Brownian plane [29, 28].

Recall the notation of Section III.5.1: we first build an infinite continuous labelled tree from the functions ζ and \widehat{W} by grafting trees onto the real line according to the Poisson point measure \mathcal{N} . More precisely, we introduce a pseudo-distance on \mathbb{R} , denoted d_ζ , defined for $s, t \in \mathbb{R}$ by $d_\zeta(s, t) = \zeta(s) + \zeta(t) - 2 \min_{u \in [s \wedge t, s \vee t]} \zeta(u)$. The space \mathcal{T} obtained by taking the quotient of \mathbb{R} by the equivalence relation $d_\zeta = 0$, endowed with the quotient metric d_ζ , is a locally compact real tree (see [29] for a similar construction). Notice that \mathcal{T} has a unique doubly-infinite geodesic: equivalently, \mathcal{T} has two ends. It follows from the construction of the Brownian snake excursion measure that the labelling \widehat{W} is compatible with the canonical projection $\pi : \mathbb{R} \rightarrow \mathcal{T}$: we keep the notation \widehat{W} for this labelling on \mathcal{T} . We then mimic Schaeffer's construction in the continuous setting: for $s, t \in \mathbb{R}$, we first define

$$D^\circ(s, t) = \widehat{W}_s + \widehat{W}_t - 2 \max \left\{ \min_{u \in [s \wedge t, s \vee t]} \widehat{W}_u, \min_{u \in [s \vee t, \infty) \cup (-\infty, s \wedge t]} \widehat{W}_u \right\}$$

and then extend $D^\circ(s, t)$ to $\mathcal{T} \times \mathcal{T}$ by setting (for $a, b \in \mathcal{T}$)

$$D^\circ(a, b) = \min \{ D^\circ(s, t) : s, t \in \mathbb{R}, \pi(s) = a, \pi(t) = b \}.$$

Finally, for all $a, b \in \mathcal{T}$, consider

$$D^*(a, b) = \inf_{a_0=a, a_1, \dots, a_p=b} \sum_{i=1}^p D^\circ(a_{i-1}, a_i)$$

where the infimum is taken over all finite sequences a_0, a_1, \dots, a_p in \mathcal{T} such that $a_0 = a$ and $a_p = b$. It is not hard to check that D^* is a pseudo-distance on \mathcal{T} (see [29, 40, 54] for similar constructions). We once more take the quotient of the space \mathcal{T} by the equivalence relation $D^* = 0$ to obtain a metric space, endowed with the quotient metric and with a distinguished point (the equivalence class of $\pi(0)$), which we call the *Brownian half-plane*.

III.6 The UIHPQ with a simple boundary

In this section we extend some of the scaling limit results on the geometry of the UIHPQ to the UIHPQ with a simple boundary, from now on denoted $\widetilde{\mathcal{H}}_\infty$, which was first introduced by Angel [8] as the local limit of quadrangulations with a simple boundary whose size and perimeter both tend to infinity in a suitable way. An interesting feature of maps with a simple boundary is that they can be used to perform surgery operations by glueing their boundaries in various ways; for example, one can fold the boundary of $\widetilde{\mathcal{H}}_\infty$ upon itself (see Figure III.13) to obtain a random infinite quadrangulation of the plane endowed with an infinite (one-ended) self-avoiding walk. One may also glue together two independent copies of $\widetilde{\mathcal{H}}_\infty$ and obtain an infinite quadrangulation of the plane, this time endowed with a doubly infinite self-avoiding walk. These models of quadrangulations with self-avoiding walks are the subject of a paper still in preparation by the author and Nicolas Curien [20], which will heavily rely on results from this section. We give an overview of results to come in Section III.7.

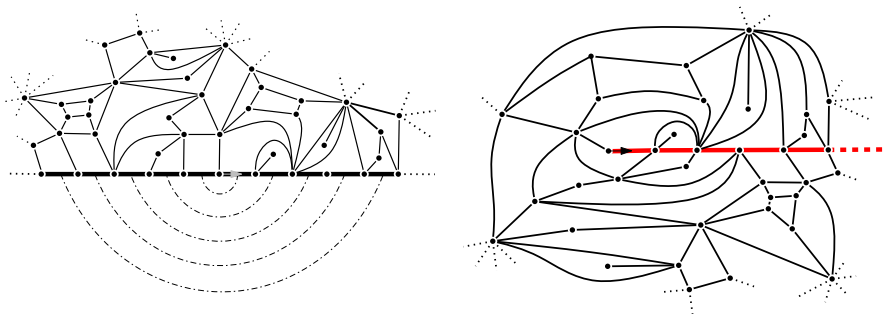


Figure III.13: How to fold the UIHPQ with a simple boundary upon itself by glueing together the two halves of its boundary.

As stated in [31, Section 5], $\widetilde{\mathcal{H}}_\infty$ can also be obtained via a pruning procedure from the UIHPQ \mathcal{H}_∞ . The pruning consists in eliminating all of the finite quadrangulations hanging from pinch points of the boundary of \mathcal{H}_∞ (see Figure III.14). Starting with the root vertex, one can follow the contour of the boundary of \mathcal{H}_∞ , thus obtaining a sequence of vertices $(x_i)_{i \in \mathbb{Z}}$, where x_0 is the root vertex and vertices may appear more than once; for each vertex y on the boundary of \mathcal{H}_∞ , consider $\text{left}(y) = \min\{i \mid x_i = y\}$ and $\text{right}(y) = \max\{i \mid x_i = y\}$; we can build a subsequence $(v_i)_{i \in \mathbb{Z}}$ of $(x_i)_{i \in \mathbb{Z}}$ by erasing all elements x_i such that there exists a vertex y for which $\text{left}(y) \leq i < \text{right}(y)$ and setting v_0 to correspond to the first vertex with non-negative index in the original sequence not to be erased. The sequence $(v_i)_{i \in \mathbb{Z}}$ is in fact a simple doubly infinite path; the infinite (random) quadrangulation lying above it, rooted in the edge v_0v_1 (oriented away from v_0), is $\widetilde{\mathcal{H}}_\infty$. The complement of $\widetilde{\mathcal{H}}_\infty$ in \mathcal{H}_∞ is a sequence of (almost surely) finite quadrangulations with a generic boundary hanging from the vertices $(v_i)_{i \in \mathbb{Z}}$, some of which may consist of a single vertex; we name such (random) quadrangulations $(\mathbf{q}_i)_{i \in \mathbb{Z}}$,

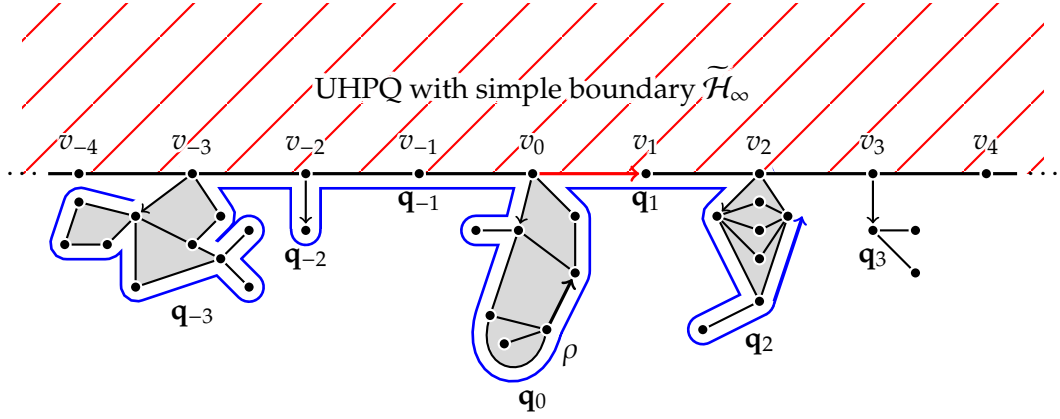


Figure III.14: The UIHPQ with a simple boundary obtained by a pruning procedure from the UIHPQ with a generic boundary. The finite quadrangulations \mathbf{q}_i are rooted in their first edge to be met when following the left-to-right contour of the boundary of the UIPQ (represented by the blue arrow) so that the root vertex of \mathbf{q}_i is the vertex v_i on the simple boundary of $\tilde{\mathcal{H}}_\infty$.

where \mathbf{q}_i includes vertex v_i (so that \mathbf{q}_0 includes the root vertex of \mathcal{H}_∞ , and possibly the entire root edge). By [31, Proposition 6], the \mathbf{q}_i 's are independent and distributed according to the so-called free Boltzmann distribution on quadrangulations with a general boundary, with the exception of \mathbf{q}_0 , which has an additional bias (see [31] for details).

We denote by \mathbf{Q}_f a free Boltzmann quadrangulation with a general boundary; the probability that $\mathbf{Q}_f = q$ for a given (rooted) quadrangulation $q \in \mathbf{Q}_{n,p}$ (with n internal faces and perimeter $2p$) is

$$\mathbb{P}(\mathbf{Q}_f = q) = \frac{1}{W(1/12, 1/8)} \left(\frac{1}{12}\right)^n \left(\frac{1}{8}\right)^p,$$

where $W(g, z)$ is the generating function defined in Section III.2.1.2, counting cardinalities of the sets $\mathbf{Q}_{n,p}$ with a weight g per inner face and \sqrt{z} per edge on the boundary; using the explicit formula (III.9) one can deduce that

$$\mathbb{E}[\text{Perimeter}(\mathbf{Q}_f)] = \left. \frac{2z\partial_z W(g, z)}{W(g, z)} \right|_{\substack{g=1/12 \\ z=1/8}} = 2. \quad (\text{III.24})$$

The area (i.e. the number of inner faces) of \mathbf{Q}_f has no first moment since $\partial_g W(g, z)$ explodes when $z = 1/8$ as $g \rightarrow 1/12$. Singularity analysis, however, shows that

$$\mathbb{P}(\text{Area}(\mathbf{Q}_f) = n) \sim \frac{[g^n]W(g, 1/8)}{W(1/12, 1/8)} = C \cdot n^{-7/4} \quad (\text{III.25})$$

for some constant $C > 0$ (whose value is not relevant for what follows).

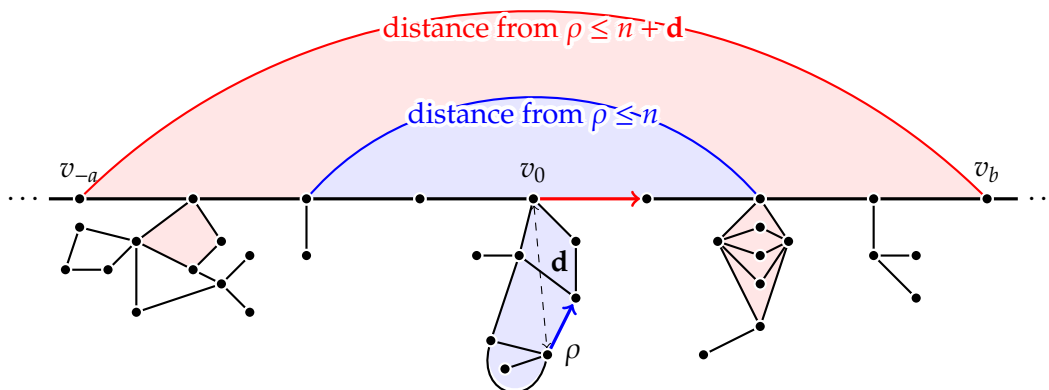


Figure III.15: A representation of the balls $[\mathcal{H}_\infty]_n$ and $[\mathcal{H}_\infty]_{n+d}$; notice that $[\tilde{\mathcal{H}}_\infty]_n \subseteq [\mathcal{H}_\infty]_{n+d}$ (in fact, it is obtained from $[\mathcal{H}_\infty]_{n+d}$ by eliminating any vertices belonging to $\cup_{i \in \mathbb{Z}} \mathbf{q}_i$, with the exception of the v_i 's).

Using the pruning procedure described above we can now deduce a result analogous to Proposition III.5.1 for the UIHPQ with a simple boundary:

Proposition III.6.1. *Let $(\tilde{X}_k)_{k \in \mathbb{Z}}$ be the process of distances to the root vertex read along the boundary of the UIHPQ with a simple boundary (which is a doubly infinite path, implicitly identified with \mathbb{Z}); then, using the same notation as in Proposition III.5.1, we have*

$$\left(\frac{\tilde{X}_{[nt]}}{\sqrt{n}} \right)_{t \in \mathbb{R}} \xrightarrow[n \rightarrow \infty]{(d)} \sqrt{3} (Z_t)_{t \in \mathbb{R}}.$$

Proof. We use the construction of the UIHPQ with a simple boundary $\tilde{\mathcal{H}}_\infty$ as the result of the pruning operation on the standard UIHPQ, as described at the beginning of this section; recall that the boundary $(v_i)_{i \in \mathbb{Z}}$ of $\tilde{\mathcal{H}}_\infty$ was constructed as a subsequence of the contour $(x_i)_{i \in \mathbb{Z}}$ of the full boundary of \mathcal{H}_∞ , so that each v_i is identified with some x_{n_i} , its leftmost occurrence in the sequence $(x_i)_{i \in \mathbb{Z}}$. It is now quite clear that $n_i - n_{i-1} - 1$ is equal to the perimeter of the quadrangulation \mathbf{q}_i , so that by the law of large numbers we get

$$\frac{n_i}{i} \xrightarrow[i \rightarrow \pm\infty]{a.s.} 1 + \mathbb{E}[\text{Perimeter}(\mathbf{Q}_f)] \stackrel{\text{(III.24)}}{=} 3.$$

This fact can be combined with Proposition III.5.1 to obtain the desired result. □

Similarly, Proposition III.5.3 can be restated for the UIHPQ with a simple boundary:

Proposition III.6.2. *Proposition III.5.3 still holds if \mathcal{H}_∞ is replaced by $\tilde{\mathcal{H}}_\infty$.*

Proof. Again, we see $\widetilde{\mathcal{H}}_\infty$ as being constructed from the UIHPQ \mathcal{H}_∞ via the pruning procedure of [31]. We will show that

$$\lim_{n \rightarrow \infty} \mathbb{P}(|\#[\mathcal{H}_\infty]_n - \#[\widetilde{\mathcal{H}}_\infty]_n| > \varepsilon n^4) = 0$$

for any positive ε , which entails the proposition.

Thanks to the pruning construction, we have $|\#[\mathcal{H}_\infty]_n - \#[\widetilde{\mathcal{H}}_\infty]_n| \leq \sum_{i=-a}^b |\mathbf{q}_i| + |\#[\mathcal{H}_\infty]_{n+\mathbf{d}} - \#[\mathcal{H}_\infty]_n|$, where \mathbf{d} is the distance between the root vertex of \mathcal{H}_∞ and the infinite component, while $-a$ and b are the minimum and maximum i such that vertex v_i is at distance n from vertex v_0 (see Figure III.15).

Without loss of generality we may then restrict ourselves to the event $\mathbf{d} < \sqrt{n}$, which is asymptotically almost sure; on the other hand, we have

$$\mathbb{P}\left(|\#[\mathcal{H}_\infty]_{n+\mathbf{d}} - \#[\mathcal{H}_\infty]_n| > \frac{\varepsilon}{2} n^4 \mid \mathbf{d} < \sqrt{n}\right) \rightarrow 0$$

as $n \rightarrow \infty$ by Proposition III.5.3.

Also, we have shown in Proposition III.6.2 that the probability of $\max\{a, b\}$ being at least $n^{2+\alpha}$ is infinitesimal in n for all positive α . Excluding the single (almost surely) finite quadrangulation \mathbf{q}_0 in order not to be forced to take the bias of its law into account, we are reduced to computing

$$\lim_{n \rightarrow \infty} \mathbb{P}\left(\sum_{0 < |i| \leq n^{2+\alpha}} |\mathbf{q}_i| > \frac{\varepsilon}{4} n^4\right),$$

where the \mathbf{q}_i 's are i.i.d. free Boltzmann quadrangulations. Since the size of \mathbf{q}_i can always be bounded from above by four times its area, we may use (III.25) to deduce that \mathbf{q}_i is stochastically dominated by a random variable in the domain of attraction of the totally asymmetric 3/4-stable random variable. In particular it follows by standard estimates [59] that there is a constant C such that

$$\lim_{n \rightarrow \infty} \mathbb{P}\left(\sum_{0 < |i| \leq n^{2+2\alpha}} |\mathbf{q}_i| > C n^{4(2+\alpha)/3}\right) = 0,$$

and we can choose α so that asymptotically $C n^{4(2+2\alpha)/3} < \varepsilon n^4/4$. □

III.7 Self-avoiding walks on the UIPQ

III.7.1 The zipper maps

We have introduced in Section III.1 the set $\widetilde{\mathcal{Q}}_{n,p}$ of rooted quadrangulations with a *simple* boundary of length $2p$ and area n . By convention, we will consider $\widetilde{\mathcal{Q}}_{0,0}$ to contain a single map consisting of only one vertex; notice that $\widetilde{\mathcal{Q}}_{0,1}$ also contains a single map,

consisting of exactly one oriented edge with two distinct end-points: such an edge is considered to be a *simple* boundary of length 2. As already remarked upon in Section III.2.1.2, $\widetilde{\mathcal{Q}}_{n,1}$, which is in fact the same as the set $\mathcal{Q}_{n,1}$ since a boundary of length two is always simple, can also be seen as the set of all (rooted) quadrangulations of the sphere with n faces (i.e. quadrangulations *without* a boundary), by identifying the two edges of the boundary, thus contracting the outerface and effectively “zipping” the quadrangulation shut.

Enumeration results for the sets $\widetilde{\mathcal{Q}}_{n,p}$ can be found in [17]; in particular, we have

Enumeration result III.1.

$$\#\widetilde{\mathcal{Q}}_{n,p} = 3^{-p} \frac{(3p)!}{p!(2p-1)!} 3^n \frac{(2n+p-1)!}{(n-p+1)!(n+2p)!}, \quad n \xrightarrow{\sim} \infty \quad C_p 12^n n^{-5/2}, \quad (\text{III.26})$$

$$C_p = \frac{1}{2\sqrt{\pi}} \frac{(3p)!}{p!(2p-1)!} \left(\frac{2}{3}\right)^p \quad p \xrightarrow{\sim} \infty \quad \frac{\sqrt{3p}}{2\pi} \left(\frac{9}{2}\right)^p. \quad (\text{III.27})$$

Consider now how the operation of “zipping up” a quadrangulation along its simple boundary may be extended from the set $\widetilde{\mathcal{Q}}_{n,1}$ to the set of all locally finite quadrangulations with a simple boundary of finite length. We may define a map $Z^{(0,p)}$ which, given a rooted quadrangulation $q \in \widetilde{\mathcal{Q}}$ with a boundary of length $2p$, yields a quadrangulation of the sphere $Z^{(0,p)}(q)$ endowed with a self-avoiding walk of length p that has the root vertex as an endpoint and starts with the root edge.

In fact, we may generalise this construction and build a function $Z^{(b,f)}$, where $b+f = p$ (and $f \geq 1$), to the set of rooted, locally finite quadrangulations with a simple boundary of length $2p$, which we call $\widetilde{\mathcal{Q}}_p$; given $q \in \widetilde{\mathcal{Q}}_p$, call e_0, \dots, e_{2p-1} the $2p$ edges of its boundary, each oriented clockwise with respect to the outerface, taken in clockwise order starting with the root edge e_0 ; we set $Z^{(b,f)}(q)$ to be the quadrangulation of the sphere obtained by identifying e_i with $-e_{2f-1-i}$, where the $-$ sign represents a change in orientation, endowed with the distinguished self-avoiding path of length p that is the image of the original cycle e_0, \dots, e_{2p-1} and rooted in the image of e_0 . The object $Z^{(b,f)}(q)$ is a rooted locally finite quadrangulation of the sphere endowed with a distinguished path of length $b+f$ which contains the root edge, and comprises b edges lying left of the root vertex and f edges lying to its right (where right and left are determined by the direction of the root edge, which is considered to be pointing towards the right); we call such a path a *self-avoiding walk of type (b, f)* . We shall call $\mathcal{Q}^{(b,f)}$ the set of rooted (locally finite) quadrangulations of the sphere endowed with a self-avoiding walk of type (b, f) and $\mathcal{Q}_n^{(b,f)} \subset \mathcal{Q}^{(b,f)}$ the set of all those that have area n . The following is clear:

Proposition III.7.1. *Given $b \geq 0, f \geq 1$ such that $b+f = p$, the mapping $Z^{(b,f)} : \widetilde{\mathcal{Q}}_{n,p} \rightarrow \mathcal{Q}_n^{(b,f)}$ is a bijection for every $n \geq 1$.*

It should then be apparent how one may want to employ random quadrangulations with a simple boundary as a tool to study self-avoiding walks on a uniform random quadrangulation of the sphere. If we call $\mathcal{Q}_n^{(b,f)}$ a uniform element of $\mathcal{Q}_n^{(b,f)}$ and let q be a

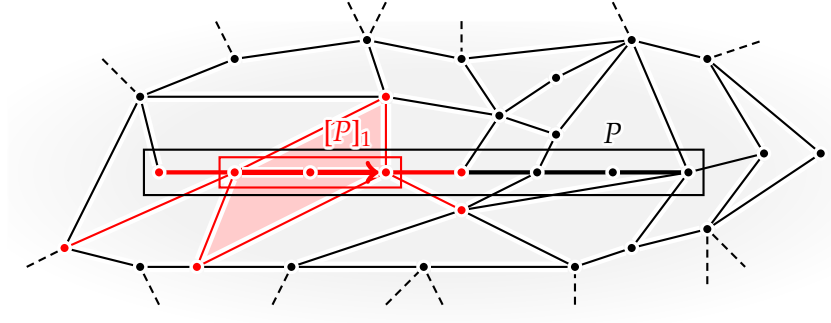


Figure III.16: The picture above represents a quadrangulation q with a SAW of type $(2, 5)$, and its ball $[q]_1$ of radius 1, which is a map endowed with a $(1, 1)$ -SAW.

fixed rooted quadrangulation with n faces, writing $\mathbf{Q}^{(b,f)} = q$ to mean that q is obtained by forgetting the distinguished SAW of $\mathbf{Q}^{(b,f)}$, we have

$$\mathbb{P}(\mathbf{Q}_n^{(b,f)} = q) = \frac{\#\text{SAW}^{(b,f)}(q)}{\#\widetilde{\mathbf{Q}}_{n,b+f}}, \quad (\text{III.28})$$

where $\text{SAW}^{(b,f)}(q)$ is the set of all self-avoiding walks of type (b, f) in the rooted quadrangulation q ; in other words, the underlying rooted quadrangulation of $\mathbf{Q}_n^{(b,f)}$ is not uniform, but chosen proportionally to the number of its self-avoiding walks of type (b, f) .

III.7.2 Annealed infinite self-avoiding walk on the UIPQ

Let us have a closer look at the maps $Z^{(b,f)} : \widetilde{\mathbf{Q}}_{b+f} \rightarrow \mathbf{Q}^{(b,f)}$. We claim that such maps are continuous for the local distance, where the local distance on $\widetilde{\mathbf{Q}}_p$ is the restriction of d_{loc} as defined on \mathbf{Q} in Section III.2.1.2, and the local distance on $\cup_{b \geq 0, f \geq 1} \mathbf{Q}^{(b,f)}$ is defined as follows: given $q \in \mathbf{Q}^{(b,f)}$ (with a distinguished self-avoiding path P) and an integer $r > 0$, we write $[q]_r$ for the rooted map with a distinguished path obtained by selecting the sub-path $[P]_r$ of P having $\min\{f, r\}$ edges after the root vertex and $\min\{b, r\}$ edges before; all vertices having distance greater than r from the path $[P]_r$ are then erased (together with edges having them as endpoints), and $[P]_r$ is made the distinguished path of $[q]_r$ (see Figure III.16). We then set

$$d_{\text{loc}}(q, q') = \left(1 + \max(0, \sup\{r \geq 1 : [q]_r = [q']_r\})\right)^{-1}$$

for $q, q' \in \cup_{b,f} \mathbf{Q}^{(b,f)}$ (where equality is that of maps with distinguished paths).

Continuity of $Z^{(b,f)}$ is quite clear: suppose you are given $q \in \widetilde{\mathbf{Q}}_{b+f}$ and a positive integer r ; then for any $q' \in \widetilde{\mathbf{Q}}_{b+f}$ such that $[q']_{b+f+r} = [q]_{b+f+r}$ one has $[Z^{(b,f)}(q)]_r = [Z^{(b,f)}(q')]_r$, because the vertices at distance at most r from the distinguished path in

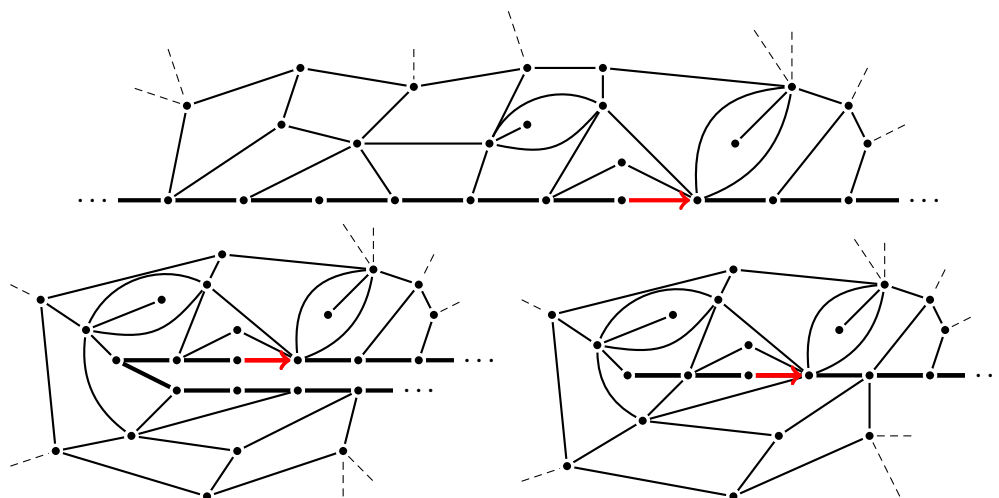


Figure III.17: The map $Z^{(2, \infty)}$ applied to a quadrangulation with an infinite boundary.

$Z^{(b, f)}(q)$ have a pre-image in q at distance at most r from the boundary of q , that is at most $r + b + f$ from the root vertex of q (since the length of the boundary is $2(b + f)$).

As a direct consequence of this and (III.7) one therefore has:

Corollary III.7.2. *For any integers $b \geq 0, f \geq 1$ the following convergence holds in distribution for the local topology, if $Q_\infty^{(b, f)}$ is taken to be $Z^{(b, f)}(\tilde{Q}_{\infty, b+f})$, where $\tilde{Q}_{\infty, b+f}$ is the UIPQ of the $2(b + f)$ -gon:*

$$Q_n^{(b, f)} \xrightarrow[n \rightarrow \infty]{(d)} Q_\infty^{(b, f)}.$$

We may now fix b and consider the local limit of $Q_\infty^{(b, f)}$ when $f \rightarrow \infty$. Consider a construction $Z^{(b, \infty)}$ performed on rooted quadrangulations with a simple *infinite* boundary to obtain rooted quadrangulations of the sphere with an infinite self-avoiding walk containing the root edge, having b edges lying left of the root vertex (that is a SAW of type (b, ∞)) as in Figure III.17. It is not hard to see that

$$Q_\infty^{(b, f)} \xrightarrow[f \rightarrow \infty]{} Z^{(b, \infty)}(\tilde{\mathcal{H}}_\infty),$$

where $\tilde{\mathcal{H}}_\infty$ is the UIHPQ with a simple boundary (and as usual the convergence is in law for the local topology).

In fact, consider the law of $[Z^{(b, f)}(\tilde{Q}_{\infty, b+f})]_r = [Q_\infty^{(b, f)}]_r$; this random map (with distinguished SAW) can be fully reconstructed as a measurable function of $[\tilde{Q}_{\infty, b+f}]_{2(b+r)}$, by an argument entirely analogous to that above. Since we know local convergence of $\tilde{Q}_{\infty, p}$ to $\tilde{\mathcal{H}}_\infty$ as $p \rightarrow \infty$, we also know that $[\tilde{Q}_{\infty, b+f}]_{2(b+r)} \rightarrow [\tilde{\mathcal{H}}_\infty]_{2(b+r)}$. The same measurable function, which consists in taking a (finite) rooted map and zipping up the rightmost path issued from the root vertex to the leftmost path to create a SAW of type $(b, 2r)$, then

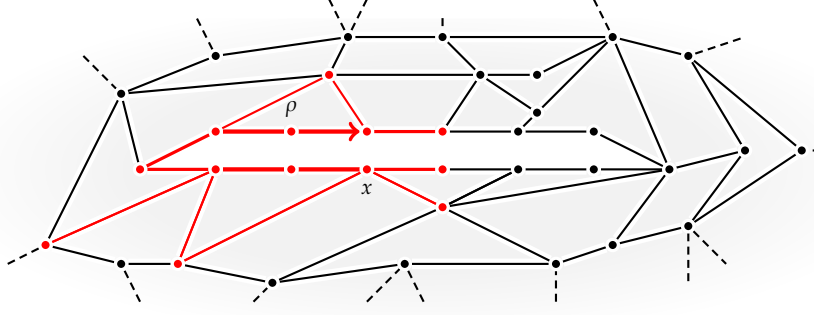


Figure III.18: A quadrangulation q' with a boundary of length 14, such that $Z^{(2,5)}(q')$ is the quadrangulation with a $(2, 5)$ -SAW, q , represented in Figure III.16; the pre-image of $[q]_1$ is coloured red: notice that it is indeed the ball one would obtain by taking $[q']_{2(b+r)}$, with $b = 2$ and $r = 1$ (thus $[q']_6$) and “zipping it up” to obtain a map with a $(2, 2)$ -SAW, then taking the ball of radius 1 (in the sense described at the beginning of this Section). This is due to the fact that vertices in the pre-image of $[q]_1$ (coloured red) have distance at most 1 from the pre-image of the distinguished path of $[q]_1$, whose vertex furthest from the root is the one labelled x , which is such that $d_{\text{gr}}(x, \rho) = 2b + r = 5$.

applying $[\cdot]_r$ as defined above, can be applied to $[\widetilde{\mathcal{H}}_\infty]_{2(b+r)}$ to obtain $[Z^{(b,\infty)}(\widetilde{\mathcal{H}}_\infty)]_r$ (see Figure III.18).

Moving on to a convergence result involving a *doubly infinite* self-avoiding walk, i.e. sending b to infinity, is more difficult. One can nonetheless show the following:

Proposition III.7.3. *We have the following convergence in distribution for the local topology:*

$$\mathcal{Q}_\infty^{(b,f)} \xrightarrow{b,f \rightarrow \infty} \mathcal{Q}_\infty^{(\infty,\infty)},$$

where $\mathcal{Q}_\infty^{(\infty,\infty)}$ is a quadrangulation with a bi-infinite self-avoiding walk obtained by glueing together two independent copies of the UIHPQ with a simple boundary, making the two roots coincide; the distinguished self-avoiding walk on $\mathcal{Q}_\infty^{(\infty,\infty)}$ is the image of the identified boundaries.

The proof of this fact (which we do not give here) relies on the fact that, as b is sent to infinity, the ball $[Z^{(b,\infty)}(\widetilde{\mathcal{H}}_\infty)]_r$ is split by its SAW of type (r, r) into two parts whose pre-images in $\widetilde{\mathcal{H}}_\infty$ will tend not to intersect each other (since they are contained in balls for the graph distance that are centred in vertices of the boundary very far from each other – namely the root vertex of $\widetilde{\mathcal{H}}_\infty$ and the vertex of the boundary that lies $2b$ steps to its left). The spatial Markov property of the UIHPQ can then be used to infer that the two balls (for $b \rightarrow \infty$) are essentially independent.

III.7.3 Annealed and quenched connective constants

The connective constant of a lattice is the exponential growth rate of the number of self-avoiding walks of type $(0, n)$, if it exists. Given an infinite quadrangulation q , we

may consider its connective constant

$$\mu(q) = \limsup_{n \rightarrow \infty} \left(\# \text{SAW}^{(0,n)}(q) \right)^{\frac{1}{n}},$$

and thus investigate the random variable $\mu(\mathcal{Q}_\infty)$, where \mathcal{Q}_∞ is the UIPQ.

We claim that methods from [37] and [7] can be adapted to show the following:

Proposition III.7.4. *The (quenched) connective constant $\mu(\mathcal{Q}_\infty)$ of the UIPQ is almost surely constant.*

This leaves the question of the actual value of $\mu(\mathcal{Q}_\infty)$; though we have for the moment no inkling of the exact value, the preceding sections allow us to give an upper bound thanks to the following estimate for the quantity $\mathbb{E}[\# \text{SAW}^{(b,f)}(\mathcal{Q}_\infty)]$:

Proposition III.7.5 (Annealed connective constant). *With the notation of (III.27), for any $b \geq 0$ and $f \geq 1$ we have*

$$\mathbb{E}[\# \text{SAW}^{(b,f)}(\mathcal{Q}_\infty)] = \frac{C_{b+f}}{C_1} = \left(\frac{9}{2} \right)^{b+f+o(b+f)}.$$

Proof. Thanks to (III.28) and (III.27), for each $n \geq 1$ we have

$$\mathbb{E}[\# \text{SAW}^{(b,f)}(\mathcal{Q}_n)] = \frac{\#\tilde{\mathcal{Q}}_{n,b+f}}{\#\tilde{\mathcal{Q}}_{n,1}} \xrightarrow{n \rightarrow \infty} \frac{C_{b+f}}{C_1}.$$

On the other hand, from the convergence of uniform quadrangulations towards the UIPQ we deduce that for any fixed pair b, f the random variables $\# \text{SAW}^{(b,f)}(\mathcal{Q}_n)$ converge in law towards $\# \text{SAW}^{(b,f)}(\mathcal{Q}_\infty)$ as $n \rightarrow \infty$. The statement of the proposition thus follows if we manage to prove that $(\# \text{SAW}^{(b,f)}(\mathcal{Q}_n))_{n \geq 0}$ is uniformly integrable. In other words, for any $\varepsilon > 0$ we want to find $A > 0$ such that $\mathbb{E}[\# \text{SAW}^{(b,f)}(\mathcal{Q}_n) \mathbf{1}_{\# \text{SAW}^{(b,f)}(\mathcal{Q}_n) > A}] \leq \varepsilon$ for all $n \geq 0$. But by definition of $\mathcal{Q}_n^{(b,f)}$ we have

$$\mathbb{E}[\# \text{SAW}^{(b,f)}(\mathcal{Q}_n) \mathbf{1}_{\# \text{SAW}^{(b,f)}(\mathcal{Q}_n) > A}] \stackrel{\text{(III.28)}}{=} \frac{\#\tilde{\mathcal{Q}}_{n,b+f}}{\#\tilde{\mathcal{Q}}_{n,1}} \mathbb{E}[\mathbf{1}_{\# \text{SAW}^{(b,f)}(\mathcal{Q}_n^{(b,f)}) > A}]. \quad (\text{III.29})$$

Since we know that $\mathcal{Q}_n^{(b,f)} \rightarrow \mathcal{Q}_\infty^{(b,f)}$ locally in distribution (see Proposition III.7.3 and the discussion above), it follows that

$$\# \text{SAW}^{(b,f)}(\mathcal{Q}_n^{(b,f)}) \xrightarrow[n \rightarrow \infty]{(d)} \# \text{SAW}^{(b,f)}(\mathcal{Q}_\infty^{(b,f)}).$$

Hence the family $(\# \text{SAW}^{(b,f)}(\mathcal{Q}_n^{(b,f)}))_{n \geq 1}$ is tight; we can consequently find A large enough for the right-hand side of (III.29) to be less than ε uniformly in $n \geq 0$ as desired. \square

Proposition III.7.4 and Proposition III.7.5 imply the following upper bound for $\mu(\mathcal{Q}_\infty)$:

Corollary III.7.6. *We have $\mu(Q_\infty) \leq \frac{9}{2}$.*

The question of whether the quenched constant coincides with the annealed constants, or in other words of whether “weak” or “strong disorder” [39, 37] holds in the case of the UIPQ remains open.

III.7.4 Singularity of $Q_\infty^{(\infty, \infty)}$ with respect to the law of the UIPQ

We give here the main result of a paper that is still in preparation by the author of this thesis and Nicolas Curien, which is the natural outcome of the last few sections, combined with Proposition III.6.2:

Theorem III.7.7. *The law of the underlying rooted quadrangulation of $Q_\infty^{(\infty, \infty)}$ is singular with respect to the law of the UIPQ Q_∞ .*

While a natural way to show this would involve comparing the number of self-avoiding walks typically found in Q_∞ to the number of self-avoiding walks in $Q_\infty^{(\infty, \infty)}$, we find that it is simpler to compare estimates for the volume of balls in the two structures, given that we have both a result concerning such a volume in the UIHPQ with a simple boundary (see Proposition III.6.2) and one – shown by Le Gall and Ménard [45] – for the volume of balls in the UIPQ.

We shall not give a proof here, but rather sketch the argument which we believe would lead to such a conclusion. From now on, with an abuse of notation, we shall write $Q_\infty^{(\infty, \infty)}$ to mean the random rooted quadrangulation of the sphere obtained by forgetting the distinguished SAW; we shall therefore use the notation $[Q_\infty^{(\infty, \infty)}]_r$ as in Section III.2.1.2, to refer to the ball of radius r (centred in the root vertex) for the graph distance d_{gr} . By Proposition III.7.3, the random variable giving the number of vertices of $Q_\infty^{(\infty, \infty)}$ at distance r or less from the root vertex, i.e. $\#[Q_\infty^{(\infty, \infty)}]_r$, is at least $\#[\tilde{\mathcal{H}}_\infty^1]_r + \#[\tilde{\mathcal{H}}_\infty^2]_r - B$, where $\tilde{\mathcal{H}}_\infty^1$ and $\tilde{\mathcal{H}}_\infty^2$ are two independent copies of the UIHPQ with a simple boundary, and B is the number of vertices in $[\tilde{\mathcal{H}}_\infty^1]_r$ that lie on the boundary; since we shall use estimates for $r^{-4}[\tilde{\mathcal{H}}_\infty^1]_r$, the random variable B will turn out to be completely irrelevant.

Already the fact that $\mathbb{E}[\mathcal{V}_h] = \frac{7}{9}\mathbb{E}[\mathcal{V}_p]$ (where \mathcal{V}_p and \mathcal{V}_h are the weak limits of $r^{-4}\#[Q_\infty]_r$ and $r^{-4}\#[\tilde{\mathcal{H}}_\infty]_r$) gives a strong indication that the two laws should be singular with respect to each other, since $2 \cdot \frac{7}{9} > 1$. In order to turn this idea into a rigorous argument, one can consider two independent copies of \mathcal{V}_h (we call them $\mathcal{V}_h^{(1)}$ and $\mathcal{V}_h^{(2)}$); with this notation, we have

$$r^{-4}\#[Q_\infty^{(\infty, \infty)}]_r \geq r^{-4}(\#[\tilde{\mathcal{H}}_\infty^1]_r + \#[\tilde{\mathcal{H}}_\infty^2]_r - B) \rightarrow \mathcal{V}_h^{(1)} + \mathcal{V}_h^{(2)} \quad \text{and} \quad r^{-4}\#[Q_\infty]_r \rightarrow \mathcal{V}_p \quad (\text{III.30})$$

in law as $r \rightarrow \infty$; also, since $\mathbb{E}[\mathcal{V}_h^{(1)} + \mathcal{V}_h^{(2)}] > \mathbb{E}[\mathcal{V}_p]$, there is $x_0 > 0$ such that

$$\mathbb{P}(\mathcal{V}_h^{(1)} + \mathcal{V}_h^{(2)} > x_0) > \mathbb{P}(\mathcal{V}_p > x_0). \quad (\text{III.31})$$

Given a quadrangulation q , set $\mathcal{X}_r(q) = 1$ if $\#[q]_r \geq x_0 r^4$ and $\mathcal{X}_r(q) = 0$ otherwise. The singularity result follows from an evaluation of the random variables $\mathcal{X}_r(Q_\infty^{(\infty, \infty)})$ and $\mathcal{X}_r(Q_\infty)$ at different scales $0 \ll r_1 \ll r_2 \ll r_3 \ll \dots$ chosen in such a way that $\mathcal{X}_{r_i}(Q_\infty^{(\infty, \infty)})$ is roughly independent of $\mathcal{X}_{r_j}(Q_\infty^{(\infty, \infty)})$ for $i \neq j$, so that one may invoke a law of large numbers.

Indeed, for any $\delta > 0$ and $r > 0$, one can always find $r' \gg r$ such that

$$\text{Cov}(\mathcal{X}_r(Q_\infty); \mathcal{X}_{r'}(Q_\infty)) \leq \delta,$$

and that the same holds for $Q_\infty^{(\infty, \infty)}$.

One then builds a sequence $0 \ll r_1 \ll r_2 \ll \dots$ such that for all $i < j$ one has $\text{Cov}(\mathcal{X}_{r_i}(Q_\infty), \mathcal{X}_{r_j}(Q_\infty)) \leq 2^{-j}$ and $\text{Cov}(\mathcal{X}_{r_i}(Q_\infty^{(\infty, \infty)}), \mathcal{X}_{r_j}(Q_\infty^{(\infty, \infty)})) \leq 2^{-j}$, so that the hypotheses for the strong law of large numbers for weakly correlated variables are satisfied, and (III.30) implies

$$\frac{1}{k} \sum_{i=1}^k \mathcal{X}_{r_i}(Q_\infty) \xrightarrow[k \rightarrow \infty]{a.s.} \mathbb{P}(\mathcal{V}_p > x_0)$$

while almost surely

$$\liminf_{k \rightarrow \infty} \frac{1}{k} \sum_{i=1}^k \mathcal{X}_{r_i}(Q_\infty^{(\infty, \infty)}) \geq \mathbb{P}(\mathcal{V}_h^{(1)} + \mathcal{V}_h^{(2)} > x_0) > \mathbb{P}(\mathcal{V}_p > x_0).$$

This implies that the event $\{\lim k^{-1} \sum_i \mathcal{X}_{r_i}(q) = \mathbb{P}(\mathcal{V}_p > x_0)\}$ has probability 1 under the law of the UIPQ and probability 0 under the law of $Q_\infty^{(\infty, \infty)}$, finally establishing singularity of the two distributions, as expected.

Bibliography

- [1] C. ABRAHAM, *Rescaled bipartite planar maps converge to the Brownian map*, arXiv:1312.5959, (2013).
- [2] R. ABRAHAM AND J.-F. DELMAS, *Local limits of conditioned Galton-Watson trees: the infinite spine case*, *Electron. J. Probab.*, 19 (2014), pp. 1–19.
- [3] D. ALDOUS, *The continuum random tree. I*, *Ann. Probab.*, 19 (1991), pp. 1–28.
- [4] ———, *The continuum random tree. II. An overview*, in *Stochastic analysis* (Durham, 1990), vol. 167 of *London Math. Soc. Lecture Note Ser.*, Cambridge Univ. Press, Cambridge, 1991, pp. 23–70.
- [5] ———, *The continuum random tree. III*, *Ann. Probab.*, 21 (1993), pp. 248–289.
- [6] J. AMBJØRN, B. DURHUUS, AND T. JONSSON, *Quantum geometry*, *Cambridge Monographs on Mathematical Physics*, Cambridge University Press, Cambridge, 1997.
- [7] O. ANGEL, *Growth and percolation on the uniform infinite planar triangulation*, *Geom. Funct. Anal.*, 13 (2003), pp. 935–974.
- [8] ———, *Scaling of percolation on infinite planar maps, I*, arXiv:0501006, (2005).
- [9] O. ANGEL AND O. SCHRAMM, *Uniform infinite planar triangulation*, *Comm. Math. Phys.*, 241 (2003), pp. 191–213.
- [10] J. BERTOIN AND I. KORTCHEMSKI, *Self-similar scaling limits of Markov chains on the positive integers*, arXiv:1412.1068, (2014).
- [11] J. BETTINELLI, *Scaling limit of random planar quadrangulations with a boundary*, *Ann. Inst. Henri Poincaré Probab. Stat.*, 51 (2015), pp. 432–477.
- [12] J. BETTINELLI, E. JACOB, AND G. MIERMONT, *The scaling limit of uniform random plane maps, via the Ambjørn–Budd bijection*, *Electron. J. Probab.*, 19 (2014), pp. no. 74, 1–16.
- [13] F. BONAHOON, *Low-dimensional geometry*, vol. 49 of *Student Mathematical Library*, American Mathematical Society, Providence, RI, 2009.

- [14] N. BONICHON, C. GAVOILLE, AND N. HANUSSE, *Canonical decomposition of outerplanar maps and application to enumeration, coding and generation*, J. Graph Algorithms Appl., 9 (2005), pp. 185–204.
- [15] J. BOUTTIER, P. DI FRANCESCO, AND E. GUITTER, *Geodesic distance in planar graphs*, Nuclear Physics, 663 (2003), pp. 535–567.
- [16] J. BOUTTIER, P. DI FRANCESCO, AND E. GUITTER, *Planar maps as labeled mobiles*, Electron. J. Combin., 11 (2004), pp. Research Paper 69, 27 pp.
- [17] J. BOUTTIER AND E. GUITTER, *Distance statistics in quadrangulations with a boundary, or with a self-avoiding loop*, J. Phys. A, 42 (2009), pp. 465208, 44.
- [18] ———, *Planar maps and continued fractions*, Comm. Math. Phys., 309 (2012), pp. 623–662.
- [19] A. CARACENI, *The Scaling Limit of Random Outerplanar Maps*, Ann. Inst. H. Poincaré Probab. Statist. (to appear), (2015).
- [20] A. CARACENI AND N. CURIEN, *Annealed models for self-avoiding walks on the UIPQ*, in preparation.
- [21] A. CARACENI AND N. CURIEN, *Geometry of the Uniform Infinite Half-Planar Quadrangulation*, arXiv:1508.00133, (2015).
- [22] G. CHARTRAND AND F. HARARY, *Planar permutation graphs*, Ann. Inst. Henri Poincaré Probab. Stat., 3 (1967), pp. 433–438.
- [23] P. CHASSAING AND B. DURHUUS, *Local limit of labeled trees and expected volume growth in a random quadrangulation*, Ann. Probab., 34 (2006), pp. 879–917.
- [24] P. CHASSAING AND G. SCHAEFFER, *Random planar lattices and integrated superBrownian excursion*, Probab. Theory Related Fields, 128 (2004), pp. 161–212.
- [25] R. CORI AND B. VAUQUELIN, *Planar maps are well labeled trees*, Canad. J. Math., 33 (1981), pp. 1023–1042.
- [26] E. CSÁKI, A. FÖLDES, AND P. RÉVÉSZ, *Transient nearest neighbor random walk and Bessel process*, J. Theoret. Probab., 22 (2009), pp. 992–1009.
- [27] N. CURIEN, B. HAAS, AND I. KORTCHEMSKI, *The CRT is the scaling limit of random dissections*, Random Structures Algorithms, (2014).
- [28] N. CURIEN AND J.-F. LE GALL, *The hull process of the Brownian plane*, arXiv:1409.4026.
- [29] ———, *The Brownian plane*, J. Theoret. Probab., 27 (2014), pp. 1249–1291.
- [30] N. CURIEN, L. MÉNARD, AND G. MIERMONT, *A view from infinity of the uniform infinite planar quadrangulation*, Lat. Am. J. Probab. Math. Stat., 10 (2013), pp. 45–88.

- [31] N. CURIEN AND G. MIERMONT, *Uniform Infinite Planar Quadrangulations with a boundary*, *Random Struct. Alg.*, (2014).
- [32] A. DEMBO AND O. ZEITOUNI, *Large deviations techniques and applications*, vol. 38 of *Stochastic Modelling and Applied Probability*, Springer-Verlag, Berlin, 2010.
- [33] S. JANSON AND S. Ö. STEFÁNSSON, *Scaling limits of random planar maps with a unique large face*, *Ann. Probab.*, 43 (2015), pp. 1045–1081.
- [34] H. KESTEN, *Subdiffusive behavior of random walk on a random cluster*, *Ann. Inst. H. Poincaré Probab. Statist.*, 22 (1986), pp. 425–487.
- [35] M. KRIKUN, *Local structure of random quadrangulations*, arXiv:0512304.
- [36] ———, *A uniformly distributed infinite planar triangulation and a related branching process*, *Zap. Nauchn. Sem. S.-Peterburg. Otdel. Mat. Inst. Steklov. (POMI)*, 307 (2004), pp. 141–174, 282–283.
- [37] H. LACOIN, *Non-coincidence of quenched and annealed connective constants on the supercritical planar percolation cluster*, *Probab. Theory Related Fields* (to appear), (2012).
- [38] J. LAMPERTI, *A new class of probability limit theorems*, *Bull. Amer. Math. Soc.*, 67 (1961), pp. 267–269.
- [39] P. LE DOUSSAL AND J. MACHTA, *Self-avoiding walks in quenched random environments*, *J. Stat. Phys.*, 64 (1991), pp. 541–578.
- [40] J.-F. LE GALL, *Random geometry on the sphere*, *Proceedings of the ICM 2014*.
- [41] ———, *Spatial branching processes, random snakes and partial differential equations*, *Lectures in Mathematics ETH Zürich*, Birkhäuser Verlag, Basel, 1999.
- [42] ———, *Random trees and applications*, *Probab. Surv.*, 2 (2005), pp. 245–311.
- [43] ———, *The topological structure of scaling limits of large planar maps*, *Invent. Math.*, 169 (2007), pp. 621–670.
- [44] ———, *Uniqueness and universality of the Brownian map*, *Ann. Probab.*, 41 (2013), pp. 2880–2960.
- [45] J.-F. LE GALL AND L. MÉNARD, *Scaling limits for the uniform infinite quadrangulation*, *Illinois J. Math.*, 54, pp. 1163–1203 (2012).
- [46] ———, *Scaling limits for the uniform infinite quadrangulation (erratum)*, available at <http://www.math.u-psud.fr/jflegall/indexbis.html>.
- [47] J.-F. LE GALL AND G. MIERMONT, *Scaling limits of random trees and planar maps*, *Lecture notes for the Clay Mathematical Institute Summer School in Buzios*, (July 11 - August 7, 2010).

- [48] J.-F. LE GALL AND F. PAULIN, *Scaling limits of bipartite planar maps are homeomorphic to the 2-sphere*, *Geom. Funct. Anal.*, 18 (2008), pp. 893–918.
- [49] J.-F. MARCKERT AND G. MIERMONT, *Invariance principles for random bipartite planar maps*, *Ann. Probab.*, 35 (2007), pp. 1642–1705.
- [50] J.-F. MARCKERT AND G. MIERMONT, *The CRT is the scaling limit of unordered binary trees*, *Random Struct. Algorithms*, 38 (2011), pp. 467–501.
- [51] J.-F. MARCKERT AND A. MOKKADEM, *Limit of normalized quadrangulations: the Brownian map*, *Ann. Probab.*, 34 (2006), pp. 2144–2202.
- [52] J.-F. MARCKERT AND A. PANHOLZER, *Noncrossing trees are almost conditioned Galton-Watson trees*, *Random Structures Algorithms*, 20 (2002), pp. 115–125.
- [53] L. MÉNARD, *The two uniform infinite quadrangulations of the plane have the same law*, *Ann. Inst. H. Poincaré Probab. Statist.*, 46 (2010), pp. 190–208.
- [54] G. MIERMONT, *Aspects of random maps*, preprint, <http://perso.ens-lyon.fr/gregory.miermont/coursSaint-Flour.pdf>.
- [55] ———, *The Brownian map is the scaling limit of uniform random plane quadrangulations*, *Acta Math.*, 210 (2013), pp. 319–401.
- [56] K. PANAGIOTOU, B. STUFLER, AND K. WELLER, *Scaling limits of random graphs from subcritical classes*, arXiv:1411.1865, (2014).
- [57] D. REVUZ AND M. YOR, *Continuous martingales and Brownian motion*, vol. 293 of *Grundlehren der Mathematischen Wissenschaften [Fundamental Principles of Mathematical Sciences]*, Springer-Verlag, Berlin, third ed., 1999.
- [58] G. SCHAEFFER, *Conjugaison d'arbres et cartes combinatoires aléatoires*. PhD thesis, (1998).
- [59] A. V. SKOROHOD, *Limit theorems for stochastic processes with independent increments*, *Teor. Veroyatnost. i Primenen.*, 2 (1957), pp. 145–177.
- [60] B. STUFLER, *The continuum random tree is the scaling limit of unlabelled unrooted trees*, arXiv:1412.6333, (2014).
- [61] ———, *Scaling limits of random outerplanar maps with independent link-weights*, arXiv:1505.07600, (2015).
- [62] M. M. SYSŁO, *Characterizations of outerplanar graphs*, *Discrete Math.*, 26 (1979), pp. 47–53.
- [63] W. T. TUTTE, *A census of planar maps*, *Canad. J. Math.*, 15 (1963), pp. 249–271.
- [64] A. ZVONKIN, *Matrix integrals and map enumeration: an accessible introduction*, *Math. Comput. Modelling*, 26 (1997), pp. 281–304.